Title

Mechanics of Lipid Bilayers with an Attached Cytoskeleton, Tilt and Distension

Author

Hendrickson, Brett Ian

Publication Date

2021

Peer reviewed|Thesis/dissertation

Mechanics of Lipid Bilayers with an Attached Cytoskeleton, Tilt and Distension

by

Brett Hendrickson

A dissertation submitted in partial satisfaction of the

requirements for the degree of

Doctor of Philosophy

in

Engineering - Mechanical Engineering

in the

Graduate Division

of the

University of California, Berkeley

Committee in charge:

Professor David Steigmann, Chair
Professor Mohammad Mofrad
Associate Professor Aaron Streets

Summer 2021

Mechanics of Lipid Bilayers with an Attached Cytoskeleton, Tilt and Distension

Abstract

Mechanics of Lipid Bilayers with an Attached Cytoskeleton, Tilt and Distension

by

Brett Hendrickson

Doctor of Philosophy in Engineering - Mechanical Engineering

University of California, Berkeley

Professor David Steigmann, Chair

The purpose of this thesis is to examine the mechanical aspects of biological lipid bilayers. Constituting the cell membranes of nearly every organism, lipid bilayers are composed of amphiphilic lipid molecules which self-assemble into bilayers in aqueous solution. They exhibit a fascinating combination of flexural resistance as in shell structures and lateral flow as in two-dimensional fluid sheets, giving rise to a host of complex phenomena. Lipid bilayers represent a promising object of inquiry for medical innovation, as dysfunctional lipid bilayers have been linked to disease formation. This work seeks to mathematically depict previously unexplored lipid bilayer phenomena.

A simple model of lipid tilt and distension inspired by parallel research in molecular dynamics is outlined and demonstrated numerically. This simple model assumes reflection symmetry of lipid molecule orientation about the bilayer midsurface. Equilibrium configurations for a membrane of this type are presented for domains containing many closely packed voids representing transmembrane proteins. Lipid tilt and distension patterns arise due to the amphipathic nature of these proteins. Then, a model for a lipid bilayer involving independent tilt fields for top and bottom leaflets of the bilayer is developed. This loosened restriction leads to a complex but more general theory. A model for a lipid bilayer with a conforming elastic cytoskeleton is then proposed and equilibrium equations are established. The spontaneous curvature of the conventional Helfrich theory is shown to arise naturally as a mechanical aspect of this system.

To my family,

and all my student peers that have supported me.

Contents

List of Figures

Acknowledgments

Completion of this manuscript and years of study at UC Berkeley has been a privilege and an immense personal struggle. I have learned a enormous deal about mechanics and about how to overcome personal tragedies and stay focused on a long term goal.

I owe much of my success to my advisor, Professor Steigmann. His advice and lectures have helped lead to me greater understanding than I could have imagined before I started graduate studies. He understood my moral reservations about certain research topics in mechanical engineering and provided me with a project that I feel proud of participating in. Professor Steigmann also connected me with unique international opportunities to travel while expanding my academic career, which I greatly appreciate.

I would also like to acknowledge the years of collaboration and camaraderie I have enjoyed with my fellow graduate students in mechanics. I have learned so much from Milad, Erden, and Rubens in particular. I could not have done this without them.

Numerous other individuals in the departmental staff have provided invaluable support, including academic advising early in my graduate career by Professor Casey.

Chapter 1

Introduction

Modern life science has emphasized interdisciplinary efforts to unravel the manner in which the molecular building blocks of living cells physically interact. As a result, continuum mechanics has become relevant in cell biology topics, such as in the study of lipid bilayers. Their coupled chemical, topological, and mechanical properties can be internally modulated with amazing precision and speed [14]. Newly acquired knowledge of lipid bilayers has been exploited in laboratories and clinical trials for use in cancer treatments, drug-delivery, drug permeability testing, and biosensor design (including rapid toxin assessment) [39]. The study of lipid bilayers has recently benefited from the increased participation of the mechanics community, improving the understanding of coupled geometric and mechanical lipid bilayer properties.

Compared to the ad-hoc nature of early lipid bilayer models, utilization of concepts from differential geometry and shell theory has produced a more coherent mathematical basis for describing lipid bilayers, yielding excellent predictive accuracy even at molecular length scales [57]. Classical theories of lipid bilayers rely on the Helfrich model in which areal energy density is established as a function of Gaussian and mean curvature. This standard approach does not allow for the tilting of lipid molecule axes away from the surface normal nor axial distension of lipids (Figure 1.1(B), (C)). However, experimental observations evidence tilt and distension manifesting in many ways, including a ripple-like effect [58].

This work seeks to expand the theoretical understanding of mechanical lipid bilayer phenomena, including tilt, distension, and other effects not included in the standard models. The theoretical additions are then demonstrated using illustrative examples numerically. The first introductory sections below give a brief discussion of the physical arrangement and biological purpose of lipid bilayer membranes in cells. The next section summarizes the background research performed by previous authors as a starting point for this thesis. The last section gives a synopsis of the theoretical improvements contained in this work.

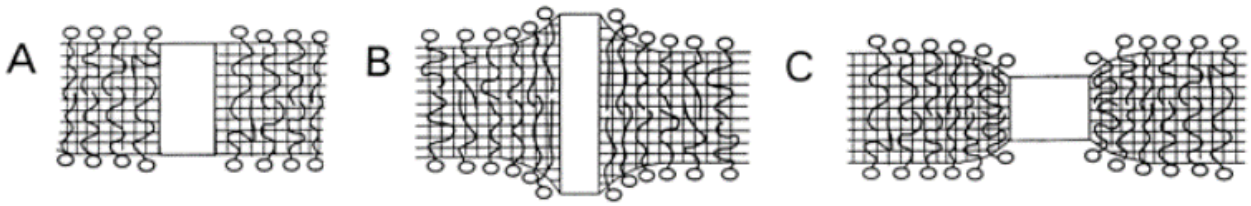

Figure 1.1: Lipid bilayer with an embedded protein. A: No tilt/distention B: Lipid distension. C: Lipid tilt [53].

1.1 Background on lipid bilayers

Membranes composed of phospholipid bilayers are an essential feature of cells. They are found in all known living cells excluding just a handful of single-celled organisms which contain monolayers [**6**]. Their essential functions are to serve as a container for the rest of the cell, separating the cell from its environment, and as a facilitator of material transport and signaling. Lipid bilayer membranes also similarly encapsulate and aid in the function of many internal organelles, including the nucleus, mitochondria and chloroplasts. Vesicle formation, in which materials are pinched into a small cavity surrounded by a lipid bilayer for transport, may take place on the surface of the Golgi complex, the endoplasmic reticulum, or form when material on the cell's boundary becomes encased in its exterior membrane. Integral membrane proteins which diffuse among the polar lipids of a membrane act as signal transducers and regulate chemical transport across the lipid barrier. Many of these proteins carry signals across the cell membrane, relaying information from the exterior to the interior of the cell, and vice versa.

The major constituent of biological membranes are phospholipid molecules exhibiting a hydrophilic head group and hydrophobic tail group. The head group is composed of a phosphate group with a negative charge, resulting in a tendency toward electrostatic attraction with polar water molecules. The tail group usually consists of two fatty acid chains. These chains are non-polar and so are induced by hydrophobic effects to accumulate in solution and exclude water molecules. Phospholipid amphiphiles that are exposed to water then tend to naturally orient themselves into two stacked leaflets with the opposite orientation. This self-assembly process forms a lipid bilayer that minimizes the interaction of water molecules with the hydrophobic tail groups and is only two molecules thick. These bilayers favor the formation of enclosed shapes, as any open boundary of the bilayer entails distortion of the phospholipids from their most favorable orientation. The precise composition of each leaflet of the bilayer is often asymmetric, resulting in slightly asymmetric mechanical properties between the top and bottom layer of the membrane.

The chemical properties of the various head and tail groups of the lipids forming a bilayer also affect membrane function. For example, tail groups modulate the phase of the

bilayer by influencing the temperature at which the bilayer transitions from a solid gel phase to a fluid phase. This fluidity allows for lateral diffusion of molecules within the bilayer, such as embedded proteins and cholesterol. Interactions between embedded molecules or structures in the bilayer may then alter the curvature of the membrane surface or convey signals across the membrane. Many biological functions extensively rely on the lateral flow of bilayer components. Another functional aspect affected by the diversity of lipids in a typical bilayer is propensity toward lipid tilt [54]. Lipids with larger head groups that have stronger interactions, such as phosphatidylcholines, generally tend to tilt from the midsurface normal direction more than lipids with smaller head groups, phosphatidylethanolamines for example [63].

1.2 Literature review

The unique mechanical properties and physiochemical functions of a biological lipid bilayer membrane emerge from its fundamental composition, formed through self-assembly of individual molecules into fluid films with extremely fine cross-sectional thickness (< 10nm) [28]. Despite this, membranes can remain stable even while encapsulating macroscopic volumes [14]. Due to the tendency of the lipid molecules to resist deviating from a parallel axial orientation relative to one another, changes in surface area associated with stretching of the membrane require a comparatively large amount of energy. This amounts to an effective stiffness akin to the bending elasticity observed in solid shell structures which can be incorporated into an energetic model of mechanical behavior by penalizing curvature.

In most physiological conditions, the lipids occur in a liquid phase. Although the polar arrangement of the lipids prevents them from flowing transversely across the hydrophobic bilayer core and switching layer en masse, lateral flow within each layer allows lipids and other embedded molecules to easily diffuse in plane across the membrane [25]. Thus, the bilayer cannot support shear stresses consistent with typical fluid behavior. These attributes imply that biological lipid bilayers can be cast as a two-dimensional fluid sheet with bending stiffness.

A vast array of theoretical models of biological lipid bilayers have been proposed and applied to study numerous physiological phenomena. One style of model relies on the balance laws and constitutive relations of the continuum mechanics of nonlinear shells [**11**]. The natural preference of lipid orientation along the midsurface normal direction lends itself to the application of Kirchhoff-Love shell theory to biomembranes. The effects of lateral fluid flow are included by imposing material symmetry through the constitutive function. The resolution of the resulting equations of motion along the normal direction generates the so-called shape equation. The resolution of the equations of motion along the tangential direction yields an equation governing the surface tension of the bilayer.

An alternate framework to the balance laws is the variational method [**11**]. In this scheme, an energy functional is proposed and its variations minimized to find equilibrium

equations. Normal variations return the shape equation and tangential variations govern surface tension. The relevant basis for the models proposed in this thesis fall under the variational method. The two approaches described can be shown to give equivalent equilibrium equations given the proper kinematic constraints [79].

In the variational approach, asymmetry in the chemical properties of the two sides of the bilayer or other influences leading to curvature at equilibrium has been included in two ways [83]. The first is known as the bilayer-coupling model. In this family of models, a constraint is applied to the area difference of the top and bottom layers of the bilayer. In the second variant, the spontaneous curvature model, curvature at equilibrium is accounted for by the incorporation of an additional term in the strain energy per unit area function called the spontaneous curvature [24].

By far the most familiar and widely used model for biomembrane mechanical behavior is due to Canham [12] with an equivalent and more commonly used form given by Helfrich [24]. The classical Canham-Helfrich theory incorporates a characteristic spontaneous curvature and a strain energy which depends on Gaussian curvature linearly and mean curvature quadratically. This model has been used successfully to study equilibrium shapes of cells and other encapsulations of lipid bilayers, especially erythrocytes, along with many other biological membrane behaviors such as the formation of invaginations, budding and other aspects of endocytosis [68, 46, 27, 44].

The Helfrich model restricts the orientation of the lipid molecules to remain fixed along the orthogonal normal direction of the membrane surface and to retain their fixed lengths. These assumptions are in accordance with the kinematic assumptions underpinning the Kirchhoff-Love theory of elastic shells, in which material filaments initially normal to the shell midsurface remain straight and normal after deformation and the thickness of the shell does not change [66]. The Helfrich model can therefore not accommodate for tilting and distension of the lipid molecules, even for situations in which tilt and distension would be energetically optimal. Models based on the Cosserat theory of shells have been applied to include lipid tilt and distension, which also reduce to the Helfrich model under application of the appropriate constraints [79].

Lipid biomembranes have been found to be modeled well by the Helfrich model for problems at scales much larger than membrane thickness such as a complete cell or vesicle [24, 12, 17, 91]. The formation of equilibrium shapes such as spheres, "dog-bones" with high aspect-ratio and the transitions between such forms are some examples [92, 23, 83]. The biconcave discoid shape of the human erythrocyte has received particular attention. Numerous membrane integral proteins and their various attachments to the internal cytoskeleton and the extracellular matrix have been found to regulate the amazing flexibility of the erythrocyte and prevent it from collapsing [47].

For problems at scales approaching membrane thickness, however, other effects such as membrane tilt and distension must be included as fields for a continuum theory to remain applicable [91]. Lipid molecule tilt and distension has been found to be a critical aspect of lipid bilayer fission [86, 87], fusion [69, 65], relaxation of stress due to membrane inclusion [33, 85, 70, 55] and endocytosis [9, 59, 80]. Theories incorporating lipid tilt and

distension have been proposed based on symmetry arguments [20, 56, 49, 81], and by deriving larger-scale areal energy integrals from smaller-scale molecular theories [5, 89, 42, 35, 37]. These approaches have not addressed the possibility of an independent tilt field for the top and bottom leaflets of the lipid bilayer.

The overview of previously completed research stated above constitutes a basis and motivation for the additions to the theory presented in this thesis. The next section summarizes this work.

1.3 Thesis summary

Parallel computational research into model protein/lipid biomembrane systems using a particle based molecular dynamics approach has supported the notion that lipid tilt and distension in the vicinity of an embedded protein affects bilayer mechanics [77, 43]. Inspired by this development from particle based methods and [77], we demonstrate a simple model involving lipid tilt and distension in Chapter 2 using the nonlinear solver package of the COMSOL Multiphysics software package. The derivation of equilibrium equations and linearization of the system is reviewed and then the nonlinear system is solved numerically and plotted for a square domain with numerous voids representing embedded proteins.

In Chapter 3, we discuss the mechanics of a lipid bilayer with a conforming cytoskeletal membrane in which the bilayer has the structure of a nematic liquid crystal and the cytoskeleton that of a simple elastic solid. Under certain conditions the cytoskeletal membrane mimics the effects of the so-called spontaneous curvature of the conventional theory of lipid membranes. The model is used to predict the classical biconcave discoid shape of red-blood cells in equilibrium. The equilibrium equations are then linearized in a Monge representation and solved and plotted for a simple state of stress using COMSOL Multiphysics.

Several competing two-dimensional models of the mechanical response of tilted lipid bilayers have been proposed in the biophysics literature. Following an idea due to Helfrich, in Chapter 4 we seek to settle this subject by deriving a two-dimensional model via asymptotic analysis of three-dimensional liquid crystal theory in which lipid length plays the role of the small parameter. Our model emerges as an example of Cosserat shell theory featuring independent sets of director fields for each of the two leaves constituting the bilayer. This appears to be the first model accommodating asymmetry in the tilt fields of the top and bottom halves of the bilayer.

Chapter 5 concludes the thesis with a review of the salient results and some suggestions for expanding on these results.

Chapter 2

Simple model including lipid tilt and distension[1]

2.1 Formulation of model

Although all biological lipid bilayer membranes share the same basic structure composed of two oppositely oriented leaflets of phospholipids enclosing their hydrophobic fatty acid tail groups, the combination of integral proteins diffusing within them varies greatly [22]. Some types of embedded proteins may be conical in shape or contain residues that interact with ionically with the hydrophilic/hydrophobic groups of the lipids composing the bilayer. These interactions are known to induce lipid tilt and distension [45, 58].

The conventional Helfrich theory of lipid bilayers constrains the lipid molecules to remain oriented along the bilayer midsurface normal direction and maintain constant length. This precludes the possibility of lipid tilting or distension in the presence of an interacting integral protein. To establish a simple model in which lipid tilt and distension is unconstrained, consider the following problem (Figure 2.1).

Far from the embedded protein, the lipid molecules are aligned with the planar midsurface normal $\boldsymbol{n} = \boldsymbol{k}$ (fixed) and are not distended. In the vicinity of the boundary between the bilayer and the integral protein, the lipid molecules become tilted and their length changes (distension) in order to shield the hydrophobic core. For simplicity, reflection symmetry of response to the embedded protein is assumed across the midsurface ω. In this case we can then model the tilt and distension as single field representing the orientation of the lipids in the top leaflet and reflect this to the bottom.

[1]The model described in this chapter emanates from a lecture given by Prof. D.J. Steigmann at UC Berkeley in September 2017 [77].

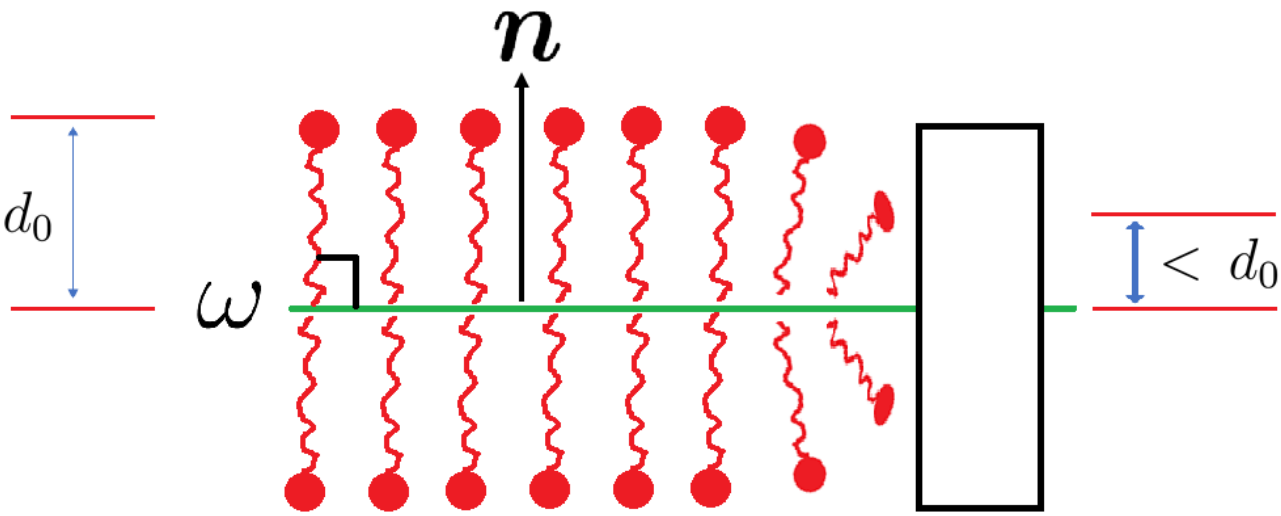

Figure 2.1: Lipid bilayer with an embedded protein. The black rectangle represents an integral protein with a hydrophobic patch. Far from the protein the lipids are of length d_0 and aligned along the normal $\boldsymbol{n}$ to the midsurface ω. In the vicinity of the protein the lipids are tilted and distended.

Define the vector field $\boldsymbol{\delta}$ aligned with the lipid molecules (Figure 2.1)

$$\boldsymbol{\delta} = \boldsymbol{\phi} + d\boldsymbol{k}, \tag{2.1}$$

where $\boldsymbol{\phi}$ is the in-plane projection of $\boldsymbol{\delta}$ onto ω and d is the projection of $\boldsymbol{\delta}$ along the normal direction.

The spatial gradient is then

$$\nabla\boldsymbol{\delta} = \nabla\boldsymbol{\phi} + \boldsymbol{k} \otimes \nabla\boldsymbol{d}. \tag{2.2}$$

We seek a strain energy function W with the functional dependence

$$W(\boldsymbol{n}, \boldsymbol{\delta}, \nabla\boldsymbol{\delta}) = W(\boldsymbol{\delta}, \nabla\boldsymbol{\delta}), \tag{2.3}$$

where dependence on $\boldsymbol{n}$ can be neglected as $\boldsymbol{n} = \boldsymbol{k}$ (a constant vector).

Propose a simple model for energy

$$W = \frac{1}{2}k|\nabla\boldsymbol{\delta}|^2 + G(\xi, d), \tag{2.4}$$

in which k is an elastic constant of the lipid molecules, $\xi = |\boldsymbol{\phi}|$, and $G(\xi, d)$ is an appropriate function of accounting for the energetic contribution of ξ and d. This ad hoc energy satisfies rotational invariance requirements such that

$$W^+ \quad = \quad W(\boldsymbol{Q}\boldsymbol{\delta}, \boldsymbol{Q}\nabla\boldsymbol{\delta}\boldsymbol{Q}^T) \quad = \quad W(\boldsymbol{\delta}, \nabla\boldsymbol{\delta}) \tag{2.5}$$

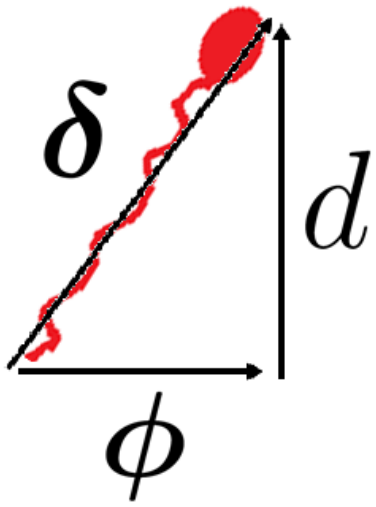

Figure 2.2: Schematic representation of lipid molecule director field $\boldsymbol{\delta}$. The field $\boldsymbol{\phi}$ is the projection of $\boldsymbol{\delta}$ onto the midsurface plane ω.

for all rotations $\boldsymbol{Q}$, and is not derived from the classical Frank energy for liquid crystals.

Expanding the strain energy function (2.4), we find

$$W = \frac{1}{2}k(\nabla\boldsymbol{\phi}\cdot\nabla\boldsymbol{\phi} + \nabla d\cdot\nabla d) + G(\xi, d). \tag{2.6}$$

Adopting a variational approach to derive equilibrium equations for the bilayer, we seek to minimize the variation of the total energy E such that

$$\dot{E} = 0, \tag{2.7}$$

in which E is the integral of the strain energy over the fixed bilayer midsurface plane ω,

$$E = \int_\omega W da. \tag{2.8}$$

Taking the variation of the integral is equivalent to integrating the variation of the integrand, so that

$$\dot{E} = \int_\omega \dot{W} da, \tag{2.9}$$

where

$$\dot{W} = \frac{\partial W}{\partial d}\dot{d} + \frac{\partial W}{\partial \boldsymbol{\phi}}\cdot\dot{\boldsymbol{\phi}} + \frac{\partial W}{\partial \nabla d}\cdot\nabla\dot{d} + \frac{\partial W}{\partial \nabla\boldsymbol{\phi}}\cdot\nabla\dot{\boldsymbol{\phi}}. \tag{2.10}$$

Noting that

$$\frac{\partial W}{\partial \nabla d}\cdot\nabla\dot{d} = \operatorname{div}\left[\left(\frac{\partial W}{\partial \nabla d}\right)^T\dot{d}\right] - \dot{d}\operatorname{div}\left(\frac{\partial W}{\partial \nabla d}\right), \tag{2.11}$$

and similarly for $\frac{\partial W}{\partial \nabla \boldsymbol{\phi}} \cdot \nabla \dot{\boldsymbol{\phi}}$, we can then apply the divergence theorem to rewrite $\dot{E} = 0$ as

$$\begin{aligned} 0 = \int_\omega \left[\frac{\partial W}{\partial d} - \operatorname{div}\left(\frac{\partial W}{\partial \nabla d}\right)\right] \dot{d} + \left[\frac{\partial W}{\partial \boldsymbol{\phi}} - \operatorname{div}\left(\frac{\partial W}{\partial \nabla \boldsymbol{\phi}}\right)\right] \dot{\boldsymbol{\phi}}\, da \\ + \int_{\partial\omega} \dot{d}\left(\frac{\partial W}{\partial \nabla d}\right) \cdot \boldsymbol{\nu} + \dot{\boldsymbol{\phi}} \cdot \left(\frac{\partial W}{\partial \nabla \boldsymbol{\phi}}\right) \boldsymbol{\nu}\, ds, \end{aligned} \tag{2.12}$$

where $\boldsymbol{\nu}$ is the unit normal vector field of the bilayer boundary $\partial\omega$. By exploiting the arbitrariness of the variations $\dot{d}$ and $\dot{\boldsymbol{\phi}}$ in (2.12), we find the resulting Euler equations are

$$\operatorname{div}\left(\frac{\partial W}{\partial \nabla \boldsymbol{\phi}}\right) = \frac{\partial W}{\partial \boldsymbol{\phi}}, \tag{2.13}$$

$$\operatorname{div}\left(\frac{\partial W}{\partial \nabla d}\right) = \frac{\partial W}{\partial d}, \tag{2.14}$$

on ω.

The boundary conditions can be assigned on $\partial\omega$ as either

$$d \quad \text{and} \quad \boldsymbol{\phi}, \tag{2.15}$$

or

$$\left(\frac{\partial W}{\partial \nabla d}\right) \cdot \boldsymbol{\nu} \quad \text{and} \quad \left(\frac{\partial W}{\partial \nabla \boldsymbol{\phi}}\right) \boldsymbol{\nu}. \tag{2.16}$$

For the form of W proposed above in (2.6), the equilibrium equations (2.13) and (2.14) then become

$$\frac{\partial W}{\partial \nabla \boldsymbol{\phi}} = k \nabla \boldsymbol{\phi}, \tag{2.17}$$

$$\frac{\partial W}{\partial \nabla d} = k \nabla d. \tag{2.18}$$

Next, solve for $\frac{\partial W}{\partial \boldsymbol{\phi}}$ by holding all variables fixed except $\boldsymbol{\phi}$ to obtain

$$\frac{\partial W}{\partial \boldsymbol{\phi}} \cdot \dot{\boldsymbol{\phi}} \quad = \quad G_\xi \dot{\xi} \quad = \quad \xi^{-1} G_\xi \boldsymbol{\phi} \cdot \dot{\boldsymbol{\phi}}, \tag{2.19}$$

which implies that

$$\frac{\partial W}{\partial \boldsymbol{\phi}} = \xi^{-1} G_\xi \boldsymbol{\phi}. \tag{2.20}$$

Noting that

$$\frac{\partial W}{\partial d} = G_d, \tag{2.21}$$

the equilbrium equations (2.17) and (2.18) can then be represented as

$$k \Delta \boldsymbol{\phi} = \xi^{-1} G_\xi \boldsymbol{\phi}, \tag{2.22}$$

$$k\Delta d = G_d, \tag{2.23}$$

where $\Delta(\cdot) = \text{div}[\nabla(\cdot)]$ is the two dimensional Laplacian on ω.

Propose a Hookean energy for G,

$$G(\xi, d) = \frac{1}{2}c(t - d_0)^2 + H(d), \tag{2.24}$$

where $t = \sqrt{d^2 + \xi^2}$, c is a material constant, and $H(d)$ is a term appended to penalize lipid collapse. This prevents t from vanishing, a highly unstable state in which the hydrophobic tail groups are exposed to the aqueous environment.

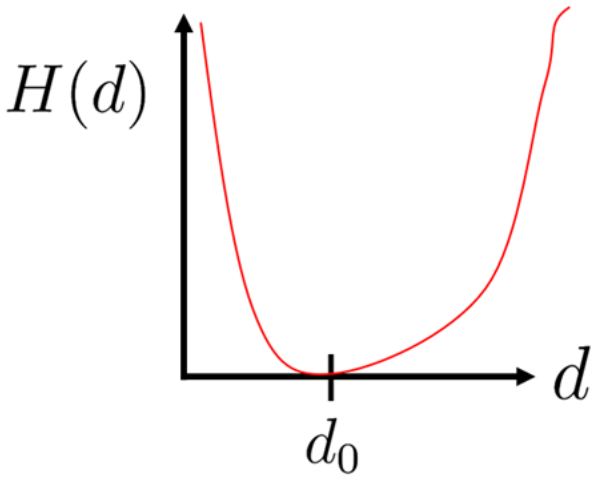

Figure 2.3: Plot of an example function for the penalizing term $H(d)$ vs. d.

$H(d)$ is defined such that (Figure 2.3)

$$H(d_0) = 0, \quad H'(d_0) = 0, \quad H''(d_0) > 0. \tag{2.25}$$

At this point the system is still nonlinear. Linearize the system about a base state trivially satisfying the nonlinear system, $(\xi, d) = (0, d_0) \Longrightarrow \boldsymbol{\phi}_0 = 0$.

$$\Rightarrow \quad \boldsymbol{\phi} \quad = \quad \boldsymbol{\phi}_0 + \dot{\boldsymbol{\phi}} \quad = \quad \dot{\boldsymbol{\phi}}, \tag{2.26}$$

$$\Rightarrow \quad d \quad = \quad d_0 + \dot{d}, \tag{2.27}$$

for small perturbations $\dot{\boldsymbol{\phi}}$ and $\dot{d}$.

Applying this linearization to the system defined by (2.22) and (2.23) yields

$$k\Delta\dot{\boldsymbol{\phi}} = (\xi^{-1}G_\xi)^{\cdot}\boldsymbol{\phi}_0 + (\xi^{-1}G_\xi)_0\dot{\boldsymbol{\phi}}, \tag{2.28}$$

$$k\Delta\dot{d} = (G_{dd})_0\dot{d} + (G_{d\xi})_0\dot{\xi}, \tag{2.29}$$

where $(\cdot)_0$ is the value of $(\cdot)$ at $\boldsymbol{\phi}_0 = \mathbf{0}$ and d_0.

For this choice of $G(\xi, d)$

$$(\xi^{-1} G_\xi)_0 = 0, \tag{2.30}$$

$$(G_{d\xi})_0 = 0, \tag{2.31}$$

$$(G_{dd})_0 = C + H''(d_0) > 0. \tag{2.32}$$

The resulting system then reduces to

$$\Delta \dot{\boldsymbol{\phi}} = \mathbf{0}, \tag{2.33}$$

$$\Delta \dot{d} = \kappa \dot{d}, \tag{2.34}$$

where $\kappa = k^{-1}(C + H''(d_0))$. Linearization of the system has thus decoupled $\boldsymbol{\phi}$ and d. Although it is now possible to solve this system analytically using modified Bessel functions and separation of variables in polar coordinates [77, 78], we seek numerical solutions to the nonlinear system in the next section.

2.2 Numerical solutions of nonlinear model

In order to generate representative plots of solutions to the nonlinear system contained within (2.22) and (2.23), we use the form of G proposed in (2.24), with $H(d)$ omitted as solutions were found to not include $d = 0$ for the domains and boundary conditions chosen. This system then takes the form

$$\Delta \boldsymbol{\phi} = c' \left(1 - \frac{d_0}{t}\right) \boldsymbol{\phi}, \tag{2.35}$$

$$\Delta d = c' \left(1 - \frac{d_0}{t}\right) d, \tag{2.36}$$

where $c' = \frac{c}{k}$ and has units of $\left[\frac{1}{\text{length}^2}\right]$

For demonstration purposes the constant c' is assigned a value of 1. The nonlinear partial differential equation solver of COMSOL Multiphysics v5.6 was then used to present representative plots of the solutions.

In Figure 2.4, a square domain with sides of length 100 nm containing an array of circular voids was solved representing a patch of a lipid bilayer containing numerous embedded proteins. The sides of the domain were assigned the boundary conditions $\boldsymbol{\phi} = \mathbf{0}$ nm and $d = 1$ nm. The boundaries representing the circular embedded proteins were assigned $\boldsymbol{\phi} = \{\text{abs}(\sin(5x))\boldsymbol{e}_x + \text{abs}(\sin(5y))\boldsymbol{e}_y\}$ nm and $d = 0.5$ nm. The resulting magnitude of the vector $\boldsymbol{\delta}$ representing the director field along the length of individual lipid molecules is

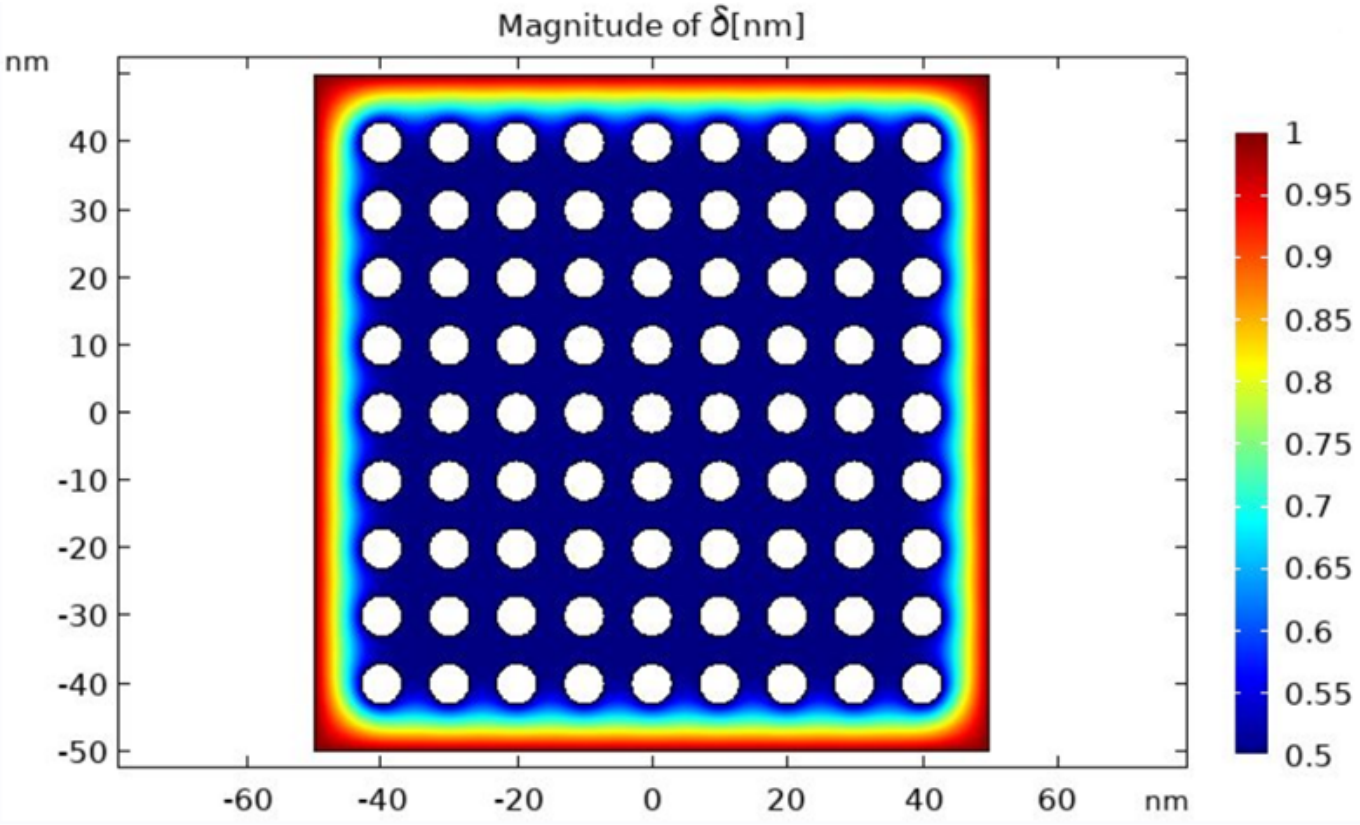

Figure 2.4: Plot of patch with numerous voids representing embedded proteins.

plotted, and varies little except in the vicinity of the square sides. Figure 2.5 is a plot of $|\phi|$ for the same data set and problem as Figure 2.4. The tilt field varies within the domain due to the location dependence of the void boundary conditions. This demonstrates a departure from models excluding lipid tilt.

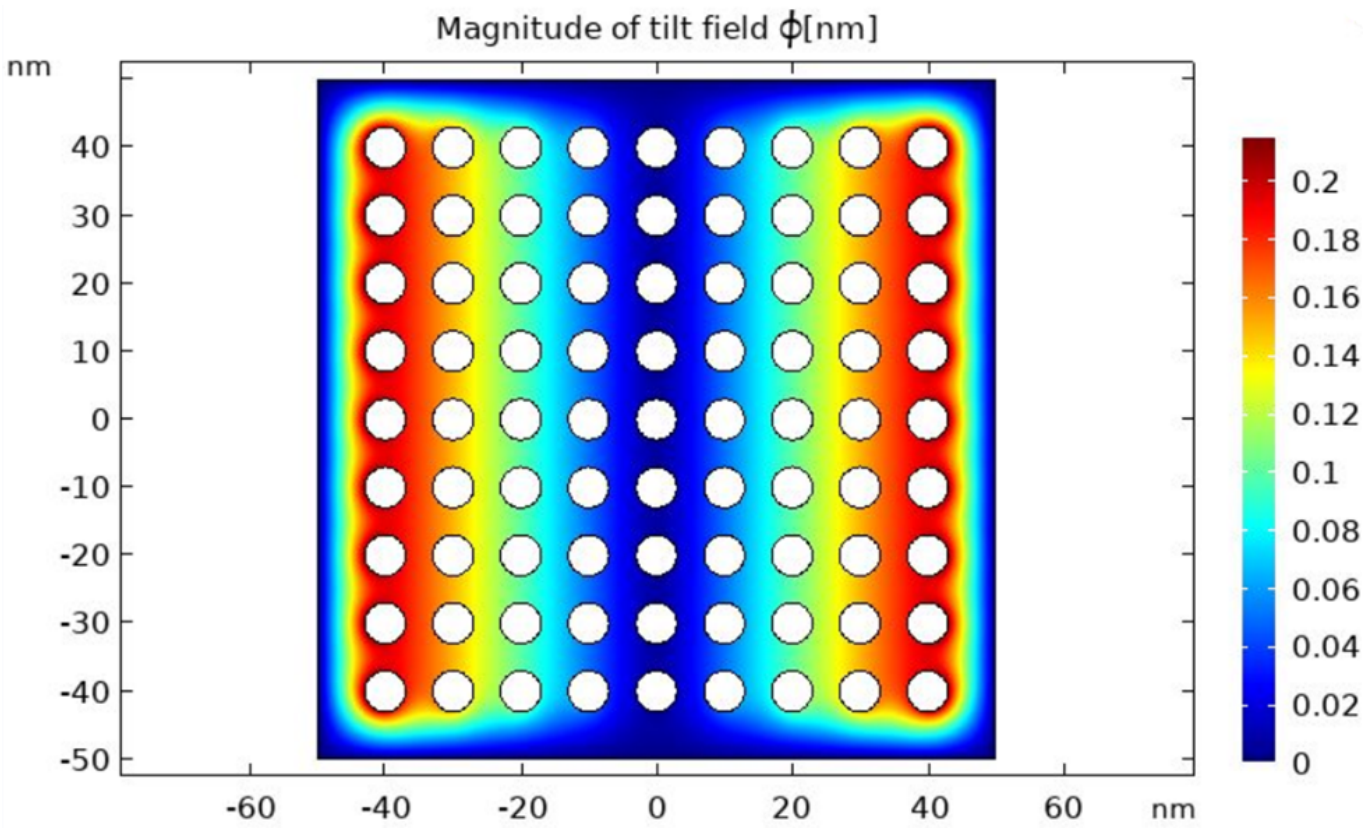

Figure 2.5: Plot of $|\phi|$ for patch with numerous voids representing embedded proteins. Same conditions as in Figure 2.4.

Chapter 3

Lipid bilayer with conforming cytoskeletal membrane [1]

3.1 Introduction

In this chapter we outline a model of the elastic response of a lipid bilayer with a conforming cytoskeletal membrane. This is intended for application to the mechanics of red-blood cells, which are known to consist of bilayers with subsurface cytoskeletal membranes formed by spectrin filaments. These membrane-associated cytoskeletons are thought to be arranged in networks that exhibit 6-fold hexagonal symmetry (Figure 3.1) [60, 10, 84, 32]. This model was recently supported by experimental evidence applying advances in super-resolution fluorescence microscopy (Figure 3.2). This technique was used in [60] to confirm a hexagonal cytoskeleton ultra-structure of triangular linkages of spectrin filaments with actin-based junctional complexes.

The basic framework of our model is similar to that underpinning Krishnaswamy's pioneering work [30] in which material points of the bilayer and cytoskeleton are assumed to be tethered by a so-called connector field while occupying distinct surfaces. The role of this connector is to maintain contact between the bilayer and cytoskeleton as they deform. In that work the bilayer is regarded as a fluid shell, as in Jenkins' model [29], and the cytoskeleton is considered to be a perfectly flexible solid membrane. Current work on the mechanics of the cytoskeleton [62, 38] suggests that the extent to which it convects with the bilayer is largely unknown. In the present chapter we therefore take the conservative view that the role of Krishnaswamy's connector is confined to maintaining congruency of the cytoskeletal and bilayer surfaces while playing no significant further role in the mechanical response.

[1] This chapter has appeared in a recent research article [40].

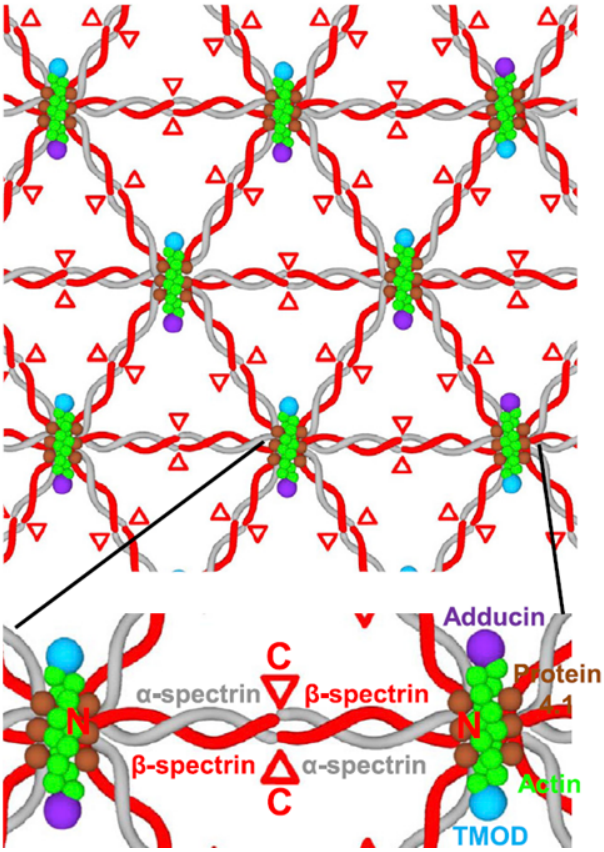

Figure 3.1: Theoretical model of human erythrocyte cytoskeleton ultra-structure consisting of hexagonal unit cells of spectrin filaments linked by actin-based junctional complexes [60], used with permission.

In Section 3.2, we develop the model of the bilayer/cytoskeleton system cia asymptotic expansion in which the bilayer is regarded as a thin nematic liquid crystal film and the cytoskeleton as a thin layer of a simple elastic solid. Certain vector fields arising in this procedure occur algebraically in the reduced model and are accordingly evaluated before proceeding further. This is explained in Section 3.3. In Section 3.4 we discuss material symmetry conditions for the cytoskeleton and bilayer. Some basic aspects of the differential geometry of surfaces [48, 13] are recalled in Section 3.5 and adapted there to the kinematics of congruent configurations of the bilayer and cytoskeleton. Equilibrium equations are deduced in Section 3.6 on the basis of a patchwise virtual-power postulate, and restrictions implied by the operative versions of the Legendre–Hadamard condition are discussed in Section 3.7. Section 3.8 demonstrates a derivation of a strain-energy function for the cytoskeleton which is such as to admit a surface having the shape of the characteristic biconcave discoid of a red-blood cell as an equilibrium state. We conclude, in Section 3.9, with a presentation of

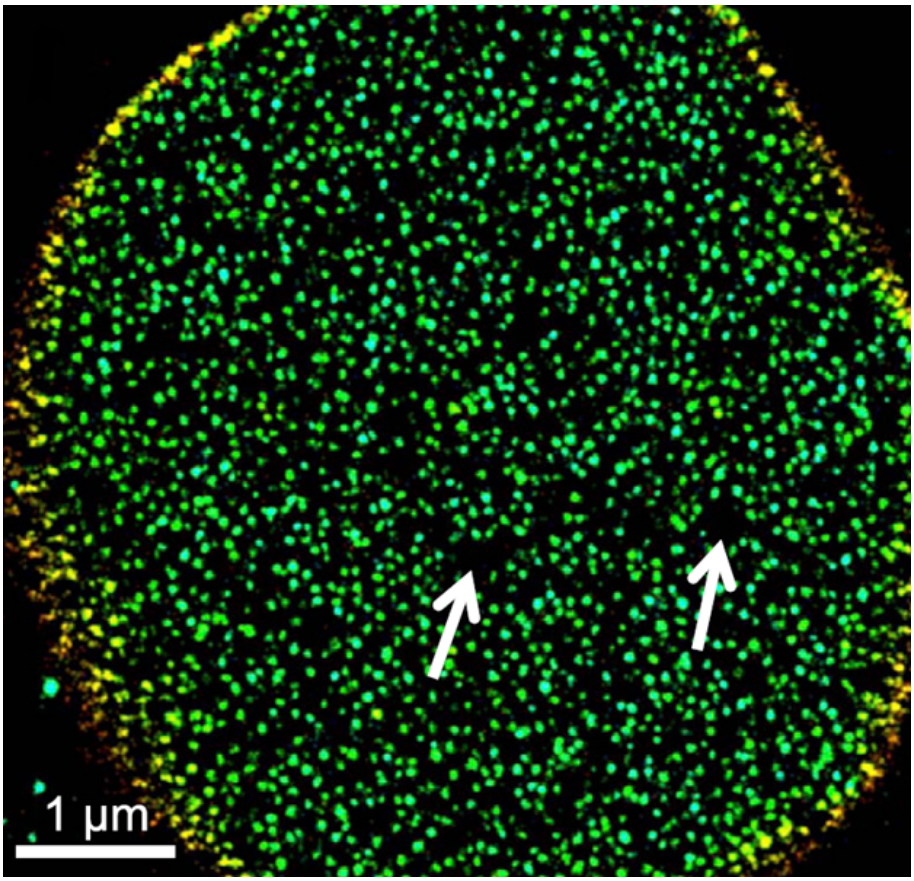

Figure 3.2: Image of human erythrocyte cytoskeleton ultra-structure obtained using super-resolution microscopy in [60] (used with permission). Statistical analysis of the image supports hexagonal arrangement model of spectrin and actin network. Arrows point to unexpected voids in the network.

numerical solutions of the shape equation for a lipid bilayer membrane with an attached cytoskeleton using COMSOL Multiphysics.

3.2 Leading-order asymptotic energy for small thickness

Consider a configuration of the bilayer-cytoskeletal combination in the shape of a prismatic cylinder generated by the parallel translation of a plane region Π forming the

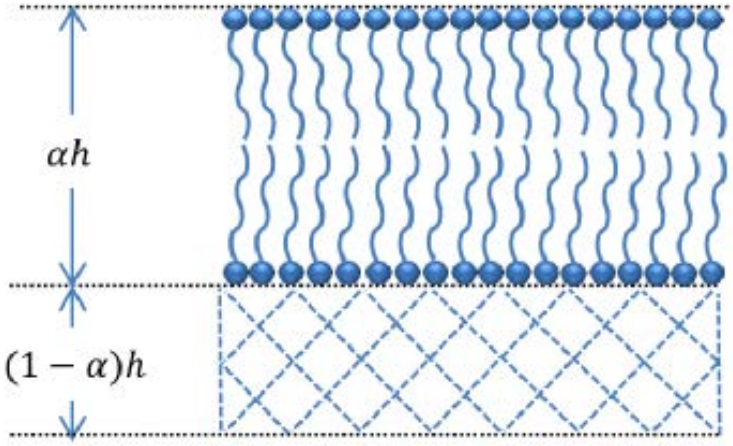

Figure 3.3: Small patch of lipid bilayer with a conforming cytoskeleton [40].

interface of the bilayer and cytoskeleton (Figure 3.3). The lipids of the bilayer are presumed to be straight, parallel and of uniform length in this configuration. The bilayer has thickness αh and the cytoskeleton $(1-\alpha)\,h$, where h is the thickness of the cylinder and $\alpha \in [0,1]$.

The energy of the cylinder is

$$\mathcal{E} = \int_{\Pi} \mathcal{U}\, dA, \tag{3.1}$$

where

$$\mathcal{U} = \int_0^{\alpha h} \mathcal{U}_b\, d\varsigma + \int_{-(1-\alpha)h}^{0} \mathcal{U}_c\, d\varsigma, \tag{3.2}$$

in which $\mathcal{U}_b$ and $\mathcal{U}_c$ respectively are the volumetric energy densities of the bilayer and cytoskeleton and ς is the through-thickness coordinate.

A central aspect of the model to be developed is that Π is assumed to convect as a material surface with respect to both the bilayer and the cytoskeleton deformations so as to maintain congruency; that is, the (possibly distinct) images of Π under the bilayer and cytoskeletal deformations are subsets of a single surface ω. We elaborate on the kinematical implications of this restriction below. Here we assume that ω can be covered completely by the images of such patches, each of which is assumed, for the sake of notational convenience, to be parametrized by a single coordinate chart.

We suppose the thickness h to be much smaller than any other length scale, l say, in a given problem. If the latter is used as the unit of length ($l = 1$), then the dimensionless thickness $h \ll 1$. Regarding $\mathcal{U}$ as a function of h, we combine Leibniz's rule with a Taylor expansion to derive

$$\mathcal{U} = hU + o\,(h)\,, \qquad \text{with} \qquad U = \alpha U_b + (1-\alpha)\,U_c, \tag{3.3}$$

in which $\mathcal{U}_b$ and $\mathcal{U}_c$ respectively are the values of $\mathcal{U}_b$ and $\mathcal{U}_c$ at $\varsigma = 0$; i.e., at their common interface Π. Accordingly,

$$\mathcal{E}/h = E + o(h)/h, \quad \text{where} \quad E = \int_\Pi U \, dA, \tag{3.4}$$

is the leading-order energy for small h.

Alternatively, in view of the fact that the thickness of the bilayer/cytoskeleton composite is on the order of molecular dimensions, it is appropriate to contemplate a direct theory based at the outset on the idea of a material surface without regard to thickness effects. However, the present asymptotic approach offers guidance as to the features that such a direct model should possess.

We assume the cytoskeleton to be a uniform elastic material with a strain energy given by

$$\mathcal{U}_c = \mathcal{W}_c(\tilde{\boldsymbol{F}}), \tag{3.5}$$

where $\tilde{\boldsymbol{F}}$ is the gradient of the cytoskeletal deformation $\hat{\chi}(\boldsymbol{x})$, with $\boldsymbol{x} \in \Pi \times [-(1-\alpha)h, 0]$, i.e., $\boldsymbol{x} = \boldsymbol{\xi} + \varsigma \boldsymbol{k}$, where $\boldsymbol{\xi}$ is the projection of $\boldsymbol{x}$ onto the plane region Π with unit normal $\boldsymbol{k}$ and $\varsigma \in [-(1-\alpha)h, 0]$. Thus, $\tilde{\boldsymbol{F}} = \hat{\boldsymbol{F}}(\boldsymbol{\xi}, \varsigma)$, where

$$\hat{\boldsymbol{F}} = \nabla \hat{\chi} + \hat{\boldsymbol{\chi}}' \otimes \boldsymbol{k}. \tag{3.6}$$

Here $(\cdot)' = \partial(\cdot)/\partial\varsigma$, $\nabla(\cdot)$ is the (two-dimensional) gradient with respect to $\boldsymbol{\xi}$, and $\hat{\chi}(\boldsymbol{\xi}, \varsigma) = \tilde{\chi}(\boldsymbol{\xi} + \varsigma \boldsymbol{k})$. Then,

$$U_c = \mathcal{W}_c(\tilde{\boldsymbol{F}}), \quad \text{where} \quad \boldsymbol{F} = \nabla \boldsymbol{r}_c + \boldsymbol{d} \otimes \boldsymbol{k}, \tag{3.7}$$

is the restriction to Π of the cytoskeletal deformation gradient, in which $\boldsymbol{r}_c(\boldsymbol{\xi}) = \hat{\chi}_{|\Pi}$ is the interfacial cytoskeletal deformation and $\boldsymbol{d}(\boldsymbol{\xi}) = \hat{\chi}'_{|\Pi}$ is the interfacial value of the normal derivative of the deformation.

Following Helfrich [24], we model the lipid bilayer as a liquid crystal with an energy density

$$\mathcal{U}_b = \mathcal{W}_b(\tilde{\boldsymbol{n}}, \tilde{\boldsymbol{D}}), \tag{3.8}$$

where $\tilde{\boldsymbol{n}}$ is a field of unit vectors specifying the local molecular orientation and $\tilde{\boldsymbol{D}} = \text{grad}\tilde{\boldsymbol{n}}$ is its (spatial) gradient. It is customary [88] to specify a constitutive function for the energy per unit current volume and to regard the liquid crystal as an incompressible medium. Accordingly $\mathcal{U}_b$ is also the energy per unit reference volume, as assumed in the foregoing. Then,

$$U_b = \mathcal{W}_b(\boldsymbol{n}, \boldsymbol{D}), \tag{3.9}$$

where $\boldsymbol{n}$ and $\boldsymbol{D}$ are the interfacial values of $\tilde{\boldsymbol{n}}$ and $\tilde{\boldsymbol{D}}$, respectively. Here, as in Helfrich's theory [24], we suppress lipid *tilt* and thus take $\boldsymbol{n}$ to be the unit-normal field to the image π_b of the interface Π in the current configuration of the lipid/cytoskeleton system. In these circumstances, we have

$$\boldsymbol{D} = \nabla_s \boldsymbol{n} + \boldsymbol{\eta} \otimes \boldsymbol{n}, \tag{3.10}$$

where $\nabla_s(\cdot)$ is the surficial gradient on π_b and $\boldsymbol{\eta}$ is the restriction to π_b of the derivative of $\tilde{\boldsymbol{n}}$ in the direction of $\tilde{\boldsymbol{n}}$. Because the latter is a field of unit vectors, we require $\boldsymbol{n}\cdot\boldsymbol{\eta}=0$ and conclude that $\boldsymbol{\eta}$ is a tangential vector field on π_b.

The Gauss and Weingarten equations of differential geometry furnish

$$\nabla_s\boldsymbol{n}=-\boldsymbol{b}, \tag{3.11}$$

where $\boldsymbol{b}$ is the symmetric curvature 2-tensor on the local tangent planes of π_b. We elaborate further in Section 3.5 below.

The energy density of the composite is thus given, in an abuse of notation, by the function

$$U(\nabla\boldsymbol{r}_c,\boldsymbol{b},\boldsymbol{d},\boldsymbol{n},\boldsymbol{\eta})=\alpha U_b(\boldsymbol{b},\boldsymbol{n},\boldsymbol{\eta})+(1-\alpha)U_c(\nabla\boldsymbol{r}_c,\boldsymbol{d}), \tag{3.12}$$

where

$$U_b(\boldsymbol{b},\boldsymbol{n},\boldsymbol{\eta})=\mathcal{W}_b(\boldsymbol{n},-b+\boldsymbol{\eta}\otimes\boldsymbol{n})\quad\text{and}\quad U_c(\nabla\boldsymbol{r}_c,\boldsymbol{d})=\mathcal{W}_c(\nabla\boldsymbol{r}_c+\boldsymbol{d}\otimes\boldsymbol{k}). \tag{3.13}$$

We observe that the dependence of the energy on the fields $\boldsymbol{d}$ and $\boldsymbol{\eta}$ is purely algebraic. This suggests a strategy, pursued in the next section, whereby we attempt to render the energy stationary with respect to these fields *a priori*.

3.3 Determination of $\boldsymbol{d}$ and $\boldsymbol{\eta}$

3.3.1 Cytoskeletal deformation

We decompose $\boldsymbol{d}$ into normal and tangential parts as

$$\boldsymbol{d}=d_n\boldsymbol{n}+(\nabla\boldsymbol{r}_c)\boldsymbol{e}, \tag{3.14}$$

where $d_n=\boldsymbol{d}\cdot\boldsymbol{n}$, e is a 2-vector on Π and $J_c\boldsymbol{n}=\boldsymbol{F}^*\boldsymbol{k}$, in which $\boldsymbol{F}^*$ is the cofactor of $\boldsymbol{F}$, and we note that $\nabla\boldsymbol{r}_c$ maps Π to the tangent plane of the image π_c of Π under the deformation at the material point in question. Here $J_c\,(=|\boldsymbol{F}^*\boldsymbol{k}|)$ and $\boldsymbol{n}$ respectively are the areal stretch of the interface due to the deformation of the cytoskeleton and the unit normal to π_c; these are determined by $\nabla\boldsymbol{r}_c$. We then have $\det\boldsymbol{F}=\boldsymbol{F}k\cdot\boldsymbol{F}^*\boldsymbol{k}=J_cd_n$ and thus require $d_n>0$.

The cytoskeletal energy is frame-invariant if and only if it depends on $\boldsymbol{F}$ via the Cauchy–Green tensor $\boldsymbol{C}=\boldsymbol{F}^T\boldsymbol{F}$; we write $\mathcal{W}_c(\boldsymbol{F})=F(\boldsymbol{C})$, where, from $(3.7)_2$ and (3.14),

$$\boldsymbol{C}=\boldsymbol{c}+\boldsymbol{\gamma}\otimes\boldsymbol{k}+\boldsymbol{k}\otimes\boldsymbol{\gamma}+(d_n^2+\boldsymbol{e}\cdot\boldsymbol{c}\boldsymbol{e})\boldsymbol{k}\otimes\boldsymbol{k}, \tag{3.15}$$

with

$$\boldsymbol{c}=(\nabla\boldsymbol{r}_c)^T(\nabla\boldsymbol{r}_c)\quad\text{and}\quad\boldsymbol{\gamma}=\boldsymbol{c}\boldsymbol{e}, \tag{3.16}$$

and we remark that

$$J_c^2=\det\boldsymbol{c}. \tag{3.17}$$

Let $G(\boldsymbol{e}) = F(\boldsymbol{C}(\boldsymbol{e}))$, where $\boldsymbol{C}(\boldsymbol{e})$ is the function obtained by fixing d_n and $\nabla \boldsymbol{r}_c$ in (3.15). We seek 2-vectors $\boldsymbol{e}$ that render G stationary. Consider materials that exhibit reflection symmetry with respect to the plane Π, i.e., $F(\boldsymbol{C}) = F(\boldsymbol{R}^T\boldsymbol{C}\boldsymbol{R})$ with $\boldsymbol{R} = \boldsymbol{I} - 2\boldsymbol{k}\otimes\boldsymbol{k}$, in which $\boldsymbol{I}$ is the three-dimensional identity. Thus,

$$\boldsymbol{R}^T\boldsymbol{C}\boldsymbol{R} = \boldsymbol{c} - \boldsymbol{\gamma}\otimes\boldsymbol{k} - \boldsymbol{k}\otimes\boldsymbol{\gamma} + (d_n^2 + \boldsymbol{e}\cdot\boldsymbol{c}\boldsymbol{e})\boldsymbol{k}\otimes\boldsymbol{k}, \tag{3.18}$$

and so reflection symmetry implies that G is an even function: $G(\boldsymbol{e}) = G(-\boldsymbol{e})$. It follows that there is a function S such that $G(\boldsymbol{e}) = S(\boldsymbol{E})$, where $\boldsymbol{E} = \boldsymbol{e}\otimes\boldsymbol{e}$. Sufficiency of this result is immediate. To establish necessity, we show that if $G(\boldsymbol{e}) = G(-\boldsymbol{e})$, then G is determined by $\boldsymbol{e}\otimes\boldsymbol{e}$, i.e., that $G(\boldsymbol{a}) = G(\boldsymbol{b})$ whenever $\boldsymbol{a}\otimes\boldsymbol{a} = \boldsymbol{b}\otimes\boldsymbol{b}$. The latter yields $a^2\boldsymbol{a} = (\boldsymbol{a}\cdot\boldsymbol{b})\boldsymbol{b}$ and $b^2\boldsymbol{b} = (\boldsymbol{a}\cdot\boldsymbol{b})\boldsymbol{a}$, where $a = |\boldsymbol{a}|$, etc. The combination of these gives $a = b$ and $a^2b^2 = (\boldsymbol{a}\cdot\boldsymbol{b})^2$. However, there is a $\theta\in\mathbb{R}$ such that $\boldsymbol{a}\cdot\boldsymbol{b} = ab\cos\theta$. Thus $\cos\theta = \pm 1$ and either of the two equations yields $\boldsymbol{b} = \pm\boldsymbol{a}$. The first alternative gives $G(\boldsymbol{a}) = G(\boldsymbol{b})$; the second yields $G(\boldsymbol{a}) = G(-\boldsymbol{b})$, so that if G is insensitive to the choice of sign, as assumed, then $G(\boldsymbol{a}) = G(\boldsymbol{b})$ whenever $\boldsymbol{a}\otimes\boldsymbol{a} = \boldsymbol{b}\otimes\boldsymbol{b}$.

Accordingly, $G_{\boldsymbol{e}} = 2(S_E)\boldsymbol{e}$ and the stationarity condition is satisfied if $\boldsymbol{e} = \boldsymbol{0}$; equation (3.15) then reduces to

$$\boldsymbol{C} = \boldsymbol{c} + d_n^2\boldsymbol{k}\otimes\boldsymbol{k}, \tag{3.19}$$

and the cytoskeletal energy is determined by $\boldsymbol{c}$ and d_n:

$$U_c = F(\boldsymbol{c} + d_n^2\boldsymbol{k}\otimes\boldsymbol{k}). \tag{3.20}$$

This is stationary with respect to $d_n(>0)$ if and only if

$$\boldsymbol{k}\cdot(F_C)\boldsymbol{k} = 0, \tag{3.21}$$

which fixes d_n in terms of $\boldsymbol{c}$.

As we are concerned with equilibria, it is appropriate to confine attention to deformations $\boldsymbol{F}$ that satisfy the strong-ellipticity condition; that is, to deformations satisfying

$$\boldsymbol{a}\otimes\boldsymbol{b}\cdot(\mathcal{W}_c)_{\boldsymbol{F}\boldsymbol{F}}[\boldsymbol{a}\otimes\boldsymbol{b}] > 0, \tag{3.22}$$

for all $\boldsymbol{a}\otimes\boldsymbol{b}\neq\boldsymbol{0}$. In these circumstances the stationarity conditions have unique solutions that minimize the energy absolutely [73].

3.3.2 The lipid bilayer

We model the lipid bilayer as a nematic liquid crystal described by Frank's energy (see [88], (3.63))

$$\mathcal{W}_b(\boldsymbol{n},\boldsymbol{D}) = k_1(\mathrm{tr}\boldsymbol{D})^2 + k_2(\boldsymbol{W}(\boldsymbol{n})\cdot\boldsymbol{D})^2 + k_3|\boldsymbol{D}n|^2 + (k_2+k_4)[\mathrm{tr}(\boldsymbol{D}^2) - (\mathrm{tr}\boldsymbol{D})^2], \tag{3.23}$$

where $k_1 - k_4$ are constants satisfying Ericksen's inequalities

$$2k_1 \geq k_2 + k_4, \quad k_2 \geq |k_4| \quad \text{and} \quad k_3 \geq 0, \tag{3.24}$$

in accordance with the assumed positive semidefiniteness of $\mathcal{W}_b(\boldsymbol{n}, \cdot)$, and $\boldsymbol{W}(\boldsymbol{n})$ is the skew tensor with axial vector $\boldsymbol{n}$, i.e., $\boldsymbol{W}(\boldsymbol{n})\boldsymbol{v} = \boldsymbol{n} \times \boldsymbol{v}$ for all $\boldsymbol{v}$. Then, with (3.10) and (3.11), we have

$$\boldsymbol{W}(\boldsymbol{n}) \cdot \boldsymbol{D} = \boldsymbol{\eta} \cdot \boldsymbol{W}(\boldsymbol{n})\boldsymbol{n} - \boldsymbol{W}(\boldsymbol{n}) \cdot \boldsymbol{b} = 0, \tag{3.25}$$

on account of the symmetry of $\boldsymbol{b}$.

Further,

$$\mathrm{tr}\boldsymbol{D} = -2H, \quad H = \frac{1}{2}\mathrm{tr}\boldsymbol{b}, \tag{3.26}$$

is the mean curvature of π_b: Combining

$$\boldsymbol{D}^2 = \boldsymbol{b}^2 - \boldsymbol{b}\boldsymbol{\eta} \otimes \boldsymbol{n}, \tag{3.27}$$

with the Cayley–Hamilton formula

$$\boldsymbol{b}^2 = 2H\boldsymbol{b} - K\boldsymbol{1} \quad \text{where} \quad K = \det\boldsymbol{b}, \tag{3.28}$$

is the Gaussian curvature of π_b and $\boldsymbol{1} = \boldsymbol{I} - \boldsymbol{n} \otimes \boldsymbol{n}$ is the (two-dimensional) identity on its local tangent plane, we arrive at

$$\mathrm{tr}(\boldsymbol{D}^2) = \mathrm{tr}(\boldsymbol{b}^2) = 4H^2 - 2K. \tag{3.29}$$

Lastly, $\boldsymbol{D}\boldsymbol{n} = \boldsymbol{\eta}$ so that, altogether,

$$\mathcal{W}_b(\boldsymbol{n}, \boldsymbol{D}) = kH^2 + \overline{k}K + k_3|\boldsymbol{\eta}|^2, \tag{3.30}$$

with

$$k = 4k_1 \quad \text{and} \quad \overline{k} = -2(k_2 + k_4). \tag{3.31}$$

For k_3 nonzero this is stationary with respect to $\boldsymbol{\eta}$ at $\boldsymbol{\eta} = \boldsymbol{0}$, and so we recover the classical Canham–Helfrich energy [24, 12]

$$U_b = kH^2 + \overline{k}K, \tag{3.32}$$

for lipid bilayers, which of course covers the possibility that k_3 vanishes. For $k_3 > 0$, it is clear that (3.32) furnishes the minimum of (3.30).

It is well known that the term in square brackets in (3.23) is a null Lagrangian in three-dimensional liquid-crystal theory [88]. This term is proportional to K, a null Lagrangian in the two-dimensional theory of lipid bilayers. Moreover, in this theory it is customary to model a possible asymmetry in bending response by introducing a variable C, the *spontaneous curvature*, via the modified energy [92]

$$U_b = k(H - C)^2 + \overline{k}K. \tag{3.33}$$

There are a number of physical effects that can give rise to a spontaneous curvature. Examples include diffusion of transmembrane proteins [1] and flexoelectricity [92]. One of our objectives in this work is to demonstrate that a conforming cytoskeletal membrane effectively mimics a spontaneous curvature under certain conditions.

With reference to (3.3) and (3.4), the net leading-order composite energy is

$$E = \int_{\Pi} \mathcal{W}\, dA, \tag{3.34}$$

where

$$W = W_b(H, K) + W_c(\boldsymbol{c}), \tag{3.35}$$

with

$$W_b(H, K) = \kappa H^2 + \overline{\kappa} K \quad \text{and} \quad W_c(\boldsymbol{c}) = (1-\alpha) F(\boldsymbol{c} + d_n^2(\boldsymbol{c})\, \boldsymbol{k} \otimes \boldsymbol{k}), \tag{3.36}$$

and with $\kappa = \alpha k$ and $\bar{\kappa} = \alpha \bar{k}$.

We adopt the conventional assumption [16] that deformations of the bilayer/cytoskeleton system conserve local surface area. This assumption is invoked for both the bilayer and cytoskeleton separately. For bilayers it is justified by bulk incompressibility in the parent theory of liquid crystals and by the suppression of lipid tilt. The presumed inextensibility of the lipids—expressed by the condition $|\boldsymbol{n}| = 1$—then implies areal incompressibility. For the cytoskeleton it is justified by empirical evidence [16] indicating that areal compressibility of the bilayer/cytoskeleton system is typically negligible; areal incompressibility, in the case of a convecting cytoskeleton, then follows from that of the bilayer. Here we impose areal incompressibility of the cytoskeleton whether or not it convects with the bilayer (for a discussion of this issue, see [30]). Accordingly, the referential areal energy density W is also the areal density in the current configuration of the system in the sense that

$$E = \int_{\pi_b} W_b\, da + \int_{\pi_c} W_c\, da, \tag{3.37}$$

where $\pi_b \subset \omega$ and $\pi_c \subset \omega$ respectively are the images of Π under the bilayer and cytoskeletal deformations.

3.4 Material symmetry

3.4.1 The cytoskeleton

Little if anything is known about the symmetry group for the cytoskeleton, regarded as a three-dimensional continuum. However, on the basis of work reported in [60] we assume that the *two-dimensional* response of the cytoskeletal membrane exhibits hexatropic symmetry relative to the plane configuration Π, characterized by mechanically equivalent unit vectors $\boldsymbol{i}_1$, $\boldsymbol{i}_2$ and $\boldsymbol{i}_3$ aligned with the filaments of the cytoskeleton (Figure 3.4).

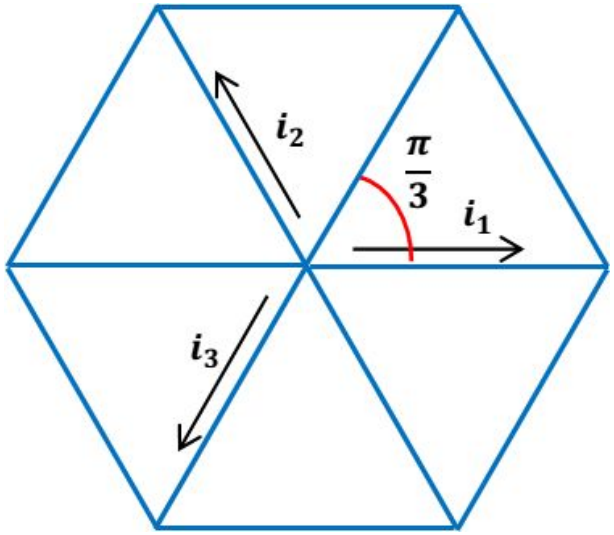

Figure 3.4: Hexagonal substructure of the cytoskeletal spectrin filament network [40].

Thus the function $W_c(\boldsymbol{c})$ is assumed to be such that [21]

$$W_c(\boldsymbol{c}) = W(\boldsymbol{R}^T\boldsymbol{c}\boldsymbol{R}), \tag{3.38}$$

for all two-dimensional orthogonal $\boldsymbol{R}$ belonging to the hexatropic symmetry group. This group is characterized in [61], where it is proved that the list $\{\mathrm{tr}\boldsymbol{c}, \mathrm{tr}(\boldsymbol{c}^2), \mathrm{tr}(\boldsymbol{h}_c\boldsymbol{c})\}$ is a function basis for hexatropic symmetry ([61], Table 1), with

$$\boldsymbol{h}_c = [(\boldsymbol{m}\cdot\boldsymbol{c})^2 - (\boldsymbol{m}'\cdot\boldsymbol{c})^2]\boldsymbol{m} - 2(\boldsymbol{m}\cdot\boldsymbol{c})(\boldsymbol{m}'\cdot\boldsymbol{c})\boldsymbol{m}', \tag{3.39}$$

in which the interposed dot is the inner product on the translation space Π' of Π, and

$$\boldsymbol{m} = \boldsymbol{e}_1\otimes\boldsymbol{e}_1 - \boldsymbol{e}_2\otimes\boldsymbol{e}_2, \quad \text{and} \quad \boldsymbol{m}' = \boldsymbol{e}_1\otimes\boldsymbol{e}_2 + \boldsymbol{e}_2\otimes\boldsymbol{e}_1, \tag{3.40}$$

with

$$\boldsymbol{e}_1 = \boldsymbol{i}_1 \quad \text{and} \quad \boldsymbol{e}_2 = (\boldsymbol{i}_2 - \boldsymbol{i}_3)/\sqrt{3}. \tag{3.41}$$

Alternatively, the Cayley–Hamilton formula yields the equivalent function basis $\{\mathrm{tr}\boldsymbol{c}, J_c, \mathrm{tr}(\boldsymbol{h}_c\boldsymbol{c})\}$ in which $J_c = 1$ by virtue of areal incompressibility. We suppress a possible explicit dependence of the strain energy on the material point $\boldsymbol{\xi} \in \Pi$ due to any nonuniformity of the material properties or of the orientation of the triad $\{\boldsymbol{i}_k\}$.

According to prevailing opinion [16, 7], the cytoskeletal membrane exhibits response that is characteristic of an isotropic material. This view must be qualified by the membrane-theoretic version of Noll's rule giving the symmetry group relative to any configuration when that relative to one of them is known, i.e., the membrane, if isotropic relative to one configuration, cannot be isotropic relative to all. Here, to avoid ambiguity, we interpret

prevailing opinion as implying isotropy relative to Π and thus do not include $\mathrm{tr}(\boldsymbol{h}_c\boldsymbol{c})$ among the arguments of the strain-energy function. Thus we assume

$$W_c(\boldsymbol{c}) = \overline{\omega}(I), \quad \text{where} \quad I = \mathrm{tr}\boldsymbol{c}, \tag{3.42}$$

for some function $\overline{\omega}(\cdot)$. Naturally, the symmetry group is thereby enlarged to the orthogonal group. However, hexatropy may be reconciled with isotropy if the strain $\boldsymbol{\epsilon}$, defined by $2\boldsymbol{\epsilon} = \boldsymbol{c} - \mathbf{1}_\Pi$, where $\mathbf{1}_\Pi$ is the identity on Π', is sufficiently small.

Hexatropy implies that the strain energy, expressed as a function of the strain, has as arguments the elements of the function basis $\{\mathrm{tr}\boldsymbol{\epsilon}, \mathrm{tr}(\boldsymbol{\epsilon}^2), \mathrm{tr}(\boldsymbol{h}_{\boldsymbol{\epsilon}}\boldsymbol{\epsilon})\}$, where $\boldsymbol{h}_{\boldsymbol{\epsilon}}$ is defined by (3.39) with $\boldsymbol{c}$ replaced by $\boldsymbol{\epsilon}$. This function basis is approximated at quadratic order in $\boldsymbol{\epsilon}$ by the basis $\{\mathrm{tr}\boldsymbol{\epsilon}, \mathrm{tr}(\boldsymbol{\epsilon}^2)\}$ for isotropy. Thus, the view expressed in the literature is consistent with the substructure of the cytoskeletal network if terms through quadratic order in $\boldsymbol{\epsilon}$ are retained in the strain-energy function. Indeed, quadratic-order energies figure prominently in Evans' and Skalak's extensive treatment [16] of cytoskeletal membranes in which isotropy is assumed at the outset.

3.4.2 The bilayer

The bilayer energy may also be interpreted in the framework of material symmetry. It is known, in the case of areal incompressibility [75, 93], that any function of the mean and Gaussian curvatures H and K may be expressed as a function, B say, of $\boldsymbol{c} = (\nabla\boldsymbol{r})^T(\nabla\boldsymbol{r})$ and the bending strain $\boldsymbol{\kappa} = (\nabla\boldsymbol{r})^T\boldsymbol{b}(\nabla\boldsymbol{r})$, where $\boldsymbol{r}(\boldsymbol{\xi})$ is the bilayer deformation, provided that

$$B(\boldsymbol{c}, \boldsymbol{\kappa}) = B(\boldsymbol{R}^T\boldsymbol{c}\boldsymbol{R}, \pm\boldsymbol{R}^T\boldsymbol{\kappa}\boldsymbol{R}), \tag{3.43}$$

for all two-dimensional unimodular $\boldsymbol{R}$ ($|\mathrm{det}\boldsymbol{R}| = 1$), with the sign chosen in accordance with that of $\mathrm{det}\boldsymbol{R}$. Here the minus sign is associated with the reflection symmetry of bilayers. This restriction has its origins in Murdoch's and Cohen's extension [6] of Noll's concept [51] of material symmetry to elastic surfaces, and comports with his use of the concept of material symmetry [52] in the interpretation of the constitutive response of liquid crystals.

3.5 Surface differential geometry

A configuration of the bilayer/cytosleletal system occupies a surface ω, which we parametrize as $\boldsymbol{r}(\theta^\alpha)$ in which θ^α, $\alpha = 1, 2$, are surface coordinates. The surface parametrization induces the tangent basis $\{\boldsymbol{a}_\alpha\}$, where $\boldsymbol{a}_\alpha = \boldsymbol{r}_{,\alpha}$; the (invertible) surface metric $a_{\alpha\beta} = \boldsymbol{a}_\alpha \cdot \boldsymbol{a}_\beta$; the dual metric $a^{\alpha\beta}$, where $(a^{\alpha\beta}) = (a_{\alpha\beta})^{-1}$; and the dual tangent basis $\{\boldsymbol{a}^\alpha\}$, with $\boldsymbol{a}^\alpha = a^{\alpha\beta}\boldsymbol{a}_\beta$. The orientation of ω is specified by the unit-normal field $\boldsymbol{n}$ defined by $\varepsilon_{\alpha\beta}\boldsymbol{n} = \boldsymbol{a}_\alpha \times \boldsymbol{a}_\beta$, where $\varepsilon_{\alpha\beta} = \sqrt{a}e_{\alpha\beta}$, with $a = \det(a_{\alpha\beta})$, is the Levi–Civita alternating tensor and $e_{\alpha\beta}$ the permutation symbol ($e_{12} = -e_{21} = 1$, $e_{11} = e_{22} = 0$).

Central to our development are the Gauss and Weingarten equations [13, 48]

$$\boldsymbol{r}_{;\alpha\beta} = b_{\alpha\beta}\boldsymbol{n} \quad \text{and} \quad \boldsymbol{n}_{,\alpha} = -b_{\alpha\beta}\boldsymbol{a}^{\beta}, \tag{3.44}$$

respectively, where

$$\boldsymbol{r}_{;\alpha\beta} = \boldsymbol{r}_{,\alpha\beta} - \Gamma^{\lambda}_{\alpha\beta}\boldsymbol{r}_{,\lambda}, \tag{3.45}$$

is the (symmetric) second covariant derivative of the surface position field. Here $\Gamma^{\lambda}_{\alpha\beta}$ are the Levi–Civita connection coefficients and $b_{\alpha\beta}$ are the coefficients of the second fundamental form on ω; these are symmetric with respect to interchange of the subscripts, and the latter induce the curvature tensor

$$\boldsymbol{b} = b_{\alpha\beta}\boldsymbol{a}^{\alpha} \otimes \boldsymbol{a}^{\beta}. \tag{3.46}$$

The surfacial gradient of the field $\boldsymbol{n}$ is $\nabla_s \boldsymbol{n} = \boldsymbol{n}_{,\alpha} \otimes \boldsymbol{a}^{\alpha}$, in accordance with (3.11) and $(3.44)_2$. Here the connection coefficients are simply the Christoffel symbols and the connection is therefore metric compatible, i.e., the covariant derivatives of the metric components vanish.

The mean and Gaussian curvatures of ω are (see $(3.26)_2$ and $(3.28)_2$)

$$H = \frac{1}{2}a^{\alpha\beta}b_{\alpha\beta} \quad \textit{and} \quad K = \frac{1}{2}\varepsilon^{\alpha\beta}\varepsilon^{\lambda\mu}b_{\alpha\lambda}b_{\beta\mu}, \tag{3.47}$$

respectively, where $\varepsilon^{\alpha\beta} = e^{\alpha\beta}/\sqrt{a}$, with $e^{\alpha\beta} = e_{\alpha\beta}$, is the contravariant alternator, and we note the relation

$$b^{\beta}_{\mu}\tilde{b}^{\mu\alpha} = Ka^{\beta\alpha}, \tag{3.48}$$

where $b^{\beta}_{\mu} = a^{\beta\alpha}b_{\alpha\mu}$ and

$$\tilde{b}^{\alpha\beta} = \varepsilon^{\alpha\lambda}\varepsilon^{\beta\mu}b_{\lambda\mu}, \tag{3.49}$$

is the cofactor of the curvature, expressible as

$$\tilde{b}^{\alpha\beta} = 2Ha^{\alpha\beta} - b^{\alpha\beta}, \tag{3.50}$$

this following on use of the identity

$$\varepsilon^{\alpha\lambda}\varepsilon^{\beta\mu} = a^{\alpha\beta}a^{\lambda\mu} - a^{\alpha\mu}a^{\beta\lambda}. \tag{3.51}$$

The Mainardi–Codazzi equations of surface theory are $b_{\lambda\mu;\beta} = b_{\lambda\beta;\mu}$ [13], or, more concisely, $\varepsilon^{\beta\mu}b_{\lambda\mu;\beta} = 0$. The metric compatibility of the connection implies that the covariant derivatives of $\varepsilon^{\alpha\lambda}$ vanish and the Mainardi–Codazzi equations are therefore equivalent to

$$\tilde{b}^{\alpha\beta}_{;\beta} = 0. \tag{3.52}$$

3.5.1 Convected coordinates and surface-fixed coordinates

The literature on lipid bilayers relies exclusively on the use of surface-fixed coordinates in the analysis of the so-called *shape equation* (see [92] for example). This formalism is entirely analogous to the spatial description of continuum mechanics in which problems are posed on a suitably parametrized fixed region of space. However, as in the latter setting, while this description often affords advantages in the solution of problems, it is a conceptual obstacle to the formulation of theories concerning material bodies. For the latter, convected coordinates that label material points furnish the appropriate alternative.

We encounter precisely the same issue in the mechanics of material surfaces, and thus pause to outline the distinction between parametrizations based on surfacefixed coordinates—analogous to the spatial coordinates of conventional continuum mechanics—and those based on convected coordinates. The relevant developments are due to Scriven [71] and summarized in Chapter 10 of Aris' book [8]. We present the main ideas in the present subsection for the sake of completeness.

Consider configurations of a surface regarded as a material manifold parametrized by a convected coordinate system ξ^α. This may be identified with the system θ^α of the previous subsection at the value $\epsilon = 0$, say, of a time-like parameter ϵ in a one-parameter family of configurations. The associated surface Ω, with parametric representation $\hat{\boldsymbol{r}}(\xi^\alpha)$, is fixed and may serve as a reference surface in a referential description of the motion. That is, we regard these coordinates as being convected in the sense that they identify, via a map $\boldsymbol{r} = \hat{\boldsymbol{r}}(\xi^\alpha, \epsilon)$, the position, associated with parameter value ϵ, of a material point occupying position $\hat{\boldsymbol{r}}(\xi^\alpha) \in \Omega$ at $\epsilon = 0$. This notion may be generalized by regarding Ω as a surface that is in one-to-one correspondence with that occupied at $\epsilon = 0$, so that it need not actually be occupied in the course of the deformation. The connection with the θ^α-parametrization of ω is provided by

$$\hat{\boldsymbol{r}}\left(\xi^\alpha, \epsilon\right) = \boldsymbol{r}\left(\theta^\alpha\left(\xi^\alpha, \epsilon\right), \epsilon\right). \tag{3.53}$$

Thus we specify the fixed surface coordinates θ^α as functions ξ^α of ϵ and subject to $\theta^\alpha\left(\xi^\alpha, 0\right) = \xi^\alpha$. We assume the relations giving θ^α in terms of ξ^α to be invertible, to reflect the notion that at fixed ϵ the coordinates θ^α can be associated with a unique material point (identified by fixed values of ξ^α). Any function, $f\left(\theta^\alpha, \epsilon\right)$, say, may then be expressed in terms of convected coordinates as $\hat{f}\left(\xi^\alpha, \epsilon\right)$, where

$$\hat{f}\left(\xi^\alpha, \epsilon\right) = f\left(\theta^\alpha\left(\xi^\alpha, \epsilon\right), \epsilon\right). \tag{3.54}$$

The variational derivative of f is its partial derivative with respect to ϵ in the convected-coordinate representation, i.e., $\dot{f} = \partial \hat{f}\left(\xi^\alpha, \epsilon\right)/\partial\epsilon$, whereas its derivative in the fixed-coordinate parametrization is $f_\epsilon = \partial f\left(\theta^\alpha, \epsilon\right)/\partial\epsilon$; these are related by $\dot{f} = f_\epsilon + \left(\theta^\alpha\right)^{\cdot} f_{,\alpha}$.

The ϵ-velocity of a material point Ω on that has been convected by the deformation to ω is $\boldsymbol{u} = \dot{\boldsymbol{r}} = \partial\hat{\boldsymbol{r}}$. We may write this in terms of components on the natural basis induced by the fixed-coordinate θ^α-parametrization:

$$\boldsymbol{u} = u^\alpha \boldsymbol{a}_\alpha + w\boldsymbol{n}. \tag{3.55}$$

This is related to the derivative $\boldsymbol{r}_\epsilon$ by

$$\boldsymbol{u} = (\theta^\alpha)^{\cdot}\, \boldsymbol{a}_\alpha + \boldsymbol{r}_\epsilon. \tag{3.56}$$

Following [8, 71] we adopt the fixed-coordinate parametrization defined by

$$\frac{d}{d\epsilon}\theta^\alpha = u^\alpha\left(\theta^\beta, \epsilon\right), \quad \theta^\alpha_{|\epsilon=0} = \xi^\alpha, \tag{3.57}$$

where the derivative is evaluated at fixed $\{\xi^\alpha\}$ and hence equal to $(\theta^\alpha)^{\cdot}$. The normal virtual velocity in (55) is then given by

$$w\boldsymbol{n} = \boldsymbol{r}_\epsilon, \tag{3.58}$$

and the convected and fixed-coordinate derivatives satisfy

$$\dot{f} = f_\epsilon + u^\alpha f_{,\alpha}. \tag{3.59}$$

We require the Lie derivative of the metric with respect to the velocity. This is simply the variational derivative $\dot{a}_{\alpha\beta}$ expressed in terms of the θ^α-parametrization. To this end we adopt convected coordinates ξ^α whose values coincide with θ^α at $\epsilon = 0$. The two sets of coordinate systems will of course differ at different values of ϵ due to the fact that material is moving with respect to the θ^α-system. Said differently, the material point located at the place with surface coordinates at $\epsilon = 0$ will have different locations at different values of and hence be associated with different values of θ^α, whereas the values of ξ^α remain invariant. Accordingly, while it is always permissible to identify ξ^α with θ^α at $\epsilon = 0$, say, it is not possible to do so over an interval of ϵ values. However, for our purposes this limitation is not restrictive. Using $\dot{a}_{\lambda\mu} = \dot{\boldsymbol{a}}_\lambda \cdot \boldsymbol{a}_\mu + \dot{\boldsymbol{a}}_\mu \cdot \boldsymbol{a}_\lambda$ and

$$\dot{\boldsymbol{a}}_\lambda = \left(\frac{\partial \boldsymbol{r}}{\partial \theta^\lambda}\right)^{\cdot} = \left[\frac{\partial \boldsymbol{r}}{\partial \xi^\mu}\left(\frac{\partial \xi^\mu}{\partial \theta^\lambda}\right)\right]^{\cdot} = \frac{\partial \boldsymbol{u}}{\partial \xi^\mu}\left(\frac{\partial \xi^\mu}{\partial \theta^\lambda}\right) + \frac{\partial \boldsymbol{r}}{\partial \xi^\mu}\left(\frac{\partial^2 \xi^\mu}{\partial \theta^\lambda \partial \theta^\alpha}\right) u^\alpha, \tag{3.60}$$

together with $\partial\xi^\mu/\partial\theta^\lambda = \delta^\mu_\lambda$ (the Kronecker delta) and hence $\partial^2\xi^\mu/\partial\theta^\lambda\partial\theta^\alpha = 0$ at $\epsilon = 0$, we derive $\dot{\boldsymbol{a}}_\alpha = \partial\boldsymbol{u}/\partial\xi^\alpha$ and

$$\dot{a}_{\lambda\mu} = \boldsymbol{u}_{,\lambda} \cdot \boldsymbol{a}_\mu + \boldsymbol{a}_\lambda \cdot \boldsymbol{u}_{,\mu}, \tag{3.61}$$

where $\boldsymbol{u}_{,\lambda} = \partial\boldsymbol{u}/\partial\theta^\lambda$ at $\epsilon = 0$.

Combining (3.55) with the Gauss and Weingarten equations yields

$$\boldsymbol{u}_{,\lambda} = \left(u_{\alpha;\lambda} - w b_{\alpha\lambda}\right)\boldsymbol{a}^\alpha + \left(u^\alpha b_{\alpha\lambda} + w_{,\lambda}\right)\boldsymbol{n}, \tag{3.62}$$

where $\boldsymbol{a}^\alpha = a^{\alpha\beta}\boldsymbol{a}_\beta$ and $u_{\alpha;\lambda}$ is the covariant derivative defined by

$$u_{\alpha;\lambda} = u_{\alpha,\lambda} - u_\beta \Gamma^\beta_{\alpha\lambda}, \tag{3.63}$$

in which $\Gamma^\beta_{\alpha\lambda}$ are the connection symbols on ω pertaining to the induced metric in the θ^α-system. Hence the desired expression:

$$\dot{a}_{\lambda\mu} = u_{\mu;\lambda} + u_{\lambda;\mu} - 2w b_{\lambda\mu}. \tag{3.64}$$

For example, if $A_{\alpha\beta}$ is the (fixed) metric on the surface Ω induced by the parametrization $\hat{\boldsymbol{r}}(\xi^\alpha)$, then the areal stretch induced by the deformation is $J = \sqrt{a/A}$, where $A = \det(A_{\alpha\beta})$ The fact that the cofactor of $a_{\alpha\beta}$ is $(a)a^{\alpha\beta}$ then implies

$$\dot{J}/J = \frac{1}{2}\alpha^{\alpha\beta}\dot{a}_{\alpha\beta}, \tag{3.65}$$

and with (3.61) this may be reduced to

$$\dot{J}/J = \boldsymbol{a}^\alpha \cdot \boldsymbol{u}_{,\alpha}. \tag{3.66}$$

3.5.2 Congruent configurations of the bilayer and cytoskeleton

This formalism may be adapted to the bilayer/cytoskeleton system by introducing one-parameter families, $\hat{\boldsymbol{r}}_c(\xi^\alpha;\epsilon_c)$ and $\hat{\boldsymbol{r}}_b(\eta^\alpha;\epsilon_b)$ of cytoskeleton and bilayer deformations respectively, in which and are convected coordinates. The surface-fixed coordinates on the cytoskeleton and bilayer are $\theta^\alpha_{(c)}\left(\xi^\beta;\epsilon_c\right)$ and $\theta^\alpha_{(b)}\left(\eta^\beta;\epsilon_b\right)$, respectively. Congruency then implies that (see (3.53))

$$\hat{\boldsymbol{r}}_c(\xi^\alpha;\epsilon_c) = \boldsymbol{r}\left(\theta^\alpha_{(c)}\left(\xi^\beta;\epsilon_c\right),\epsilon_c\right) \quad \text{and} \quad \hat{\boldsymbol{r}}_b(\eta^\alpha;\epsilon_b) = \boldsymbol{r}\left(\theta^\alpha_{(b)}\left(\eta^\beta;\epsilon_b\right),\epsilon_b\right), \tag{3.67}$$

where $\boldsymbol{r}(\theta^\alpha,\epsilon)$ is the surface-fixed parametrization of ω.

We stipulate that $\xi^\alpha = \theta^\alpha_{(c)}\left(\xi^\beta;0\right)$ and $\eta^\alpha = \theta^\alpha_{(b)}\left(\eta^\beta;0\right)$; further, that $\theta^\alpha_{(c)}\left(\xi^\beta;0\right) = \theta^\alpha_{(b)}\left(\eta^\beta;0\right) = \theta^\alpha$, so that

$$\hat{\boldsymbol{r}}_b(\eta^\alpha;0) = \boldsymbol{r}(\theta^\alpha) = \hat{\boldsymbol{r}}_c(\xi^\alpha;0), \tag{3.68}$$

where, for the sake of brevity, we write $\boldsymbol{r}(\theta^\alpha)$ in place of $\boldsymbol{r}(\theta^\alpha,0)$. In this way we construct convected coordinates ξ^α and η^α that coincide, at $\epsilon_c,\epsilon_b = 0$, with specified surface-fixed coordinates θ^α on ω. This is tantamount to adopting the place $\boldsymbol{r}(\theta^\alpha)$ occupied by material points of the bilayer (at $\epsilon_b = 0$) and cytoskeleton (at $\epsilon_c = 0$) as their common reference position.

With reference to $(3.57)_1$ we define the tangential virtual velocities

$$u^\alpha = \frac{d}{d\epsilon_c}\theta^\alpha_{(c)|\epsilon_c=0} \quad \text{and} \quad v^\alpha = \frac{d}{d\epsilon_b}\theta^\alpha_{(b)|\epsilon_b=0}, \tag{3.69}$$

of the cytoskeleton and bilayer, respectively, and assume, in keeping with congruency, that the normal virtual velocities have a common value, w say:

$$\left.\frac{\partial \boldsymbol{r}}{\partial \epsilon_b}\right|_{\epsilon_b=0} = \left.\frac{\partial \boldsymbol{r}}{\partial \epsilon_c}\right|_{\epsilon_c=0} = w\boldsymbol{n}, \tag{3.70}$$

(see (3.58)). Then the virtual velocities of the bilayer and cytoskeleton are

$$\boldsymbol{u}(\theta^\alpha) = \dot{\boldsymbol{r}}_b = u^\alpha \boldsymbol{a}_\alpha + w\boldsymbol{n}, \tag{3.71}$$

and

$$\boldsymbol{v}\left(\theta^{\alpha}\right)=\dot{\boldsymbol{r}}_{c}=v^{\alpha}\boldsymbol{a}_{\alpha}+w\boldsymbol{n}, \tag{3.72}$$

respectively, where

$$\dot{\boldsymbol{r}}_{b}=\left.\frac{\partial\hat{\boldsymbol{r}}_{b}}{\partial\epsilon_{b}}\right|_{\epsilon_{b}=0}\quad and\quad \dot{\boldsymbol{r}}_{c}=\left.\frac{\partial\hat{\boldsymbol{r}}_{c}}{\partial\epsilon_{c}}\right|_{\epsilon_{c}=0}. \tag{3.73}$$

The identification of $\boldsymbol{n}\cdot u$ with $\boldsymbol{n}\cdot v$ also features in a model proposed in [38].

The formula (3.64) for the variation of the surface metric applies as it stands to the cytoskeleton if the superposed dot is interpreted as a derivative with respect to ϵ_c (evaluated at $\epsilon_c=0$). It also applies to the bilayer if the superposed dot is interpreted as a derivative with respect to ϵ_b (evaluated at $\epsilon_b=0$), with v_μ substituted in place of u_μ.

To interpret the cytoskeletal deformation tensor $\nabla\boldsymbol{r}_c$ (see $(3.7)_2$) in this framework, let the patch Π be parametrized in the form $\boldsymbol{\xi}(\xi^{\alpha})$. This parametrization induces the tangent basis $\boldsymbol{A}_{\alpha}=\boldsymbol{\xi}_{,\alpha}$, metric $A_{\alpha\beta}=\boldsymbol{A}_{\alpha}\cdot\boldsymbol{A}_{\beta}$, dual metric $A^{\alpha\beta}$, and dual basis $\boldsymbol{A}^{\alpha}$. Then,

$$\nabla\boldsymbol{r}_{c}=\boldsymbol{a}_{\alpha}\otimes\boldsymbol{A}^{\alpha}, \tag{3.74}$$

and the surfacial Cauchy–Green deformation tensor is

$$\boldsymbol{c}=a_{\alpha\beta}\boldsymbol{A}^{\alpha}\otimes\boldsymbol{A}^{\beta}. \tag{3.75}$$

The areal dilation induced by the deformation is

$$J_{c}=\sqrt{\det\boldsymbol{c}}=\sqrt{a/A}. \tag{3.76}$$

3.6 Energy, virtual power and equilibrium

3.6.1 Energy and power

To obtain equilibrium equations and edge conditions we invoke the virtual-power principle for the simply-connected patch Π. We account for areal incompressibility by extending the energy to unconstrained states and introducing appropriate Lagrange-multiplier fields. Reference may be made to Section 5.10 of [11], for example, for an exposition of this idea together with some of its applications to continuum mechanics. From (3.34)–(3.37), the extended energy of the patch is

$$E=\int_{\Pi}\left[J_{b}W_{b}+J_{c}W_{c}+\lambda_{b}\left(J_{b}-1\right)+\lambda_{c}\left(J_{c}-1\right)\right]dA+\int_{\partial\Pi}\tilde{\mu}\left(J_{b}-1\right)dS, \tag{3.77}$$

where $\lambda_{b,c}$ and $\tilde{\mu}$ are Lagrange multiplier fields. We have included a multiplier on the boundary because, as we show below, the tangential and normal derivatives of the virtual bilayer velocity $\boldsymbol{v}$, which figure in the expression for the variation of the energy, are constrained by

areal incompressibility. To our knowledge this effect has not been discussed in the literature on bilayers. However, similar terms are known to play a role in the mechanics of continua of second grade [26, 74, 90], — as exemplified by lipid bilayers — in the presence of constraints on the first-order gradients.

Having proposed an expression for the extended energy, we identify equilibria with those states that satisfy

$$\dot{E} = P, \tag{3.78}$$

where P is the virtual power imparted to the patch. The form that this power takes is deduced in the course of the ensuing development. Here the superposed dot refers to a Gateaux derivative with respect to either ϵ_c or ϵ_b (evaluated at ϵ_c and ϵ_b equal to zero) or to both simultaneously.

3.6.2 Tangential equilibrium of the cytoskeletal membrane.

For example, consider variations that preserve the bilayer configuration. These are $\boldsymbol{u}(\theta^\alpha) = u^\alpha \boldsymbol{a}_\alpha$ and $\boldsymbol{v} = 0$, and yield

$$\dot{E} = \int_{\pi_c} \left[\dot{W}_c + (W_c + \lambda_c)\, \dot{J}_c / J_c \right] da, \tag{3.79}$$

in which variation of λ_c has been suppressed as this merely returns the areal incompressibility constraint. In the extended (unconstrained) formalism, $J_c W_c$ is the cytoskeletal energy density on Π. Thus, in the case of isotropy, for example, we make the identification

$$J_c W_c = \bar{\omega}\,(I)\,, \quad \text{with} \quad I = a_{\lambda\mu} A^{\lambda\mu}, \tag{3.80}$$

which reduces to (3.42) when the constraint is in effect. This depends via (3.75) and (3.76) on the surfacial Cauchy–Green tensor $\boldsymbol{c}$ and thus evolves in response to variations $\dot{a}_{\alpha\beta}$ of the surface metric. Accordingly, we write

$$(J_c W_c)^{\cdot} = \frac{1}{2} J_c \Sigma^{\alpha\beta} \dot{a}_{\alpha\beta}, \quad \text{with} \quad \frac{1}{2} J_c \Sigma^{\alpha\beta} = (J_c W_c)_{\boldsymbol{c}} \cdot \boldsymbol{A}^\alpha \otimes \boldsymbol{A}^\beta, \tag{3.81}$$

which we combine with (3.65) to obtain

$$\dot{W}_c + (W_c + \lambda_c)\, \dot{J}_c / J_c = \frac{1}{2} \sigma^{\alpha\beta} \dot{a}_{\alpha\beta}, \quad \text{with} \quad \sigma^{\alpha\beta} = \Sigma^{\alpha\beta} + \lambda_c a^{\alpha\beta}. \tag{3.82}$$

We note that $\Sigma^{\alpha\beta} = \Sigma^{\beta\alpha}$, and thus $\sigma^{\alpha\beta} = \sigma^{\beta\alpha}$, by virtue of the symmetry of $(J_c W_c)_{\boldsymbol{c}}$. For example, in the case of isotropy, we have from (3.75) and (3.80) that $(J_c W_c)_{\boldsymbol{c}} = \bar{\omega}'\,(I)\, \mathbf{1}_\Pi$, yielding

$$J_c \Sigma^{\alpha\beta} = 2\bar{\omega}'\,(I)\, A^{\alpha\beta}. \tag{3.83}$$

Combining this symmetry with (3.64) (with $w = 0$) we derive $\frac{1}{2}\sigma^{\alpha\beta}\dot{a}_{\alpha\beta} = \sigma^{\alpha\beta}u_{\alpha;\beta}$ and then convert (3.79) via Stokes' theorem to

$$\dot{E} = \int_{\partial\pi_c} \sigma^{\alpha\beta}\nu_\beta u_\alpha \, ds - \int_{\pi_c} \sigma^{\alpha\beta}{}_{;\beta} u_\alpha \, da, \tag{3.84}$$

where $\nu_\beta = \varepsilon_{\alpha\beta}\tau^\alpha$, in which $\tau^\alpha = d\theta^\alpha/ds$ are the components of the rightward unit normal to $\partial\pi_c$ with arclength parametrization $\theta^\alpha(s)$; i.e., $\boldsymbol{\nu} = \boldsymbol{\tau} \times \boldsymbol{n}$, where $\boldsymbol{\tau} = d\boldsymbol{r}(\theta^\alpha(s))$ and $\boldsymbol{n}$ respectively are the unit tangent to $\partial\pi_c$ and the unit surface normal.

From (3.78) it follows that the virtual power is of the form

$$P = \int_{\partial\pi_c} t^\alpha_{(c)} u_\alpha \, ds + \int_{\pi_c} g^\alpha_{(c)} u_\alpha \, da, \tag{3.85}$$

and, with no further restrictions on u_α, that

$$\sigma^{\alpha\beta}{}_{;\beta} + g^\alpha_{(c)} = 0, \quad \text{in} \quad \pi_c \quad \text{and} \quad t^\alpha_{(c)} = \sigma^{\alpha\beta}\nu_\beta, \quad \text{on} \quad \partial\pi_c, \tag{3.86}$$

in which $g^\alpha_{(c)}$ and $t^\alpha_{(c)}$ respectively are the distributed tangential force (per unit area) and the tangential edge traction (force per unit length) acting on the cytoskeleton. From these relations it is clear that $\sigma^{\alpha\beta}$ plays the role of the cytoskeletal Cauchy stress. Equation $(3.82)_2$ then yields the interpretation of λ_c as a reactive surface tension. Here, to compensate for having suppressed variation with respect to the multiplier λ_c, it is necessary to impose $J_c = 1$ *a posteriori*. Thus, in the case of isotropy, we use $(3.82)_2$ in (3.86) with

$$\Sigma^{\alpha\beta} = 2\bar{\omega}'(I)\, A^{\alpha\beta}. \tag{3.87}$$

3.6.3 Variational derivative of the bilayer energy

We pause to discuss some formulae of a general nature valid for arbitrary bilayer virtual velocities v and subsequently specialize these to derive the tangential equilibrium equations.

First we note that because J_b and W_b depend on the surface position field through its first and second derivatives with respect to the coordinates, it follows that there are vector fields $\boldsymbol{N}^\alpha$ and $\boldsymbol{M}^\alpha$ such that

$$\dot{W}_b + (W_b + \lambda_b)\, \dot{J}_b/J_b = \boldsymbol{N}^\alpha \cdot \boldsymbol{v}_{,\alpha} + \boldsymbol{M}^{\alpha\beta} \cdot \boldsymbol{v}_{;\alpha\beta}, \tag{3.88}$$

where $\boldsymbol{v} = \dot{\boldsymbol{r}}_b$ is the virtual velocity and $\boldsymbol{v}_{;\alpha\beta} = \boldsymbol{v}_{,\alpha\beta} - \Gamma^\lambda_{\alpha\beta}\boldsymbol{v}_{,\lambda}$ is the second covariant derivative of $\boldsymbol{v}$. This is symmetric in the subscripts; therefore, no generality is lost by imposing $\boldsymbol{M}^{\alpha\beta} = \boldsymbol{M}^{\beta\alpha}$.

For example [2],

$$\dot{H} = \frac{1}{2}a^{\alpha\beta}\boldsymbol{n} \cdot \boldsymbol{v}_{;\alpha\beta} - b^{\alpha\beta}\boldsymbol{a}_\beta \cdot \boldsymbol{v}_{,\alpha} \quad \text{and} \quad \dot{K} = \tilde{b}^{\alpha\beta}\boldsymbol{n} \cdot \boldsymbol{v}_{;\alpha\beta} - 2K\boldsymbol{a}^\alpha \cdot \boldsymbol{v}_{,\alpha}, \tag{3.89}$$

whereas (see (3.66))

$$\dot{J}_b/J_b = \boldsymbol{a}^\alpha \cdot \boldsymbol{v}_{,\alpha}. \tag{3.90}$$

Using $\dot{W}_b = 2\kappa H\dot{H} + \bar{\kappa}\dot{K}$ (from $(3.36)_1$) we thus derive

$$\boldsymbol{N}^\mu = N^{\mu\beta}\boldsymbol{a}_\beta \quad \text{and} \quad \boldsymbol{M}^{\mu\beta} = M^{\mu\beta}\boldsymbol{n}, \tag{3.91}$$

with

$$N^{\mu\beta} = \left(\lambda_b + \kappa H^2 - \bar{\kappa}K\right) a^{\mu\beta} - 2\kappa H b^{\mu\beta} \quad \text{and} \quad \boldsymbol{M}^{\mu\beta} = \kappa H a^{\mu\beta} + \bar{\kappa}\tilde{b}^{\mu\beta}. \tag{3.92}$$

Proceeding, we have

$$\boldsymbol{N}^\alpha \cdot \boldsymbol{v}_{,\alpha} + \boldsymbol{M}^{\alpha\beta} \cdot \boldsymbol{v}_{;\alpha\beta} = \varphi^\alpha_{;\alpha} - \boldsymbol{v} \cdot \boldsymbol{T}^\alpha_{;\alpha}, \tag{3.93}$$

where

$$\boldsymbol{T}^\alpha = \boldsymbol{N}^\alpha - \boldsymbol{M}^{\alpha\beta}_{;\beta}, \tag{3.94}$$

with

$$\boldsymbol{M}^{\alpha\beta}_{;\beta} = \boldsymbol{M}^{\beta\alpha}_{;\beta}\boldsymbol{n} - \boldsymbol{M}^{\beta\alpha}b^\mu_\beta \boldsymbol{a}_\mu, \tag{3.95}$$

and

$$\varphi^\alpha = \boldsymbol{T}^\alpha \cdot \boldsymbol{v} + \boldsymbol{M}^{\alpha\beta} \cdot \boldsymbol{v}_{,\beta}, \tag{3.96}$$

in which (3.91), (3.94) and (3.95) together give

$$\boldsymbol{T}^\alpha = \left(N^{\alpha\mu} + M^{\alpha\beta}b^\mu_\beta\right)\boldsymbol{a}_\mu - \boldsymbol{M}^{\alpha\beta}_{;\beta}\boldsymbol{n}. \tag{3.97}$$

Combining (3.88) and (3.96) with Stokes' theorem furnishes

$$\int_{\pi_b} \left[\dot{W}_b + (W_b + \lambda_b)\,\dot{J}_b/J_b\right] da = \int_{\partial\pi_b} \varphi^\alpha v_\alpha \, ds - \int_{\pi_b} \boldsymbol{v} \cdot \boldsymbol{T}^\alpha_{;\alpha} \, da, \tag{3.98}$$

where $\boldsymbol{\nu} = \nu_\alpha \boldsymbol{a}^\alpha$ is the exterior unit normal $\partial\pi_b$ and

$$\boldsymbol{v} \cdot \boldsymbol{T}^\alpha_{;\alpha} = v_\mu \boldsymbol{a}^\mu \cdot \boldsymbol{T}^\alpha_{;\alpha} + w\boldsymbol{n} \cdot \boldsymbol{T}^\alpha_{;\alpha}, \tag{3.99}$$

with

$$\boldsymbol{a}^\mu \cdot \boldsymbol{T}^\alpha_{;\alpha} = \left(N^{\alpha\mu} + M^{\alpha\beta}b^\mu_\beta\right)_{;\alpha} + \boldsymbol{M}^{\alpha\beta}_{;\beta}b^\mu_\alpha, \tag{3.100}$$

and

$$\boldsymbol{n} \cdot \boldsymbol{T}^\alpha_{;\alpha} = \left(N^{\alpha\mu} + M^{\alpha\beta}b^\mu_\beta\right) b_{\mu\alpha} - \boldsymbol{M}^{\beta\alpha}_{;\beta\alpha}. \tag{3.101}$$

In the first term on the right-hand side of (3.98) we use the normal-tangential decomposition

$$\boldsymbol{v}_{,\beta} = \tau_\beta \boldsymbol{v}' + \nu_\beta \boldsymbol{v}_\nu, \tag{3.102}$$

where $\boldsymbol{\tau} = \tau_\alpha \boldsymbol{a}^\alpha = \boldsymbol{n} \times \boldsymbol{\nu}$, is the unit tangent to $\partial\pi_b$, $\boldsymbol{v}' = \tau^\alpha \boldsymbol{v}_{,\alpha} = d\boldsymbol{v}/ds$ is the tangential derivative of $\boldsymbol{v}$, and $\boldsymbol{v}_\nu = \nu^\alpha \boldsymbol{v}_{,\alpha}$ is the normal derivative. The term involving the tangential

derivative is integrated by parts. If $\partial\pi_b$ is piecewise smooth in the sense that its tangent $\boldsymbol{\tau}$ is piecewise continuous, with discontinuities at a finite number of corners, then

$$\int_{\partial\pi_b} \varphi^\alpha \nu_\alpha \, ds = \int_{\partial\pi_b} \left(\left\{ \boldsymbol{T}^\alpha \nu_\alpha - \left(\boldsymbol{M}^{\alpha\beta} \nu_\alpha \tau_\beta \right)' \right\} \cdot \boldsymbol{v} + \boldsymbol{M}^{\alpha\beta} \nu_\alpha \nu_\beta \cdot \boldsymbol{v}_\nu \right) ds - \sum \boldsymbol{M}^{\alpha\beta} \left[\nu_\alpha \tau_\beta \right]_i \cdot \boldsymbol{v}_i, \tag{3.103}$$

in which the square bracket refers to the forward jump as a corner of the boundary is traversed, and the sum ranges over all corners. Thus, $[\cdot] = (\cdot)_+ - (\cdot)_-$, where the subscripts $\pm$ respectively identify limits as a corner located at arclength station s is approached through larger and smaller values of arclength.

3.6.3.1 Tangential bilayer equilibrium

Consider variations with $\boldsymbol{v}$ and $\boldsymbol{v}_\nu$ vanishing on $\partial\pi_b$ (and at corners) that preserve the configuration of the cytoskeleton, i.e., $\boldsymbol{u} = \boldsymbol{0}$ and $\boldsymbol{v} = v_\mu \boldsymbol{a}^\mu$ in the interior of π_b. For these we have

$$\dot{E} = \int_{\pi_b} \left[\dot{W}_b + \left(W_b + \lambda_b \right) \dot{J}_b / J_b \right] da = - \int_{\pi_b} v_\mu \boldsymbol{a}^\mu \cdot \boldsymbol{T}^\alpha_{;\alpha} \, da, \tag{3.104}$$

in which variation of λ_b has been suppressed, and it follows, from (3.78), that the virtual power is of the form

$$P = \int_{\pi_b} g^\mu_{(b)} v_\mu \, da, \tag{3.105}$$

where $g^\mu_{(b)}$ is a tangential force (per unit area) acting on the bilayer. Because v_μ is unrestricted, we arrive at

$$\left(N^{\alpha\mu} + M^{\alpha\beta} b^\mu_\beta \right)_{;\alpha} + M^{\alpha\beta}_{;\beta} b^\mu_\alpha + g^\mu_{(b)} = 0, \quad \text{in} \quad \pi_b. \tag{3.106}$$

To reduce this we use (3.50), (3.52) and (3.92) to infer that

$$N^{\alpha\mu} + M^{\alpha\beta} b^\mu_\beta = \left(\lambda_b + \kappa H^2 \right) a^{\alpha\mu} - \kappa H b^{\alpha\mu}, \tag{3.107}$$

with divergence

$$\left(N^{\alpha\mu} + M^{\alpha\beta} b^\mu_\beta \right)_{;\alpha} = a^{\alpha\mu} \left(\lambda_b \right)_{,\alpha} + 2\kappa H a^{\alpha\mu} H_{,\alpha} - \kappa b^{\alpha\mu} H_{,\alpha} - \kappa H b^{\alpha\mu}_{;\alpha}, \tag{3.108}$$

and combination with (see $(3.92)_2$)

$$M^{\alpha\beta}_{;\beta} = \kappa a^{\alpha\beta} H_{,\beta}, \tag{3.109}$$

furnishes

$$\left(N^{\alpha\mu} + M^{\alpha\beta} b^\mu_\beta \right)_{;\alpha} + M^{\alpha\beta}_{;\beta} b^\mu_\alpha = a^{\alpha\mu} \left(\lambda_b \right)_{,\alpha} + \kappa H \left(2 a^{\alpha\mu} H_{,\alpha} - b^{\alpha\mu}_{;\alpha} \right), \tag{3.110}$$

in which the second parenthetical term on the right is $\left(2H a^{\mu\alpha} - b^{\mu\alpha} \right)_{;\alpha} = \tilde{b}^{\mu\alpha}{}_{;\alpha}$. Then, with (3.52), equation (3.110) reduces simply to

$$a^{\alpha\mu} \left(\lambda_b \right)_{,\alpha} + + g^\mu_{(b)} = 0. \tag{3.111}$$

3.6.3.2 Comoving bilayer and cytoskeleton

If the cytoskeleton is anchored to the bilayer such as to convect with it, then $\boldsymbol{u} = \boldsymbol{v}$ in $\pi^* = \pi_b \cap \pi_c$. Choosing variations such that $\boldsymbol{u}$, $\boldsymbol{v}$ and $\boldsymbol{v}_\nu$ vanish on $\partial\pi^*$ and $\boldsymbol{v} = v_\mu \boldsymbol{a}^\mu$ in π^*, with $\boldsymbol{u}$, $\boldsymbol{v}$ vanishing in $\omega \setminus \pi^*$, we obtain

$$\dot{E} = \int_{\pi^*} \left[\dot{W} + (W + \lambda)\, \dot{J}/J \right] da, \tag{3.112}$$

with $W = W_b + W_c$, $\lambda = \lambda_b + \lambda_c$ and $\dot{J}/J = v^\mu_{;\mu}$. We could proceed from this statement to derive the relevant balance equation directly, but it is more illuminating to combine (3.84) and (3.104) to arrive at

$$\dot{E} = -\int_{\pi^*} \left\{ \sigma^{\mu\alpha}_{;\alpha} + a^{\alpha\mu} \left(\lambda_b\right)_{,\alpha} \right\} v_\mu \, da. \tag{3.113}$$

The associated virtual power therefore has the form

$$P = \int_{\pi^*} g^\mu v_\mu \, da, \tag{3.114}$$

and with v_μ unrestricted, $(3.86)_1$ and (3.111) then deliver

$$g^\mu = g^\mu_{(b)} + g^\mu_{(c)}. \tag{3.115}$$

Equivalently,

$$\left(\Sigma^{\mu\alpha} + \lambda a^{\mu\alpha}\right)_{;\alpha} + g^\mu = 0, \tag{3.116}$$

in which the term in parentheses is the effective Cauchy stress for the bilayer/cytoskeleton composite subjected to a net tangential force g^μ.

3.6.4 Normal equilibrium of the bilayer and cytoskeleton

Having exhausted the consequences of the virtual-power statement for tangential variations, we proceed next to normal variations. In view of (3.71) and (3.72), these involve the bilayer and cytoskeleton together. Taking variations as in the previous subsection, now with $\boldsymbol{u} = \boldsymbol{v} = w\boldsymbol{n}$, with reference to (3.64), $(3.82)_1$ and (3.98) we obtain

$$\dot{E} = -\int_{\pi^*} w \left(\sigma^{\alpha\beta} b_{\alpha\beta} + \boldsymbol{n} \cdot \boldsymbol{T}^\alpha_{;\alpha} \right) da, \tag{3.117}$$

and conclude that the associated power has the form

$$P = \int_{\pi^*} pw \, da \tag{3.118}$$

where p is the net lateral pressure acting on the surface in the direction of $\boldsymbol{n}$. Thus, with (3.101) and with w unrestricted, we arrive at

$$\sigma^{\alpha\beta}b_{\alpha\beta} + \left(N^{\alpha\mu} + M^{\alpha\beta}b^{\mu}_{\beta}\right) b_{\mu\alpha} - \boldsymbol{M}^{\beta\alpha}_{;\beta\alpha} + p = 0, \quad \text{in} \quad \pi^*. \tag{3.119}$$

To reduce this we use (3.92), finding that

$$\left(N^{\alpha\mu} + M^{\alpha\beta}b^{\mu}_{\beta}\right) b_{\mu\alpha} = 2\lambda_b H + 2\kappa H^3 - \kappa H b^{\alpha\mu}b_{\mu\alpha}. \tag{3.120}$$

The final term on the right is $b^{\alpha\mu}b_{\mu\alpha} = \mathrm{tr}(\boldsymbol{b}^2)$, and with (3.29) and (3.109), equation (3.119) becomes

$$\kappa\left[\Delta H + 2H\left(H^2 - K\right)\right] - 2\lambda_b H = \sigma^{\alpha\beta}b_{\alpha\beta} + p, \tag{3.121}$$

where

$$\Delta H = a^{\alpha\beta}H_{;\alpha\beta} = \frac{1}{\sqrt{a}}\left(\sqrt{a}a^{\alpha\beta}H_{,\beta}\right)_{,\alpha} \tag{3.122}$$

is the surfacial Laplacian of H.

Equation (3.121) is the classical *shape equation* for lipid bilayers in which the right-hand side is the pressure transmitted to the bilayer [67, 29, 50]. Thus the cytoskeleton, if curved, transmits an effective pressure to the bilayer that persists when the net pressure p acting on the system vanishes. Vice versa, the bilayer transmits an equal but opposite pressure to the cytoskeleton.

We may rewrite (3.121) in the form

$$\kappa\left[\Delta H + 2H\left(H^2 - K\right)\right] = \left(\Sigma^{\alpha\beta} + \lambda a^{\mu\alpha}\right) b_{\alpha\beta} + p. \tag{3.123}$$

This is the appropriate equation to use if the cytoskeleton convects with the bilayer because the parenthetical term on the right is then subject to (3.116), and in this setting extends the system obtained in [26] for strain-free deformations in which the entire metric, and not just the local areal stretch, is constrained, with $T^{\alpha\beta} = \Sigma^{\alpha\beta} + \lambda a^{\mu\alpha}$, in which the $\Sigma^{\alpha\beta}$ are constitutively indeterminate, then serving as the operative Lagrange multipliers.

3.6.5 Edge conditions

Boundary conditions are of limited relevance in this subject because bilayers typically form closed surfaces. Nevertheless, in the present approach based on the notion of patchwise equilibrium, they deliver expressions for the various actions at the edge of a patch which are of independent interest. Further, a number of models that entail boundary interactions are available in the literature [2, 26, 64].

With the foregoing Euler equations satisfied on ω, the variation of the energy reduces, with the aid of (3.77), (3.84) and (3.98), to

$$\dot{E} = \int_{\partial\pi^*} \left(\sigma^{\alpha\beta}\nu_\beta u_\alpha + \varphi^\alpha \nu_\alpha + \mu \dot{J}_b/J_b\right) ds, \tag{3.124}$$

where $\mu ds = (\tilde{\mu} J_b) dS$ and φ^α is defined by (3.96).

We note, from (3.90) and (3.102), that the constraint $J_b = 1$ yields $\boldsymbol{\tau}\cdot\boldsymbol{v}' + \boldsymbol{v}\cdot\boldsymbol{v}_\mu = 0$, implying that the normal and tangential derivatives of $\boldsymbol{v}$ on $\partial\pi^*$ are not independent. Because $\boldsymbol{v}'$ is determined by $\boldsymbol{v}_{|\partial\pi^*}$, it follows that $\boldsymbol{v}$ and $\boldsymbol{v}_\nu$ cannot be specified independently. In the extended formulation, this restriction is relaxed and an associated Lagrange multiplier μ is introduced. Then, with (3.103) we obtain

$$\dot{E} = \int_{\partial\pi^*} \left\{ \sigma^{\alpha\beta}\nu_\beta u_\alpha + \left[\boldsymbol{T}^\alpha \nu_\alpha - \left(\boldsymbol{M}^{\alpha\beta}\nu_\alpha\tau_\beta + \mu\boldsymbol{\tau} \right)' \right] \cdot \boldsymbol{v} + \left(\boldsymbol{M}^{\alpha\beta}\nu_\alpha\nu_\beta + \mu\boldsymbol{\nu} \right) \cdot \boldsymbol{v}_\nu \right\} ds \\ - \sum \left[\boldsymbol{M}^{\alpha\beta}\nu_\alpha\tau_\beta + \mu\boldsymbol{\tau} \right]_i \cdot \boldsymbol{v}_i. \quad (3.125)$$

The virtual power is thus expressible in the form

$$P = \int_{\partial\pi^*} \left(\boldsymbol{t}_c \cdot \boldsymbol{u} + \boldsymbol{t}_b \cdot \boldsymbol{v} + \boldsymbol{\mu} \cdot \boldsymbol{v}_\nu \right) ds + \sum \boldsymbol{f}_i \cdot \boldsymbol{v}_i, \quad (3.126)$$

where $\boldsymbol{t}_c$, $\boldsymbol{t}_b$, and $\boldsymbol{f}_i$ respectively are the cytoskeletal and bilayer tractions and the double force and corner forces acting on the bilayer patch. Accordingly,

$$\begin{gathered} \boldsymbol{t}_c = \sigma^{\alpha\beta}\nu_\beta \boldsymbol{a}_\beta, \quad \boldsymbol{t}_b = \boldsymbol{T}^\alpha \nu_\alpha - \left(M^{\alpha\beta}\nu_\alpha\tau_\beta \boldsymbol{n} + \mu\boldsymbol{\tau} \right)', \\ \boldsymbol{\mu} = M\boldsymbol{n} + \mu\boldsymbol{\nu} \quad \text{and} \quad \boldsymbol{f}_i = -\left[M^{\alpha\beta}\nu_\alpha\tau_\beta \boldsymbol{n} + \mu\boldsymbol{\tau} \right]_i, \quad \text{with} \quad M = M^{\alpha\beta}\nu_\alpha\nu_\beta. \end{gathered} \quad (3.127)$$

The first of these is just the condition $(3.86)_2$ on $\partial\pi^*$.

The couple acting on the interior of $\partial\pi^*$ is

$$\boldsymbol{c} = \boldsymbol{r} \times \boldsymbol{t} + \boldsymbol{r}_\nu \times \boldsymbol{\mu}, \quad (3.128)$$

where $\boldsymbol{t} = \boldsymbol{t}_b + \boldsymbol{t}_c$ is the net traction and $\boldsymbol{r}_\nu = \nu^\alpha \boldsymbol{r}_{,\alpha} = \boldsymbol{\nu}$. Thus,

$$\boldsymbol{c} - \boldsymbol{r} \times \boldsymbol{t} = -M\boldsymbol{\tau}, \quad (3.129)$$

a pure bending couple acting at the edge that does not involve the multiplier μ. However, it is not appropriate to assign the couple in a boundary-value problem. Rather, information about μ is furnished by the specification of the double force [82].

If the bilayer and cytoskeleton are comoving, then $(3.127)_{3,4}$ remain in effect but $(3.127)_{1,2}$ are replaced by the single equation

$$\boldsymbol{t} = \left(\boldsymbol{T}^\alpha + \sigma^{\alpha\beta}\boldsymbol{a}_\beta \right) \nu_\alpha - \left(M^{\alpha\beta}\nu_\alpha\tau_\beta \boldsymbol{n} + \mu\boldsymbol{\tau} \right)'. \quad (3.130)$$

3.7 Legendre-Hadamard Conditions

If the cytoskeleton convects with the bilayer, then because the effective energy involves the spatial derivatives of a single deformation field through the second order, the operative Legendre–Hadamard necessary condition for energy minimizers entails perturbation of the latter only, at fixed values of the first derivatives [34]. Because the cytoskeletal energy involves only first derivatives, the operative Legendre–Hadamard condition then involves the bilayer energy alone. For the energy $(3.36)_1$, this yields the nonnegativity of the bending modulus k [3], as implied by $(3.24)_1$ and $(3.31)_1$.

If the cytoskeleton and bilayer are not comoving, then the membrane-theoretic version of the Legendre–Hadamard condition is applicable, and implies that, at an arbitrary material point p, say, the cytoskeletal energy, regarded as a function of $\nabla \boldsymbol{r}_c$, is locally convex with respect to perturbations of the form

$$\boldsymbol{u}_{,\alpha} = \boldsymbol{a} k_\alpha, \tag{3.131}$$

i.e.,

$$a^\mu k_\alpha = u^\mu_{;\alpha} - w b^\mu_\alpha \quad \text{and} \quad a k_\alpha = u^\mu b_{\mu\alpha} + w_{,\alpha}, \tag{3.132}$$

with $a^\mu = \boldsymbol{a} \cdot \boldsymbol{a}^\mu$ and $a = \boldsymbol{a} \cdot \boldsymbol{n}$, subject to $\boldsymbol{a}^\alpha \cdot \boldsymbol{a} k_\alpha = 0$ on account of areal incompressibility (see (3.66)). Thus, areal incompressibility imposes the restriction

$$a^{\alpha\beta} a_\beta k_\alpha = 0, \tag{3.133}$$

where $a_\beta = a_{\beta\mu} a^\mu$.

The operative Legendre–Hadamard condition is [76]

$$\boldsymbol{a} \cdot \left(\boldsymbol{E}^{\alpha\beta} k_\alpha k_\beta \right) \boldsymbol{a} \geq 0, \tag{3.134}$$

for arbitrary $\boldsymbol{a} k_\alpha$ subject to (3.133), where

$$\boldsymbol{E}^{\alpha\beta} = 2 \frac{\partial W}{\partial a_{\alpha\beta}} \boldsymbol{I} + 4 \frac{\partial^2 W}{\partial a_{\alpha\mu} \partial a_{\beta\lambda}} \boldsymbol{a}_\mu \otimes \boldsymbol{a}_\lambda, \tag{3.135}$$

in which $W(a_{\alpha\beta}) = W_c(a_{\mu\lambda} \boldsymbol{A}^\mu \otimes \boldsymbol{A}^\lambda)$. Then, with $(3.81)_1$, specialized to $J_c = 1$, we require

$$\Sigma^{\alpha\beta} k_\alpha k_\beta |\boldsymbol{a}|^2 + 4 \frac{\partial^2 W}{\partial a_{\alpha\mu} \partial a_{\beta\lambda}} a_\mu k_\alpha a_\lambda k_\beta \geq 0, \tag{3.136}$$

where $\Sigma^{\alpha\beta}$ is the constitutively determined part of the cytoskeletal Cauchy stress.

This condition yields a nontrivial restriction on W even if the bilayer remains undisturbed; i.e., if $w = 0$.

The choice $a = a\boldsymbol{n}$ ($a_\beta = 0$) conforms to (3.133) and reduces (3.136) to

$$\Sigma^{\alpha\beta} k_\alpha k_\beta \geq 0, \tag{3.137}$$

implying that the energetic part of the stress is positive semidefinite in energy minimizing states. In the absence of constraints, this implies, in accordance with a restriction proposed in [72], that the Cauchy stress is positive semidefinite.

For example, in the case of isotropy (see (3.87)), (3.137)) reduces to $\bar{\omega}'(I)\,|\boldsymbol{k}|^2 \geq 0$, where $|\boldsymbol{k}|^2 = A^{\alpha\beta}k_\alpha k_\beta$, and is thus satisfied if and only if

$$\bar{\omega}'(I) \geq 0, \tag{3.138}$$

whereas the full Legendre–Hadamard inequality (3.136), in the case of isotropy, is

$$\bar{\omega}'(I)\,|\boldsymbol{a}|^2|\boldsymbol{k}|^2 + 2\bar{\omega}''(I)\,(k^\alpha a_\alpha)^2 \geq 0, \tag{3.139}$$

with $k^\alpha = A^{\alpha\beta}k_\beta$.

3.8 Equivalent monolayers with spontaneous curvature

3.8.1 Equilibrium of monolayers

We expect the conforming cytoskeleton to confer asymmetry in the bending response of the bilayer/cytoskeleton composite, whereas that of an isolated bilayer is symmetric in the sense that the energy $(3.36)_1$ is the invariant under $\boldsymbol{b} \to -\boldsymbol{b}$. Asymmetric bending is also a feature of conventional monolayers, consisting of one sheet of oriented lipids instead of two of opposing orientation (Figure 3.3). Conventionally, this asymmetry is modelled by introducing a spontaneous curvature $C(\theta^\alpha)$ [92] via the energy

$$W(H, K; \theta^\alpha) = \kappa\,(H - C)^2 + \bar{\kappa}K. \tag{3.140}$$

The existence of these distinct models of asymmetric bending leads us to search for conditions under which they might be equivalent.

Proceeding as in Section 3.3, we derive (3.97) but with (3.92) replaced by

$$\begin{aligned} N^{\alpha\mu} = \left\{\lambda_m + \kappa\,(H - C)^2 - \bar{\kappa}K\right\} a^{\alpha\mu} - 2\kappa\,(H - C)\,b^{\alpha\mu}, \\ \text{and} \quad M^{\alpha\mu} = \kappa\,(H - C)\,a^{\alpha\mu} + \bar{\kappa}\tilde{b}^{\alpha\mu}, \end{aligned} \tag{3.141}$$

where λ_m is a Lagrange multiplier associated with the areal incompressibility of the monolayer. Then with some labor we find that (3.111) is replaced by

$$a^{\alpha\mu}\left[(\lambda_m)_{,\alpha} - 2\kappa\,(H - C)\,C_{,\alpha}\right] + g^\mu_{(m)} = 0, \tag{3.142}$$

where $g^\mu_{(m)}$ is a tangential distribution of force on the monolayer; and, in the absence of the cytoskeleton, that (3.121) is replaced by

$$\kappa\left[\Delta(H - C) + 2\,(H - C)\left(2H^2 - K\right) - 2H\,(H - C)^2\right] - 2\lambda_m H = p, \tag{3.143}$$

where p is the pressure exerted on the monolayer.

Evidently, (3.142) corresponds to (3.111) if $C_{,\alpha}$ vanishes, i.e., if the spontaneous curvature is uniform. In this case we have

$$\kappa\left[\Delta H + 2H\left(H^2 - K\right)\right] - 2\lambda_m H = p + 2\kappa C\left(CH - K\right), \tag{3.144}$$

which corresponds to (3.121), provided that $\lambda_m = \lambda_b$ and the cytoskeletal stress $\sigma^{\alpha\beta}$ satisfies

$$\sigma^{\alpha\beta} b_{\alpha\beta} = 2\kappa C\left(CH - K\right). \tag{3.145}$$

Equations (3.47) and (3.49) furnish $2H = a^{\alpha\beta} b_{\alpha\beta}$ and $2K = \tilde{b}^{\alpha\beta} b_{\alpha\beta}$ so a *sufficient condition* for such correspondence is

$$\sigma^{\alpha\beta} = \kappa C\left(C a^{\alpha\beta} - \tilde{b}^{\alpha\beta}\right), \tag{3.146}$$

provided that no tangential force is acting on the cytoskeleton. For, this expression for the stress is automatically divergence-free and $(3.86)_1$ requires that the tangential force vanish.

We observe, noting (3.123), that this same correspondence may be established between the monolayer and the comoving cytoskeleton if $\lambda_m = 0$ and if $\lambda_c = \lambda$ in $(3.82)_2$.

These correspondences must be qualified by the fact that the constitutive response of the cytoskeleton cannot be expected to yield (3.146) in general. Nevertheless, in the absence of tangential forces, the latter allows us to dispense with $(3.86)_1$ or (3.116), which would otherwise pose significant obstacles to analysis. Thus, we view (3.146) simply as a device for generating potential solutions by selecting from among a number of explicit solutions that are available for monolayers with constant spontaneous curvature [92]. Remarkably, these include the characteristic biconcave discoid shape of red-blood cells in equilibrium.

3.8.2 Biconcave discoid

Consider a surface of revolution described by

$$\boldsymbol{r}\left(\theta^\alpha\right) = r\boldsymbol{e}_r\left(\theta\right) + z\left(r\right)\boldsymbol{k}, \tag{3.147}$$

where $r(=\theta^1)$ is the radius from the symmetry axis directed along the fixed unit vector $\boldsymbol{k}$, $\theta(=\theta^1)$ is the azimuthal angle, and $\boldsymbol{e}_r(\theta)$ is a radial unit vector orthogonal to the axis of symmetry at azimuth θ. Let $\psi(\boldsymbol{r})$ be the angle defining the slope of a meridian: $\tan\psi = z'(r)$. Then with reference to Section 3.5, we compute

$$\boldsymbol{a}_1 = \boldsymbol{e}_r\left(\theta\right) + \tan\psi\boldsymbol{k}, \quad \boldsymbol{a}_2 = r\boldsymbol{e}_\theta\left(\theta\right), \tag{3.148}$$

where $\boldsymbol{e}_\theta = \boldsymbol{e}_r'(\theta)$; the metric and dual metric

$$\left(a_{\alpha\beta}\right) = \operatorname{diag}\left(\sec^2\psi, r^2\right), \quad \left(a^{\alpha\beta}\right) = \operatorname{diag}\left(\cos^2\psi, r^{-2}\right); \tag{3.149}$$

the curvature

$$(b_{\alpha\beta}) = \operatorname{diag}(\psi' \sec\psi, r\sin\psi); \tag{3.150}$$

the mean and Gaussian curvatures

$$2H = r^{-1}(r\sin\psi)' \quad \text{and} \quad K = r^{-1}\psi'\sin\psi\cos\psi; \tag{3.151}$$

and the curvature cofactor

$$\left(\tilde{b}^{\alpha\beta}\right) = \operatorname{diag}\left(r^{-1}\sin\psi\cos^2\psi, r^{-2}\psi'\cos\psi\right). \tag{3.152}$$

The Laplacian of the mean curvature, needed in (3.144), is (see (3.122))

$$\Delta H = r^{-1}\cos\psi\left[(r\cos\psi)H'\right]'. \tag{3.153}$$

Consider the particular surface of revolution described by

$$\sin\psi = r\left(d\ln r + b\right), \tag{3.154}$$

where b, d are constants. Following the procedure outlined in Section 3.3 of [92] and adjusting for differences in notation, with some effort it may be verified that (3.154) solves the shape equation (3.144) for a monolayer with a constant spontaneous curvature, provided that

$$\lambda_m = 0, \quad p = 0 \quad d = 2C, \tag{3.155}$$

and no tangential distributed force is acting.

In [92] this surface is described in terms of the dimensionless radius

$$x = r/\bar{r}, \quad \text{where} \quad \bar{r} = \exp\left(-b/d\right), \tag{3.156}$$

is such that $\sin\psi(\bar{r}) = 0$, which we use to recast (3.154) as

$$\sin\psi = \beta x\ln x, \quad \text{with} \quad \beta = 2C\bar{r}. \tag{3.157}$$

Following [92], we fix $\beta < 0$ with $|\beta| < 0$, corresponding to a negative spontaneous curvature. Evidently, $\sin\psi$ vanishes at $x = 0$ and $x = 1$ and is maximized at $x = e^{-1}$. Because $\sin\psi \leq 1$ the domain of the variable x is $[0, x_e]$, where

$$x_e\ln x_e = |\beta|^{-1}, \tag{3.158}$$

which yields a unique $x_e > 1$ [92]. This is the dimensionless equatorial radius, where $\sin\psi = -1$.

To obtain the shape of the surface we integrate $\tan\psi = \varsigma'(x)$, where $\varsigma(x) = z(r)/\bar{r}$. Thus,

$$\varsigma(x) = \int_{x_e}^{x} \frac{\beta t\ln t}{\sqrt{1-\beta^2t^2\left(\ln t\right)^2}}dt, \tag{3.159}$$

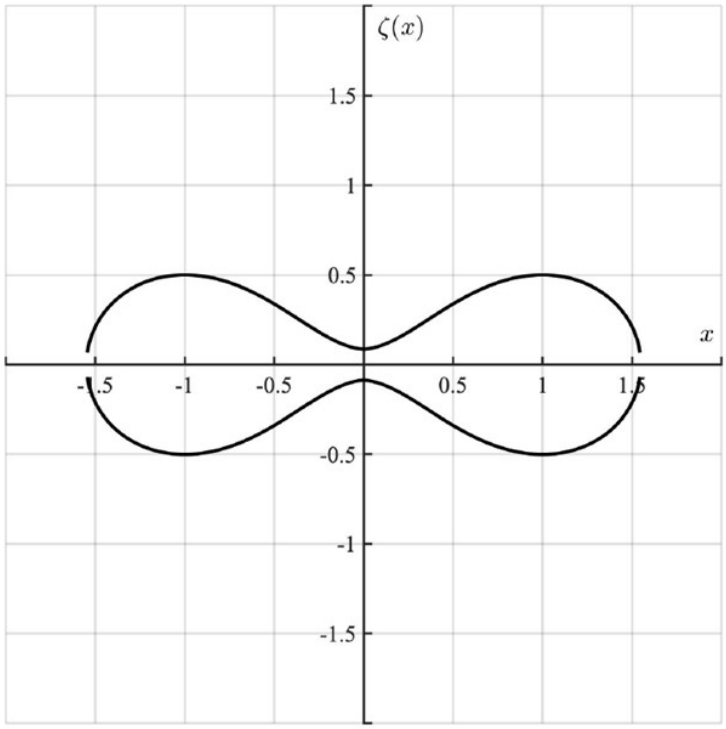

Figure 3.5: Biconcave discoid (β = -1.4721) [40].

in which we have chosen the positive root for the cosine and normalized to $\varsigma(x_e) = 0$. A numerical quadrature furnishes the upper half of a biconcave discoid, depicted in Figure 3.5. This is extended by rotational and reflection symmetry to the entire discoid.

Some insight into the mechanics of the system may be gained by computing the transverse shear traction S acting on a parallel of latitude. Assuming the component of the double force to vanish on a parallel, we find, from $(3.92)_2$ and $(3.127)_2$, that $S = \boldsymbol{n} \cdot \boldsymbol{T}^{\alpha} \nu_{\alpha}$, where

$$\boldsymbol{n} = \cos\psi \boldsymbol{k} - \sin\psi \boldsymbol{e}_r \quad \textit{and} \quad \boldsymbol{\nu} = \cos\psi \boldsymbol{e}_r + \sin\psi \boldsymbol{k}, \tag{3.160}$$

are the surface normal and the normal to a parallel, respectively. Then $(3.92)_2$ and (3.97) furnish $S = -M^{\alpha\beta}_{;\beta} \nu_{\alpha} = -\kappa \nu^{\alpha} H_{,\alpha}$, i.e.,

$$S = -\kappa \cos\psi H'(r), \tag{3.161}$$

which may be reduced, using (3.151), (3.154) and $(3.155)_3$, to

$$S = -2\kappa C r^{-1} \cos\psi. \tag{3.162}$$

This vanishes at the equator, where $\sin\psi = -\pi/2$, and therefore meets a necessary condition for reflection symmetry of the surface with respect to the equatorial plane. For, if

there were a nonzero shear traction transmitted by the material below the equator to that above, then equilibrium would require that it be balanced by an equal and opposite traction exerted by the part of the membrane above the equator on that below, and this would destroy reflection symmetry. However, the biconcave discoid is not free standing. There is a point force $F\boldsymbol{k}$ acting at the pole, where $\psi = 0$, given by

$$F = -2\pi \lim_{r\to 0} (rS) = 4\pi\kappa C, \tag{3.163}$$

which was overlooked in [92].

3.8.3 Mapping a plane cytoskeletal disc to a biconcave discoid

To adapt (3.154) to the bilayer/cytoskeleton composite, we must select a suitable configuration relative to which the constitutive framework (3.87) for an isotropic cytoskeleton, say, may be implemented. Because the literature is ambiguous concerning this issue, we consider a plane disc for the sake of illustration, and seek a strain-energy function which is such as to admit (3.154) as an equilibrium configuration in the absence of any distributed tangential forces acting on the bilayer or cytoskeleton.

We parametrize the disc by the position function $\boldsymbol{\xi}(\theta^\alpha) = \rho(r)\boldsymbol{e}_r(\theta)$ (see (6)). The induced tangent basis elements, $\boldsymbol{A}_\alpha = \boldsymbol{\xi}_{,\alpha}$, are

$$\boldsymbol{A}_1 = \rho'(r)\,\boldsymbol{e}_r(\theta) \quad \textit{and} \quad \boldsymbol{A}_2 = \rho(r)\,\boldsymbol{e}_\theta(\theta), \tag{3.164}$$

and the metric and dual metric are

$$(A_{\alpha\beta}) = \operatorname{diag}\left[(\rho')^2, \rho^2\right], \quad \left(A^{\alpha\beta}\right) = \operatorname{diag}\left[(\rho')^{-2}, \rho^{-2}\right]. \tag{3.165}$$

With $J_c = \sqrt{a/A}$, where $a = \det(a_{\alpha\beta})$ and $A = \det(A_{\alpha\beta})$, we obtain

$$J_c = r\sec\psi/(\rho\rho'), \tag{3.166}$$

and

$$I = a_{\alpha\beta}A^{\alpha\beta} = J_c^2(\rho/r)^2 + (r/\rho)^2. \tag{3.167}$$

Areal incompressibility then yields

$$I = (\rho/r) + (r/\rho)^2, \tag{3.168}$$

and furnishes a differential equation for $\rho(r)$:

$$\rho\rho' = r\sec\psi. \tag{3.169}$$

This integrates to

$$\left(\frac{X}{x}\right)^2 = \frac{2}{x^2}\int_0^x t\sec\psi(t)\,dt, \quad \text{where} \quad X = \rho/\bar{r}, \tag{3.170}$$

and we have imposed $X = 0$ at $x = 0$ (Figure 3.4).

The constitutive part of the stress is given by (3.87). We combine this with $(3.82)_2$, (3.87) and (3.146) to derive the system

$$\begin{aligned} \lambda_c \cos^2\psi + 2\bar{\omega}'(I)(\rho')^{-2} &= -\kappa C r^{-1}\sin\psi\cos^2\psi + \kappa C^2\cos^2\psi, \\ \lambda_c r^{-2} + 2\bar{\omega}'(I)\rho^{-2} &= -\kappa C r^{-2}\psi'\cos\psi + \kappa C^2 r^{-2}, \end{aligned} \tag{3.171}$$

which also applies in the case of a comoving cytoskeleton if the multiplier λ_c is replaced by λ. Eliminating this multiplier, we obtain

$$2\bar{\omega}'(I)\left[(\rho')^{-2} - (r/\rho)^2\cos^2\psi\right] = -\kappa C\cos^2\psi\left(r^{-1}\sin\psi - \psi'\cos\psi\right), \tag{3.172}$$

which may be simplified by using (3.166) to reduce the left-hand side. On the righthand side we use (3.154), finding that

$$r^{-1}\sin\psi - \psi'\cos\psi = -d. \tag{3.173}$$

Then, with (3.155) we have

$$\bar{\omega}'(I)\left[(\rho/r)^2 - (r/\rho)^2\right] = \kappa C^2, \tag{3.174}$$

where, from (3.168),

$$\left[(\rho/r)^2 - (r/\rho)^2\right]^2 = I^2 - 3. \tag{3.175}$$

With $\cos\psi \in (0,1]$ almost everywhere on the biconcave discoid (Figure 3.5), equation (3.169) implies that $\rho/r(= X/x) > 1$ almost everywhere (Figure 3.6). Then $(\rho/r)^2 - (r/\rho)^2 > 0$ and (3.174), (3.175) deliver

$$\bar{\omega}'(I) = \kappa C^2/\sqrt{I^2-4}, \tag{3.176}$$

which is meaningful if $I > 2$ (as required by (3.175)) and satisfies (3.138). Thus,

$$\bar{\omega}(I) = \kappa C^2 \ln\left[\frac{1}{2}\left(I + \sqrt{I^2-4}\right)\right], \tag{3.177}$$

normalized to $\bar{\omega}(2) = 0$.

We are not able to show that (3.176) satisfies the full Legendre–Hadamard inequality (3.139). However, as previously noted, the latter is not relevant if the cytoskeleton and bilayer are comoving.

3.9 Linearized shape equation in Monge parametrization

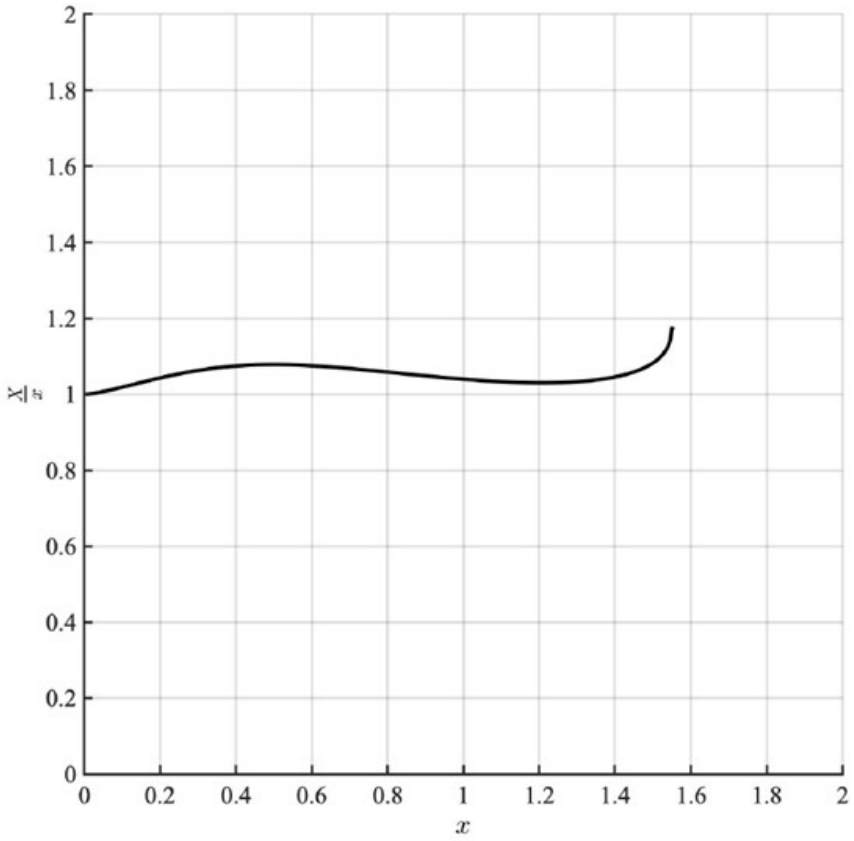

Figure 3.6: Map from the biconcave discoid to the plane disc (β = -1.4721) [40].

In this section we seek to demonstrate additional numerical solutions for the results above using the COMSOL Multiphysics nonlinear solver software. The procedure relies on a linearization of the shape equations for a lipid bilayer with a conforming hexatropic cytoskeleton using a Monge parametrization. The geometric quantities to be parametrized and then linearized in this way are contained within (3.123),

$$\kappa[\Delta H + 2H(H^2 - K)] = (\Sigma^{\alpha\beta} + \lambda a^{\alpha\beta})b_{\alpha\beta} + p, \tag{3.178}$$

where κ is a material constant, H is mean curvature, K is Guassian curvature, $\Sigma^{\alpha\beta}$ are stress components, $a^{\alpha\beta}$ is the dual metric, $b_{\alpha\beta}$ are the components of the curvature tensor, and p is a uniform pressure.

3.9.1 Monge parametrization

To this end, we follow [15, 2] by considering a Monge parametrization in which the membrane and attached cytoskeleton system is defined by its height $z(\boldsymbol{\theta})$ above a plane p, in which $\boldsymbol{\theta}$ denotes position on p. Then the position $\boldsymbol{r}(\theta^\alpha)$ of a particle on the membrane midsurface ω is given by

$$\boldsymbol{r}(\theta^\alpha) = \boldsymbol{\theta} + z(\boldsymbol{\theta})\boldsymbol{k}. \tag{3.179}$$

Let p be parametrized by a system of orthonormal coordinates θ^α with basis $\{\boldsymbol{e}_\alpha\}$ so that

$$\boldsymbol{\theta} = \theta^\alpha \boldsymbol{e}_\alpha, \tag{3.180}$$

which implies that ω is completely characterized by $z(\boldsymbol{\theta})$. Combining this with the definition $\boldsymbol{a}_\alpha = \boldsymbol{r}_{,\alpha}$, we find

$$\boldsymbol{a}_\alpha = \boldsymbol{e}_\alpha + z_{,\alpha}\boldsymbol{k}. \tag{3.181}$$

The components of the metric tensor $a_{\alpha\beta} = \boldsymbol{a}_\alpha \cdot \boldsymbol{a}_\beta$ on ω then reduce to

$$a_{\alpha\beta} = \delta_{\alpha\beta} + z_{,\alpha} z_{,\beta}, \tag{3.182}$$

which in turn reduces $\boldsymbol{n}(\theta^\alpha)$, defined above by $\varepsilon_{\alpha\beta}\boldsymbol{n} = \boldsymbol{a}_\alpha \times \boldsymbol{a}_\beta$, to

$$\boldsymbol{n} = (\boldsymbol{k} - \nabla_p z)\sqrt{a}, \tag{3.183}$$

where $\nabla_p z = z_{,\alpha}\boldsymbol{e}_\alpha$ is the gradient on plane p, and

$$a = \det(a_{\alpha\beta}) = 1 + |\nabla_p z|^2. \tag{3.184}$$

Proceeding with the consequences of parametrization, we note that

$$b_{\alpha\beta} = z_{,\alpha\beta}/\sqrt{a}, \tag{3.185}$$

where the curvature tensor $\boldsymbol{b} = b_{\alpha\beta}\boldsymbol{a}^\alpha \otimes \boldsymbol{a}^\beta$, and

$$\begin{aligned} \boldsymbol{a}^1 &= \frac{1}{a}\{[1 + (z_{,2})^2](\boldsymbol{e}_1 + z_{,1}\boldsymbol{k}) - z_{,1}z_{,2}(\boldsymbol{e}_2 + z_{,2}\boldsymbol{k})\}, \\ \boldsymbol{a}^2 &= \frac{1}{a}\{[1 + (z_{,1})^2](\boldsymbol{e}_1 + z_{,2}\boldsymbol{k}) - z_{,1}z_{,2}(\boldsymbol{e}_2 + z_{,1}\boldsymbol{k})\}, \end{aligned} \tag{3.186}$$

where $\boldsymbol{a}^\alpha = a^{\alpha\beta}\boldsymbol{a}_\beta$ and $(a^{\alpha\beta}) = (a_{\alpha\beta})^{-1}$ have been used.

3.9.2 Linearization in Monge parametrization

To linearize the quantities in (3.123) in their Monge representations, consider the case where gradients of $z(\boldsymbol{\theta})$ are small enough so that their products may be neglected. This leads to a linearization of equations (3.182 - 3.186) such that

$$a \approx 1, \quad \boldsymbol{n} \approx \boldsymbol{k} - \nabla_p z, \quad \boldsymbol{a}^\alpha \approx \boldsymbol{e}_\alpha + z_{,\alpha}\boldsymbol{k}, \quad \boldsymbol{b} \approx \nabla_p^2 z. \tag{3.187}$$

The mean curvature $H = \frac{1}{2}a^{\alpha\beta}b_{\alpha\beta}$ then becomes

$$H \approx \frac{1}{2}\delta_{\alpha\beta}z_{,\alpha\beta} = \frac{1}{2}\Delta_p z, \tag{3.188}$$

where $\Delta_p z = \mathrm{tr}(\nabla_p^2 z)$ is the Laplacian operator on p, and the Guassian curvature $K = \frac{1}{2}\varepsilon^{\alpha\beta}\varepsilon^{\lambda\mu}b_{\alpha\lambda}b_{\beta\mu}$ is then

$$K \approx 0. \tag{3.189}$$

Next, we proceed to linearize the shape equations for a bilayer with an attached comoving cytoskeleton (3.123),

$$\kappa\left\{\Delta_p\left(\frac{1}{2}\Delta_p z\right) + 2\left(\frac{1}{2}\Delta_p z\right)\left[\cancel{\left(\frac{1}{2}\Delta_p z\right)^2}^{\,0} - 0\right]\right\} = (\Sigma^{\alpha\beta} + \lambda\delta_{\alpha\beta})z_{,\alpha\beta} + p, \tag{3.190}$$

which simplifies to

$$\frac{\kappa}{2}(z_{,xxxx} + z_{,yyyy} + 2z_{,xxyy}) = (\Sigma^{\alpha\beta} + \lambda\delta_{\alpha\beta})z_{,\alpha\beta} + p. \tag{3.191}$$

Now prescribe a simple state of stress $\Sigma^{\alpha\beta} = \sigma a^{\alpha\beta} \approx \sigma\delta_{\alpha\beta}$. The linearized shape equations are then

$$z_{,xxxx} + z_{,yyyy} + 2z_{,xxyy} = \eta(z_{,xx} + z_{,yy}) + p' \tag{3.192}$$

where $\eta = \frac{2(\sigma+\lambda)}{\kappa}$, and $p' = \frac{2p}{\kappa}$. This shape equation, for which $\Sigma^{\alpha\beta} = \sigma a^{\alpha\beta}$, can now be solved for equilibrium shapes.

3.9.3 Plot of example equilibrium configuration

We now seek to visualize the vertical displacement of a circular patch of radius 10×10^{-4} [m] of an initially flat lipid bilayer with an attached cytoskeletal membrane as a function of Cartesian coordinates, $z(x, y)$. For demonstration purposes we assign simplifying values for the constants such that

$$(\sigma + \lambda) = 1, \quad \kappa = 2, \tag{3.193}$$

where the dimensions of $\{\sigma, \lambda\}$ are $\left[\frac{\text{force}}{\text{length}}\right]$, and the dimensions of κ are [force $\times$ length]. This reduces (3.192) to

$$z_{,xxxx} + z_{,yyyy} + 2z_{,xxyy} = z_{,xx} + z_{,yy} + p. \tag{3.194}$$

The value of the net pressure p is then assigned a value of 1000 MPa. We then assign clamped boundary conditions at the edges of the patch to complete the problem. The results shown in Figure 3.7 were solved and plotted using COMSOL Multiphysics v5.6.

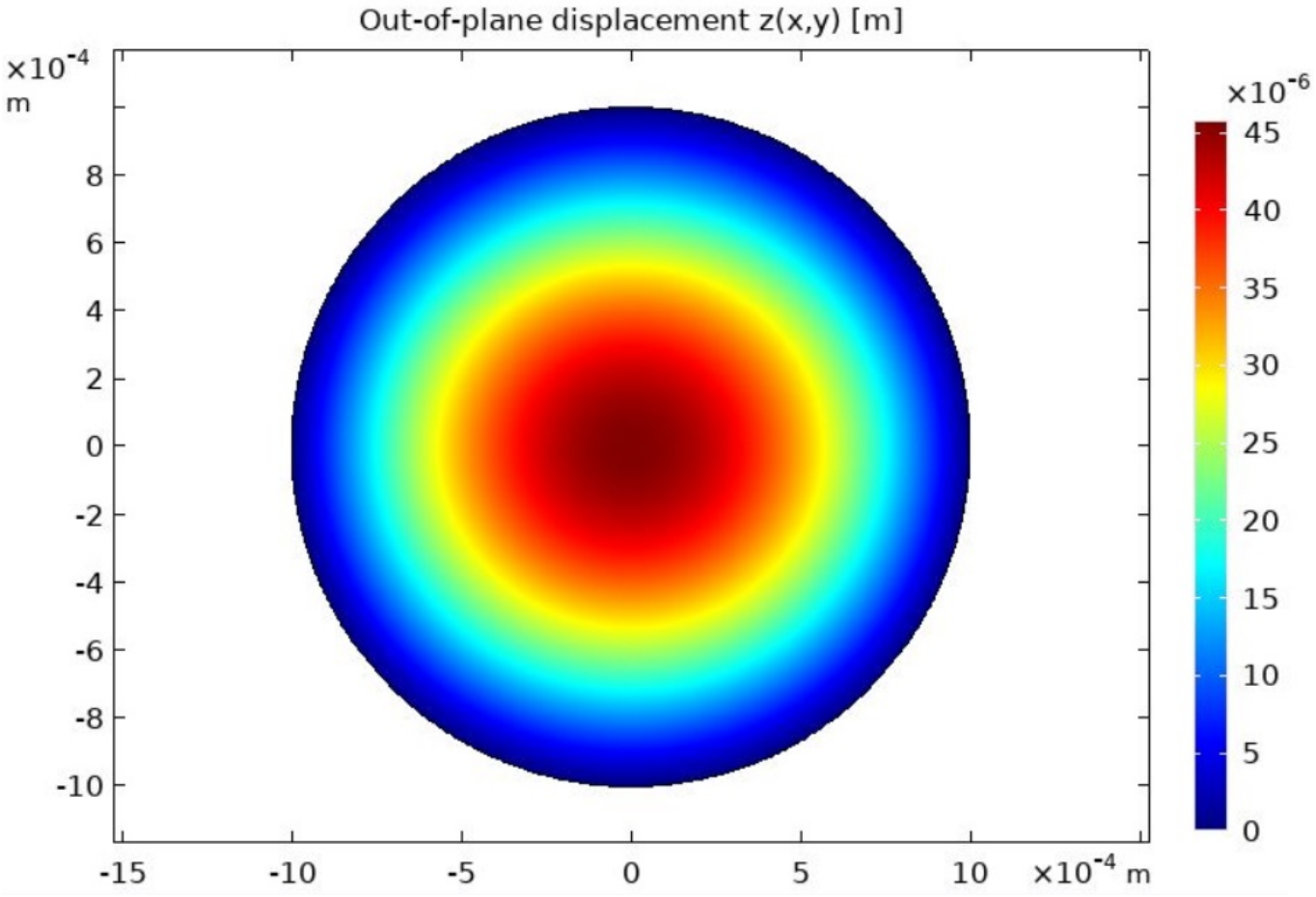

Figure 3.7: Plot of circular patch with simple stress state and uniform pressure.

The results match the expected outcome: the formation of a bubble with maximum vertical displacement of the membrane attained in the center of the circular domain. Although this is a rather academic example, as cell turgor rarely exceeds 2 MPa [31] even in plant cells and the constants were chosen to simplify the equation, it does demonstrate the approximate response of a lipid bilayer/cytoskeleton system response to a net lateral pressure.

Chapter 4

Equations of equilibrium for asymmetric tilted lipid bilayers [1]

4.1 Introduction

In this chapter we extend the classical Canham-Helfrich model of lipid bilayer surfaces [12, 24] to accommodate lipid tilt, defined as deviation from the surface normal of a director field aligned locally with the axes of the lipids. Tilt typically manifests itself as a kinematical accommodation between the lipids of the bilayer membrane and embedded transmembrane structures such as inclusions and proteins [18]. A basic model of tilt was advanced by Helfrich [24] on the assumption that liquid phases of lipid bilayers may be modeled as thin liquid crystal films. This fruitful idea was further developed in [92] to achieve a predictive model of the interplay between tilt and surface geometry in equilibrium. These works rest on the premise that lipid bilayers may be modeled at the outset as elastic surfaces endowed with fields of directors representing the local orientations of the lipid molecules. An associated surfacial energy density is obtained by effectively assigning Frank's energy [19] for bulk liquid crystals directly to the surface of the bilayer. Further refinements of this concept, culminating in several competing models of tilted bilayers, are described in [18, 37, 58, 36].

In the present chapter we pursue an alternative approach based on asymptotic analysis of three dimensional liquid crystal theory in which lipid length - on the order of molecular dimensions - plays the role of the small parameter. While this procedure may be criticized on the grounds that an actual bilayer cannot be regarded as a three-dimensional continuum, our confidence in it is nevertheless justified by the fact that it yields precisely the classical Canham-Helfrich surface model at leading order when tilt is suppressed [4]. Moreover, the asymptotic framework offers guidance as to the features that a direct two-

[1] This chapter has appeared in a recent research article [41].

dimensional surface model should possess. Among these are additional non-standard director fields representing the restrictions to the surface of the curvatures of the three-dimensional lipid trajectories [74].

Following a brief outline of the basic constitutive framework of three-dimensional liquid-crystal theory in Section 4.2, in Section 4.3 we derive the leading-order two-dimensional energy for asymmetric bilayers consisting of congruent leaflets having distinct properties and director fields. In Section 4.4 this is combined with a virtual-power postulate to obtain coupled equilibrium and boundary conditions for the surface and the leaflet director fields. The response functions figuring in the theory are derived in Section 4.5. These are valid for any bulk energy density in the considered class. They are specialized to energies of Frank type in Section 4.6. Owing to the complexity of the model we limit ourselves merely to its derivation in the hope that the community may find it useful for application to specific problems involving lipid tilt.

4.2 Liquid-crystal energies

We model both leaves of the bilayer as nematic liquid crystals. Lipid molecules are polar, in contrast to the non-polar molecules of conventional nematics. Accordingly, the unit-vector field $\tilde{\boldsymbol{d}}$ defining the molecular orientation is physically significant, i.e., the energy is not invariant under $\tilde{\boldsymbol{d}} \longrightarrow -\tilde{\boldsymbol{d}}$. The most general quadratic energy that takes this into account is ([88]; eq. (3.36))

$$\begin{aligned}\mathcal{W}(\tilde{\boldsymbol{d}},\tilde{\boldsymbol{D}}) = k_1(\mathrm{tr}\tilde{\boldsymbol{D}})^2 + k_2(\boldsymbol{W}(\tilde{\boldsymbol{d}})\cdot\tilde{\boldsymbol{D}})^2 + k_3|\tilde{\boldsymbol{D}}\tilde{\boldsymbol{d}}|^2 + (k_2+k_4)[\mathrm{tr}(\tilde{\boldsymbol{D}}^2) - (\mathrm{tr}\tilde{\boldsymbol{D}})^2] \\ +a_0 + [a_1 + a_2\boldsymbol{W}(\tilde{\boldsymbol{D}})\cdot\tilde{\boldsymbol{D}}]\mathrm{tr}\tilde{\boldsymbol{D}} + a_3\boldsymbol{W}(\tilde{\boldsymbol{d}})\cdot\tilde{\boldsymbol{D}}.\end{aligned} \tag{4.1}$$

where

$$\tilde{\boldsymbol{D}} = \mathrm{grad}\tilde{\boldsymbol{d}}, \tag{4.2}$$

is the spatial gradient of $\tilde{\boldsymbol{d}}$, $\boldsymbol{W}(\tilde{\boldsymbol{d}})$ is the skew tensor with axial vector $\tilde{\boldsymbol{d}}$, i.e.

$$\boldsymbol{W}(\tilde{\boldsymbol{d}})\boldsymbol{v} = \tilde{\boldsymbol{d}}\times\boldsymbol{v}, \tag{4.3}$$

for all v, and where k_{1-4} are constants satisfying Ericksen's inequalities

$$2k_1 \geq k_2 + k_4, \quad k_2 \geq |k_4| \quad \text{and} \quad k_3 \geq 0, \tag{4.4}$$

in accordance with the assumed convexity of the function $\mathcal{W}(\tilde{\boldsymbol{d}},\cdot)$. Here the dot interposed between tensor variables is the Euclidean inner product, i.e., $\mathbf{A}\cdot\mathbf{B} = \mathrm{tr}(\mathbf{A}\mathbf{B}^T)$, where tr is the trace and $\boldsymbol{B}^T$ is the transpose of $\boldsymbol{B}$.

We use superposed tildes to identify three-dimensional fields. The same variables, without tildes, are used in the remainder of the paper to denote the restrictions of these fields to the surface of the bilayer.

A more conventional representation of $\mathcal{W}$ is obtained on noting that

$$\mathrm{tr}\tilde{\boldsymbol{D}} = \mathrm{div}\tilde{\mathbf{d}}, \tag{4.5}$$

the spatial divergence of $\tilde{\mathbf{d}}$ and [88]

$$\boldsymbol{W}\left(\tilde{\mathbf{d}}\right)\cdot\mathbf{D} = \tilde{\mathbf{d}}\cdot\mathrm{curl}\tilde{\mathbf{d}}, \tag{4.6}$$

where curl is the spatial curl. The third term in the expression for $\mathcal{W}$ is conventionally written in terms of the curl via the identication ([88], eq. (3.24))

$$\tilde{\boldsymbol{D}}\tilde{\mathbf{d}} = \mathrm{curl}\ \tilde{\mathbf{d}}\times\tilde{\mathbf{d}}. \tag{4.7}$$

The chiral terms involving $a_{0,1,2,3}$ account for the polarity of the lipids, whereas Frank's energy ([19], [88] eq. (3.63)), obtained on setting $a_{0,1,2,3} = 0$ pertains to conventional non-polar nematics.

4.3 Leading-order asymptotic energy

Let $t^{\pm}$ respectively be the fixed, uniform lengths of the lipid molecules comprising the upper and lower leaflets of the bilayer, and let $\mathcal{E}^{\pm}$ be the leaflet energies. We assume that $t^{\pm}$ are much smaller than any other length scale, l say, in the system, and adopt the latter as the unit of length ($l = 1$), so that $t^{\pm} \ll 1$. The total bilayer energy,

$$\mathcal{E} = \mathcal{E}^{+} + \mathcal{E}^{-}, \tag{4.8}$$

satisfies

$$\mathcal{E}/t = \alpha^{+}\left(\mathcal{E}^{+}/t^{+}\right) + \alpha^{-}\left(\mathcal{E}^{-}/t^{-}\right), \tag{4.9}$$

where $t = t^{+} + t^{-}$and $\alpha^{\pm} = t^{\pm}/t$ with $\alpha^{+} + \alpha^{-} = 1$.

In Section 1.3 of [78] it is proved that

$$\mathcal{E}^{\pm}/t^{\pm} = E^{\pm} + o\left(t^{\pm}\right)/t^{\pm}, \tag{4.10}$$

where

$$E^{\pm} = \int_{\omega} W^{\pm} da, \tag{4.11}$$

in which

$$W^{\pm} = |d_n^{\pm}|\mathcal{W}^{\pm}\left(\boldsymbol{d}^{\pm}, \boldsymbol{D}^{\pm}\right), \tag{4.12}$$

where $\mathcal{W}^{\pm}$ are the volumetric leaflet energy densities having possibly distinct material constants, $\boldsymbol{d}^{\pm} = \tilde{\boldsymbol{d}}^{\pm}_{|\omega}$ are the restrictions of the leaflet director fields to the interfacial surface ω, $\boldsymbol{D}^{\pm} = \tilde{\boldsymbol{D}}^{\pm}{}_{|\omega}$ are the restrictions of their spatial gradients to the surface, and

$$d_n^{\pm} = \boldsymbol{d}^{\pm}\cdot\boldsymbol{n}^{\pm}, \tag{4.13}$$

in which

$$\boldsymbol{n}^+ = -\boldsymbol{n}^- = \boldsymbol{n}, \tag{4.14}$$

where $\boldsymbol{n}$ is the field of unit normals to ω (Figure 4.1).

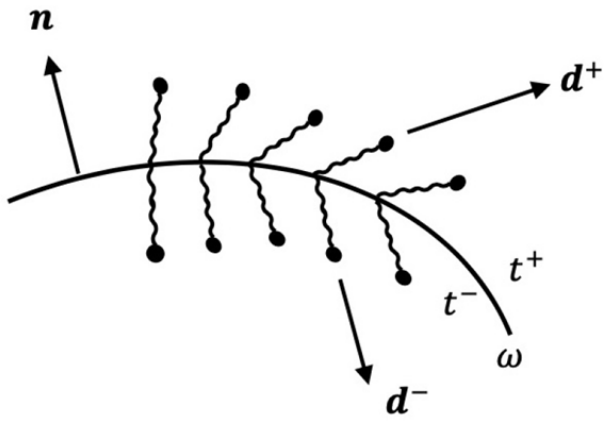

Figure 4.1: Typical patch of director fields on the bilayer surface.

Accordingly, the limit of small t we have $\mathcal{E}/t \to E$, where

$$E = \alpha^+ E^+ + \alpha^- E^-. \tag{4.15}$$

Thus Et is the leading-order energy for small t.

Further, in [78] it is proved that

$$\boldsymbol{D}^\pm = \nabla \boldsymbol{d}^\pm + \left(d_n^\pm\right)^{-1} \left[\boldsymbol{\eta}^\pm - \left(\nabla \boldsymbol{d}^\pm\right) \boldsymbol{d}^\pm\right] \otimes \boldsymbol{n}^\pm, \tag{4.16}$$

provided that $d_n^\pm \neq 0$, where $\nabla(\cdot)$ is the two-dimensional surficial gradient on ω and

$$\boldsymbol{\eta}^\pm = \boldsymbol{D}^\pm \boldsymbol{d}^\pm, \tag{4.17}$$

are the restrictions to ω of the directional derivatives of $\tilde{\boldsymbol{d}}^\pm$ in the directions $\tilde{\boldsymbol{d}}^\pm$. These are the nonstandard director fields identified in the Introduction, representing the curvatures of the trajectories aligned locally with the lipid molecules. Because $\tilde{\boldsymbol{d}}^\pm$ are unit vectors, we require

$$\boldsymbol{d}^\pm \cdot \boldsymbol{\eta}^\pm = 0 \tag{4.18}$$

on ω.

The energy densities in (4.11) are thus given by the functions

$$W^\pm\left(\boldsymbol{n}^\pm, \boldsymbol{d}^\pm, \nabla \boldsymbol{d}^\pm, \boldsymbol{\eta}^\pm\right) = d_n^\pm \mathcal{W}^\pm\left(\boldsymbol{d}^\pm, \boldsymbol{D}^\pm\right) + H^\pm\left(d_n^\pm\right). \tag{4.19}$$

Ad hoc terms $H^{\pm}\left(d_n^{\pm}\right)$ have been appended to penalize configurations having $d_n^{\pm}=0$ in which the hydrophobic tail groups of the lipids are exposed to the surrounding aqueous solution - a highly energetic and unstable condition. We have also assumed $d_n^{\pm}>0$ in accordance with the arrangement of lipids depicted in Figure 4.1, and we note, from (4.14), that

$$d_n^{+}=\boldsymbol{d}^{+}\cdot\boldsymbol{n} \quad \text{and} \quad d_n^{-}=-\boldsymbol{d}^{-}\cdot\boldsymbol{n}. \tag{4.20}$$

We observe that in the expressions for $\boldsymbol{D}^{\pm}$, and hence those for $\mathcal{W}^{\pm}$, the signs of $\boldsymbol{n}^{\pm}$ are immaterial. Accordingly, these expressions are unaltered if the orientation $\boldsymbol{n}$ of ω is substituted in place of $\boldsymbol{n}^{\pm}$. The energy is subject to constraints consisting of (4.18) and

$$|d^{\pm}|=1. \tag{4.21}$$

Among the many possibilities for the penalty terms, the choices

$$H^{\pm}\left(d_n^{\pm}\right)=-c^{\pm}\ln|d_n^{\pm}|, \tag{4.22}$$

in which $c^{\pm}$ are positive constants, seem to be the simplest and most tractable.

For the purposes of deriving equilibrium equations we write the surface gradient $\nabla\boldsymbol{d}$, again with superscripts $^{\pm}$ as appropriate, in the form

$$\nabla\boldsymbol{d}=\boldsymbol{d}_{,\alpha}\otimes\boldsymbol{a}^{\alpha}, \tag{4.23}$$

where $\boldsymbol{d}_{,\alpha}=\partial\boldsymbol{d}/\partial\theta^{\alpha}$, in which $\theta^{\alpha}\,(\alpha=1,2)$ are coordinates on ω and $\boldsymbol{a}^{\alpha}$ are the basis one-forms on the tangent plane of ω at the point with coordinates θ^{α}. These are related to the tangent basis $\boldsymbol{a}_{\alpha}=\boldsymbol{r}_{,\alpha}\,(=\partial\boldsymbol{r}/\partial\theta^{\alpha})$ in which $\boldsymbol{r}\left(\theta^1,\theta^2\right)$, is the position field on ω with metric $a_{\alpha\beta}=\boldsymbol{a}_{\alpha}\cdot\boldsymbol{a}_{\beta}$, by $\boldsymbol{a}^{\alpha}=a^{\alpha\beta}\boldsymbol{a}_{\beta}$, where $a^{\alpha\beta}$ is the dual metric, i.e., $\left(a^{\alpha\beta}\right)=\left(a_{\alpha\beta}\right)^{-1}$. The orientation of ω is defined by

$$\boldsymbol{n}=\frac{1}{2}\epsilon^{\alpha\beta}\boldsymbol{a}_{\alpha}\times\boldsymbol{a}_{\beta}, \tag{4.24}$$

where $\epsilon^{\alpha\beta}=e^{\alpha\beta}/\sqrt{a}$ is the contravariant permutation tensor, in which $e^{\alpha\beta}$ is the permutation symbol $(e^{12}=-e^{21}=1;e^{11}=e^{22}=0)$ and $a=\det\left(a_{\alpha\beta}\right)$. Accordingly, the leaflet energies may be expressed in the form

$$U^{\pm}\left(\boldsymbol{a}_{\alpha},\boldsymbol{d}^{\pm},\boldsymbol{d}_{,\alpha}^{\pm},\boldsymbol{\eta}^{\pm}\right)=W^{\pm}\left(\boldsymbol{n},\boldsymbol{d}^{\pm},\nabla\boldsymbol{d}^{\pm},\boldsymbol{\eta}^{\pm}\right), \tag{4.25}$$

and the net energy is

$$E=\alpha^{+}E^{+}+\alpha^{-}E^{-}, \tag{4.26}$$

with

$$E^{\pm}=\int_{\omega}U^{\pm}\left(\boldsymbol{a}_{\alpha},\boldsymbol{d}^{\pm},\boldsymbol{d}_{,\alpha}^{\pm},\boldsymbol{\eta}^{\pm}\right)da. \tag{4.27}$$

4.4 Equilibrium

Following standard practice, we regard equilibria as states that satisfy the virtual-power statement

$$\dot{E}^* = P, \tag{4.28}$$

where P is the virtual power of external agencies acting on the bilayer, the superposed dot is used to denote a variational derivative (evaluated at the considered equilibrium state), and

$$E^* = \alpha^+ \left(E^*\right)^+ + \alpha^- \left(E^*\right)^-, \tag{4.29}$$

with

$$\left(E^*\right)^\pm = \int_\omega \left[U^\pm \left(\boldsymbol{a}_\alpha, \boldsymbol{d}^\pm, \boldsymbol{d}^\pm_{,\alpha}, \boldsymbol{\eta}^\pm\right) + \frac{1}{2}\lambda^\pm \left(\boldsymbol{d}^\pm \cdot \boldsymbol{d}^\pm - 1\right) + \mu^\pm \boldsymbol{d}^\pm \cdot \boldsymbol{\eta}^\pm \right] da \tag{4.30}$$

being the extended energy, where $\lambda^\pm$, $\mu^\pm$ are Lagrange multiplier fields associated with the constraints (4.18) and (4.21). Importantly, the variational problem (4.28) is entirely unconstrained, and $U^\pm$ are to be treated as extensions of the actual leaflet energies from their original domains, namely the manifolds defined by the constraints [11]. In this respect our treatment differs from that found in [88], where Lagrange multipliers are avoided and variations are computed on a constraint manifold directly.

For the purpose of computing the variation of the extended energy, we write

$$\left(E^*\right)^\pm = \int_{\Omega^\pm} \Phi^\pm dA, \tag{4.31}$$

with

$$\Phi^\pm = J^\pm U^\pm + \frac{1}{2}\Lambda^\pm \left(\boldsymbol{d}^\pm \cdot \boldsymbol{d}^\pm - 1\right) + \Pi^\pm \boldsymbol{d}^\pm \cdot \boldsymbol{\eta}^\pm, \tag{4.32}$$

where $\Lambda^\pm = J^\pm \lambda^\pm$, $\Pi^\pm = J^\pm \mu^\pm$, and $J^\pm = \sqrt{a/A^\pm}$ are the areal dilations of the leaflets in which $A^\pm$ are the values of a on reference surfaces $\Omega^\pm$, on which the positions of the lipid molecules constituting the leaflets, but not their orientations, are fixed. The variational derivatives are then computed treating the lipid molecules, and thus $\Omega^\pm$ as fixed. In a departure from convention, we do not impose constraints on the areal dilations because such constraints are not implied by the bulk incompressibility of liquid crystals [74].

We consider the possibility that the upper and lower leaflets may slide relative to each other while remaining congruent to ω, and thus allow for distinct, but congruent, reference surfaces $\Omega^\pm$. Accordingly,

$$\dot{E}^* = \alpha^+ \left(\dot{E}^*\right)^+ + \alpha^- \left(\dot{E}^*\right)^-, \tag{4.33}$$

where

$$\left(\dot{E}^*\right)^\pm = \int_{\Omega^\pm} \dot{\Phi}^\pm dA = \int_\omega J_\pm^{-1} \dot{\Phi}^\pm da, \tag{4.34}$$

and the virtual power is

$$P = \alpha^+ P^+ + \alpha^- P^-, \tag{4.35}$$

with

$$P^\pm = \left(\dot{E}^*\right)^\pm. \tag{4.36}$$

We suppress variations of the Lagrange multipliers $\Lambda^\pm$ and $\Pi^\pm$ in the computation of $\dot{\Phi}^\pm$ as these merely return the constraints as the relevant Euler equations. The latter are therefore to be appended to the final system of equilibrium conditions.

In addition to the multipliers, the functions $\Phi^\pm$ depend on the list $\{\boldsymbol{a}_\alpha, \boldsymbol{d}^\pm, \boldsymbol{d}^\pm_{,\alpha}, \boldsymbol{\eta}^\pm\}$. For each leaflet of the bilayer, we define

$$J\boldsymbol{N}^\alpha = \Phi_{\boldsymbol{a}_\alpha}, \quad J\boldsymbol{M}^\alpha = \Phi_{\boldsymbol{d}_{,\alpha}}, \quad J\boldsymbol{m} = \Phi_{\boldsymbol{d}} \quad \textit{and} \quad J\boldsymbol{l} = \Phi_{\boldsymbol{\eta}}, \tag{4.37}$$

where $\Phi_{\boldsymbol{a}_\alpha}$, etc., are partial derivatives with respect to the indicated variables, and with $^\pm$ labels appended as appropriate. Then,

$$J^{-1}\dot{\Phi} = \boldsymbol{N}^\alpha \cdot \boldsymbol{u}_{,\alpha} + \boldsymbol{M}^\alpha \cdot \dot{\boldsymbol{d}}_{,\alpha} + \boldsymbol{m} \cdot \dot{\boldsymbol{d}} + \boldsymbol{l} \cdot \dot{\boldsymbol{\eta}}, \tag{4.38}$$

where $\boldsymbol{u} = \dot{\boldsymbol{r}}$ is the virtual velocity of the lipids on ω, the interposed dots are scalar products, and we regard the coordinates θ^α as being convected with the lipids, so that $\dot{a}_\alpha = (\boldsymbol{r}_{,\alpha})^{\cdot} = \dot{\boldsymbol{r}}_{,\alpha}$ and $(\boldsymbol{d}_{,\alpha})^{\cdot} = \dot{\boldsymbol{d}}_{,\alpha}$.

For each leaflet, Stokes' theorem, applied to (4.36), then furnishes

$$P = \int_{\partial\omega} \left(\boldsymbol{N}^\alpha \nu_\alpha \cdot \boldsymbol{u} + \boldsymbol{M}^\alpha \nu_\alpha \cdot \dot{\boldsymbol{d}}\right) ds + \int_\omega \left[\left(\boldsymbol{m} - \boldsymbol{M}^\alpha_{;\alpha}\right) \cdot \dot{\boldsymbol{d}} + \boldsymbol{l} \cdot \dot{\boldsymbol{\eta}} - \boldsymbol{N}^\alpha_{;\alpha} \cdot \boldsymbol{u}\right] da, \tag{4.39}$$

where $\boldsymbol{N}^\alpha_{;\alpha} = \left(\sqrt{a}\right)^{-1} \left(\sqrt{a}\boldsymbol{N}^\alpha\right)_{,\alpha}$, etc., is the covariant surface divergence on ω and ν_α are the components of the unit normal $\boldsymbol{\nu} = \nu_\alpha \boldsymbol{a}^\alpha$ to the edge $\partial\omega$ lying in the tangent plane to ω.

We conclude that essential boundary conditions entail the specification of position $\boldsymbol{r}$ and orientation $\boldsymbol{d}$ on subsets of $\partial\omega$, the latter corresponding to the *hard anchoring* condition of conventional liquid crystal theory [88]. For example, the individual leaflet director tractions, power-conjugate to $\dot{\boldsymbol{d}}^\pm$, are

$$\boldsymbol{p}^\pm = \boldsymbol{M}^\alpha_\pm \nu_\alpha. \tag{4.40}$$

As we are allowing the leaflets to undergo relative slipping while remaining congruent to ω, the leaflet virtual velocities are of the form

$$\boldsymbol{u}^\pm = u^\alpha_\pm \boldsymbol{a}_\alpha + w\boldsymbol{n}, \tag{4.41}$$

in which the normal velocity w is common to both leaflets and $u^\alpha_\pm = \dot{\theta}^\alpha_\pm$ are the tangential leaflet velocities at the lipids with coordinates θ^α on ω. In effect we stipulate that the convected coordinates attached to the individual leaflets coincide, *at* the considered equilibrium state, with the coordinates θ^α used to parametrize ω, but that they depart from the latter

in the course of variation [40]. Accordingly, (4.39) furnishes tangential leaflet edge force densities

$$t^{\pm}_{\beta} = \boldsymbol{a}_{\beta} \cdot \boldsymbol{N}^{\alpha}_{\pm} \nu_{\alpha}, \tag{4.42}$$

which are power-conjugate to $\dot{u}^{\alpha}_{\pm}$ and the shear-force density

$$S = \boldsymbol{n} \cdot \boldsymbol{N}^{\mu} \nu_{\mu}, \tag{4.43}$$

power-conjugate to w, where

$$N^{\mu} = \alpha^{+} \boldsymbol{N}^{\mu}_{+} + \alpha^{-} \boldsymbol{N}^{\mu}_{-}. \tag{4.44}$$

In the same way, assuming there are no virtual power terms associated with variation of $\boldsymbol{d}^{\pm}$ or $\boldsymbol{\eta}^{\pm}$ in the interior of ω, we conclude, from (4.28), (4.33) and (4.39), that

$$\left(\boldsymbol{M}^{\alpha}_{\pm}\right)_{;\alpha} = \boldsymbol{m}^{\pm}, \quad \text{and} \quad \boldsymbol{l}^{\pm} = \boldsymbol{0} \quad \text{on} \quad \omega; \tag{4.45}$$

and if $f^{\pm}_{\beta}$ are tangential areal force densities acting on the leaflets, that

$$\boldsymbol{a}_{\beta} \cdot \left(\boldsymbol{N}^{\alpha}_{\pm}\right)_{;\alpha} + f^{\pm}_{\beta} = 0 \quad \text{on} \quad \omega, \tag{4.46}$$

whereas the net lateral pressure p exerted on ω satisfies

$$\boldsymbol{n} \cdot \boldsymbol{N}^{\mu}_{;\mu} + p = 0 \quad \text{on} \quad \omega, \tag{4.47}$$

this generalizing the well known *shape equation* of conventional bilayer theory in which lipid tilt is suppressed.

Some insight into the nature of the director tractions may be gained by considering the overall equilibrium of the bilayer under rigid-body variations. These are of the form $\boldsymbol{u} = \boldsymbol{\omega} \times \boldsymbol{r} + \boldsymbol{a}$, $\dot{\boldsymbol{d}}^{\pm} = \boldsymbol{\omega} \times \boldsymbol{d}^{\pm}$ and $\dot{\boldsymbol{\eta}}^{\pm} = \boldsymbol{\omega} \times \boldsymbol{\eta}^{\pm}$, where $\boldsymbol{a}$ and $\boldsymbol{\omega}$ are constant vectors. Because the liquid-crystal energy (4.1) is invariant under such variations [88], the same is true of the extended bilayer energy (4.32), and (4.28) thus reduces to $P = 0$, i.e.,

$$\boldsymbol{a} \cdot \left(\int_{\partial\omega} \boldsymbol{t} ds + \int_{\omega} \boldsymbol{f} da \right) + \boldsymbol{\omega} \cdot \left[\int_{\partial\omega} (\boldsymbol{c} + \boldsymbol{r} \times \boldsymbol{t})\, ds + \int_{\omega} \boldsymbol{r} \times \boldsymbol{f} da \right] = 0, \tag{4.48}$$

where, from (4.40)-(4.47),

$$\boldsymbol{t} = \left(\alpha^{+} t^{+}_{\beta} + \alpha^{-} t^{-}_{\beta}\right) \boldsymbol{a}^{\beta} + S\boldsymbol{n}, \quad \boldsymbol{f} = \left(\alpha^{+} f^{+}_{\beta} + \alpha^{-} f^{-}_{\beta}\right) \boldsymbol{a}^{\beta} + p\boldsymbol{n} \tag{4.49}$$

are the net edge and areal force densities, respectively, and

$$\boldsymbol{c} = \alpha^{+} \boldsymbol{d}^{+} \times \boldsymbol{p}^{+} + \alpha^{-} \boldsymbol{d}^{-} \times \boldsymbol{p}^{-}. \tag{4.50}$$

The arbitrariness of $\boldsymbol{a}$ and $\boldsymbol{\omega}$ then furnishes the global force and moment balances

$$\int_{\partial\omega} \boldsymbol{t} ds + \int_{\omega} \boldsymbol{f} da = \boldsymbol{0} \quad \text{and} \quad \int_{\partial\omega} (\boldsymbol{c} + \boldsymbol{r} \times \boldsymbol{t})\, ds + \int_{\omega} \boldsymbol{r} \times \boldsymbol{f} da = \boldsymbol{0} \tag{4.51}$$

and hence the interpretation of $\boldsymbol{c}$ as a couple traction on $\partial\omega$.

4.5 Response functions

To render the model explicit we require expressions for the derivatives listed in (4.37). To this end we combine (4.19), (4.25) and (4.32) with the chain rule. Thus,

$$\dot{U} = \dot{d}_n \left[\mathcal{W} + H'\left(d_n\right)\right] + d_n \left(\mathcal{W}_{\boldsymbol{d}} \cdot \dot{\boldsymbol{d}} + \mathcal{W}_{\boldsymbol{D}} \cdot \dot{\boldsymbol{D}}\right) \tag{4.52}$$

in each leaflet, with labels $^{\pm}$ appended as appropriate, where $\mathcal{W}_{\boldsymbol{d}}$ and $\mathcal{W}_{\boldsymbol{D}}$ are the derivatives of the extended (unconstrained) bulk energy, and (cf. (4.16))

$$\begin{aligned}\dot{\boldsymbol{D}} = (\nabla \boldsymbol{d})^{\cdot} - d_n^{-2}\dot{d}_n \left[\boldsymbol{\eta} - (\nabla \boldsymbol{d})\, \boldsymbol{d}\right] \otimes \boldsymbol{n} + d_n^{-1} \left[\boldsymbol{\eta} - (\nabla \boldsymbol{d})\, \boldsymbol{d}\right] \otimes \dot{\boldsymbol{n}} \\ + d_n^{-1} \left[\dot{\boldsymbol{\eta}} - (\nabla \boldsymbol{d})^{\cdot}\, \boldsymbol{d} - (\nabla \boldsymbol{d})\, \dot{\boldsymbol{d}}\right] \otimes \boldsymbol{n},\end{aligned} \tag{4.53}$$

with (cf. (4.20))

$$\dot{d}_n^{\pm} = \pm(\dot{\boldsymbol{d}}^{\pm} \cdot \boldsymbol{n} + \boldsymbol{d}^{\pm} \cdot \dot{\boldsymbol{n}}) \tag{4.54}$$

and

$$(\nabla \boldsymbol{d})^{\cdot} = \dot{\boldsymbol{d}}_{,\alpha} \otimes \boldsymbol{a}^{\alpha} + \boldsymbol{d}_{,\alpha} \otimes \dot{\boldsymbol{a}}^{\alpha}. \tag{4.55}$$

For example, to compute the derivative $U_{\boldsymbol{\eta}}$ we fix $\boldsymbol{d}$, $\boldsymbol{a}_{\alpha}$ (hence $\boldsymbol{n}$) and $\nabla \boldsymbol{d}$, obtaining $\dot{\boldsymbol{D}} = d_n^{-1} \dot{\boldsymbol{\eta}} \otimes \boldsymbol{n}$. Then, (4.52) furnishes

$$U_{\boldsymbol{\eta}} \cdot \dot{\boldsymbol{\eta}} = \mathcal{W}_{\boldsymbol{D}} \cdot \dot{\boldsymbol{\eta}} \otimes \boldsymbol{n} = (\mathcal{W}_{\boldsymbol{D}})\, \boldsymbol{n} \cdot \dot{\boldsymbol{\eta}}. \tag{4.56}$$

Because U is the extended energy, the variation $\dot{\boldsymbol{\eta}}$ is arbitrary; thus,

$$U_{\boldsymbol{\eta}} = (\mathcal{W}_{\boldsymbol{D}})\, \boldsymbol{n}. \tag{4.57}$$

With reference to (4.32) we have $\Phi_{\boldsymbol{\eta}} \cdot \dot{\boldsymbol{\eta}} = J(U_{\boldsymbol{\eta}} + \mu \boldsymbol{d}) \cdot \dot{\boldsymbol{\eta}}$, and $(4.37)_4$ then gives

$$\boldsymbol{l} = U_{\boldsymbol{\eta}} + \mu \boldsymbol{d}. \tag{4.58}$$

Next, we fix $\boldsymbol{d}$ and $\boldsymbol{a}_{\alpha}$, obtaining $\dot{\boldsymbol{D}} = (\nabla \boldsymbol{d})^{\cdot} - d_n^{-1} (\nabla \boldsymbol{d})^{\cdot}\, \boldsymbol{d} \otimes \boldsymbol{n}$. Using the rule $\boldsymbol{a} \cdot \boldsymbol{A}\boldsymbol{b} = \boldsymbol{a} \otimes \boldsymbol{b} \cdot \boldsymbol{A}$, we find that

$$U_{\boldsymbol{d},\alpha} \cdot \dot{\boldsymbol{d}}_{,\alpha} = \left[d_n \mathcal{W}_{\boldsymbol{D}} - (\mathcal{W}_{\boldsymbol{D}})\, \boldsymbol{n} \otimes \boldsymbol{d}\right] \cdot (\nabla \boldsymbol{d})^{\cdot}, \quad \text{with} \quad (\nabla \boldsymbol{d})^{\cdot} = \dot{\boldsymbol{d}}_{,\alpha} \otimes \boldsymbol{a}^{\alpha}, \tag{4.59}$$

and (4.32), (4.52) and $(4.37)_2$ combine to yield

$$\boldsymbol{M}^{\alpha} = d_n\, (\mathcal{W}_{\boldsymbol{D}})\, \boldsymbol{a}^{\alpha} - d^{\alpha}\, (\mathcal{W}_{\boldsymbol{D}})\, \boldsymbol{n}. \tag{4.60}$$

According to $(4.45)_2$, (4.57) and (4.58), $(\mathcal{W}_{\boldsymbol{D}})\boldsymbol{n} = -\mu \boldsymbol{d}$ in *equilibrium*, yielding the leaflet contribution $\boldsymbol{p} = d_n \boldsymbol{d} \times (\mathcal{W}_{\boldsymbol{D}})\boldsymbol{\nu}$ to the couple traction on $\partial\omega$.

The computation of $U_{\boldsymbol{d}}$ proceeds in the same way. Fixing $\boldsymbol{a}_\alpha$, $\boldsymbol{\eta}$, and $\nabla\boldsymbol{d}$, we have

$$U_{\boldsymbol{d}} \cdot \dot{\boldsymbol{d}} = \dot{d}_n \mathcal{W} + d_n \mathcal{W}_{\boldsymbol{d}} \cdot \dot{\boldsymbol{d}} - d_n^{-2} \dot{d}_n \left[\boldsymbol{\eta} - (\nabla \boldsymbol{d})\, \boldsymbol{d}\right] \cdot (\mathcal{W}_{\boldsymbol{D}})\, \boldsymbol{n} - d_n^{-1} (\nabla \boldsymbol{d})\, \dot{\boldsymbol{d}} \cdot (\mathcal{W}_{\boldsymbol{D}})\, \boldsymbol{n}. \quad (4.61)$$

As we are concerned with the equilibrium value of $U_{\boldsymbol{d}}$, we simplify matters by combining $(4.45)_2$, (4.57) and (4.58) to find that $\boldsymbol{\eta} \cdot (\mathcal{W}_{\boldsymbol{D}})\, \boldsymbol{n} = -\mu \boldsymbol{\eta} \cdot \boldsymbol{d}$, which vanishes by (4.18); and $(\nabla \boldsymbol{d})\, \boldsymbol{d} \cdot (\mathcal{W}_{\boldsymbol{D}})\, \boldsymbol{n} = -\mu \boldsymbol{d} \cdot (\nabla \boldsymbol{d})^T\, \boldsymbol{d}$, in which $(\nabla \boldsymbol{d})^T\, \boldsymbol{d}$ vanishes because $\boldsymbol{d}$ is a unit vector. The last term in (4.61) is disposed of similarly, and with (4.54) we obtain

$$U_{\boldsymbol{d}} = d_n \mathcal{W}_{\boldsymbol{d}} \pm \left[\mathcal{W} + H'(d_n)\right] \boldsymbol{n}, \quad (4.62)$$

again at equilibrium, with the sign pertaining to the leaflet in question, and where, for H as in (4.22),

$$H'_{\pm}\left(d_n^{\pm}\right) = \mp c^{\pm} / |d_n^{\pm}|. \quad (4.63)$$

Combining this result with (4.32) and $(4.37)_3$, we arrive at

$$\boldsymbol{m} = U_{\boldsymbol{d}} + \lambda \boldsymbol{d} + \mu \boldsymbol{\eta}. \quad (4.64)$$

The derivation of the expressions for the response functions $\boldsymbol{N}^\alpha$ is substantially more involved. We fix $\boldsymbol{d}$, $\boldsymbol{\eta}$ and $\boldsymbol{d}_{,\alpha}$, and use (4.32) to infer that

$$\Phi_{\boldsymbol{a}_\alpha} \cdot \dot{\boldsymbol{a}}_\alpha = J \left(\dot{U} + U \dot{J}/J\right), \quad (4.65)$$

where $\dot{U}$ is given by (4.52) with

$$\dot{\boldsymbol{D}} = (\nabla \boldsymbol{d})^{\cdot} - d_n^{-2} \dot{d}_n \left[\boldsymbol{\eta} - (\nabla \boldsymbol{d})\, \boldsymbol{d}\right] \otimes \boldsymbol{n} - d_n^{-1} (\nabla \boldsymbol{d})^{\cdot}\, \boldsymbol{d} \otimes \boldsymbol{n} + d_n^{-1} \left[\boldsymbol{\eta} - (\nabla \boldsymbol{d})\, \boldsymbol{d}\right] \otimes \dot{\boldsymbol{n}} \quad (4.66)$$

in which

$$(\nabla \boldsymbol{d})^{\cdot} = \boldsymbol{d}_{,\alpha} \otimes \dot{\boldsymbol{a}}^\alpha. \quad (4.67)$$

Then,

$$\begin{aligned} \mathcal{W}_{\boldsymbol{D}} \cdot \dot{\boldsymbol{D}} = \mathcal{W}_{\boldsymbol{D}} \cdot (\nabla \boldsymbol{d})^{\cdot} - d_n^{-2} \dot{d}_n \left[\boldsymbol{\eta} - (\nabla \boldsymbol{d})\, \boldsymbol{d}\right] \cdot (\mathcal{W}_{\boldsymbol{D}})\, \boldsymbol{n} - d_n^{-1} (\nabla \boldsymbol{d})^{\cdot}\, \boldsymbol{d} \cdot (\mathcal{W}_{\boldsymbol{D}})\, \boldsymbol{n} \\ + d_n^{-1} \left[\boldsymbol{\eta} - (\nabla \boldsymbol{d})\, \boldsymbol{d}\right] \cdot (\mathcal{W}_{\boldsymbol{D}})\, \dot{\boldsymbol{n}} \end{aligned} \quad (4.68)$$

wherein the 2nd term on the right-hand side again vanishes in equilibrium. The rule $\boldsymbol{A} \cdot \boldsymbol{a} \otimes \boldsymbol{b} = \boldsymbol{b} \cdot \boldsymbol{A}^T \boldsymbol{a}$ may then be used to arrive at

$$d_n \mathcal{W}_{\boldsymbol{D}} \cdot \dot{\boldsymbol{D}} = \left[d_n (\mathcal{W}_{\boldsymbol{D}})^T - \boldsymbol{d} \otimes (\mathcal{W}_{\boldsymbol{D}})\, \boldsymbol{n}\right] \boldsymbol{d}_{,\alpha} \cdot \dot{\boldsymbol{a}}^\alpha + (\mathcal{W}_{\boldsymbol{D}})^T \left[\boldsymbol{\eta} - (\nabla \boldsymbol{d})\, \boldsymbol{d}\right] \cdot \dot{\boldsymbol{n}}. \quad (4.69)$$

Noting that $[\boldsymbol{d} \otimes (\mathcal{W}_{\boldsymbol{D}})\, \boldsymbol{n}] \boldsymbol{d}_{,\alpha} = -\mu (\boldsymbol{d} \cdot \boldsymbol{d}_{,\alpha}) \boldsymbol{d}$ at equilibrium, which vanishes by (4.21), from (4.52) we derive

$$\dot{U} = \pm \left[\mathcal{W} + H'(d_n)\right] \boldsymbol{d} \cdot \dot{\boldsymbol{n}} + (\mathcal{W}_{\boldsymbol{D}})^T \left[\boldsymbol{\eta} - (\nabla \boldsymbol{d})\, \boldsymbol{d}\right] \cdot \dot{\boldsymbol{n}} + d_n (\mathcal{W}_{\boldsymbol{D}})^T \boldsymbol{d}_{,\alpha} \cdot \dot{\boldsymbol{a}}^\alpha. \quad (4.70)$$

To secure the desired result this must be expressed as a linear form in $\dot{\boldsymbol{a}}_\alpha$. Start by expressing the variation $\dot{\boldsymbol{n}}$ in terms of $\dot{\boldsymbol{a}}_\alpha$ through writing (4.24) in the form

$$J\boldsymbol{n} = \frac{1}{2}\mu^{\alpha\beta}\boldsymbol{a}_\alpha \times \boldsymbol{a}_\beta, \tag{4.71}$$

where $\mu^{\alpha\beta} = J\epsilon^{\alpha\beta} = e^{\alpha\beta}/\sqrt{A}$. Then,

$$\dot{\boldsymbol{n}} = \epsilon^{\alpha\beta}\dot{\boldsymbol{a}}_\alpha \times \boldsymbol{a}_\beta - (\dot{J}/J)\boldsymbol{n}, \tag{4.72}$$

so that the 2nd term on the right-hand side of (4.70) may be reduced to

$$(\mathcal{W}_{\boldsymbol{D}})^T [\boldsymbol{\eta} - (\nabla \boldsymbol{d})\, \boldsymbol{d}] \cdot \dot{\boldsymbol{n}} = \epsilon^{\alpha\beta}\boldsymbol{a}_\beta \times (\mathcal{W}_{\boldsymbol{D}})^T [\boldsymbol{\eta} - (\nabla \boldsymbol{d})\, \boldsymbol{d}] \cdot \dot{\boldsymbol{a}}_\alpha - (\dot{J}/J) [\boldsymbol{\eta} - (\nabla \boldsymbol{d})\, \boldsymbol{d}] \cdot (\mathcal{W}_{\boldsymbol{D}})\, \boldsymbol{n}, \tag{4.73}$$

in which, as before, the 2nd term on the right vanishes. Continuing this procedure, consider the inner product $\dot{\boldsymbol{n}} \cdot \boldsymbol{n}$ which renders

$$\dot{J}/J = \epsilon^{\alpha\beta}\dot{\boldsymbol{a}}_\alpha \times \boldsymbol{a}_\beta \times \boldsymbol{n}, \tag{4.74}$$

where $\boldsymbol{a}_\beta \times \boldsymbol{n} = \epsilon_{\lambda\beta}\boldsymbol{a}^\lambda$ and $\epsilon_{\lambda\beta}$ is the covariant permutation tensor. With $\epsilon^{\alpha\beta}\epsilon_{\lambda\beta} = \delta^\alpha_\lambda$ (the Kronecker delta), we arrive at

$$\dot{J}/J = \boldsymbol{a}^\alpha \cdot \dot{\boldsymbol{a}}_\alpha. \tag{4.75}$$

To obtain $\dot{\boldsymbol{a}}_\alpha$ in terms of $\dot{\boldsymbol{a}}^\alpha$, use $\dot{\boldsymbol{a}}^\alpha = (a^{\alpha\beta}\boldsymbol{a}_\beta)^{\cdot}$ with $\dot{a}^{\alpha\beta} = -a^{\alpha\nu}a^{\beta\mu}\dot{a}_{\nu\mu}$, which follows from the identity $a^{\alpha\gamma}a_{\gamma\beta} = \delta^\alpha_\beta$. Using $a_{\nu\mu} = \boldsymbol{a}_\nu \cdot \boldsymbol{a}_\mu$, we then obtain

$$\dot{a}^{\alpha\beta} = -a^{\beta\mu}\boldsymbol{a}^\alpha \cdot \dot{\boldsymbol{a}}_\mu - a^{\alpha\mu}\boldsymbol{a}^\beta \cdot \dot{\boldsymbol{a}}_\mu \tag{4.76}$$

and finally

$$\dot{a}^\alpha = a^{\alpha\beta}\dot{\boldsymbol{a}}_\beta - [(a^{\alpha\beta}\boldsymbol{a}^\mu + a^{\beta\mu}\boldsymbol{a}^\alpha) \cdot \dot{\boldsymbol{a}}_\beta]\boldsymbol{a}_\mu. \tag{4.77}$$

Using (4.77), the 3rd term on the right-hand side of (4.70) may be written

$$d_n\, (\mathcal{W}_{\boldsymbol{D}})^T\, \boldsymbol{d}_{,\alpha} \cdot \dot{\boldsymbol{a}}^\alpha = d_n \left\{ a^{\alpha\beta}\, (\mathcal{W}_{\boldsymbol{D}})^T\, \boldsymbol{d}_{,\beta} - [\boldsymbol{d}_{,\beta} \cdot (\mathcal{W}_{\boldsymbol{D}})\, \boldsymbol{a}_\mu] \left(a^{\alpha\beta}\boldsymbol{a}^\mu + a^{\alpha\mu}\boldsymbol{a}^\beta\right) \right\} \cdot \dot{\boldsymbol{a}}_\alpha. \tag{4.78}$$

On combining these results with $(4.37)_1$, (4.65) and (4.75), we finally obtain the rather formidable formula

$$\begin{aligned} \boldsymbol{N}^\alpha = U\boldsymbol{a}^\alpha + \epsilon^{\alpha\beta}\boldsymbol{a}_\beta \times (\mathcal{W}_{\boldsymbol{D}})^T [\boldsymbol{\eta} - (\nabla \boldsymbol{d})\, \boldsymbol{d}] \pm [\mathcal{W} + H'\,(d_n)] \left(\epsilon^{\alpha\beta}\boldsymbol{a}_\beta \times \boldsymbol{d} - d_n\boldsymbol{a}^\alpha\right) \\ + d_n \left\{ a^{\alpha\beta}\, (\mathcal{W}_{\boldsymbol{D}})^T\, \boldsymbol{d}_{,\beta} - [\boldsymbol{d}_{,\beta} \cdot (\mathcal{W}_{\boldsymbol{D}})\, \boldsymbol{a}_\mu] \left(a^{\alpha\beta}a^\mu + a^{\alpha\mu}a^\beta\right) \right\}. \end{aligned} \tag{4.79}$$

The foregoing results are valid for any Galilean-invariant function $\mathcal{W}(\boldsymbol{d}, \boldsymbol{D})$ and are therefore applicable to bilayers composed of extensible lipids, provided that the constraints (4.18) and (4.21) are relaxed and the associated multipliers λ, μ are suppressed.

4.6 Computation of $\mathcal{W}_{\boldsymbol{D}}$ and $\mathcal{W}_{\boldsymbol{d}}$

To complete the specification of the response functions we require expressions for $\mathcal{W}_{\boldsymbol{D}}$ and $\mathcal{W}_{\boldsymbol{d}}$. The former is obtained by fixing $\boldsymbol{d}$ in (4.1) and (4.53), yielding

$$\begin{aligned}\mathcal{W}_{\boldsymbol{D}}\cdot\dot{\boldsymbol{D}} = (a_1+a_2\boldsymbol{W}(\boldsymbol{d})\cdot\boldsymbol{D}+2k_1\mathrm{tr}\boldsymbol{D})\,\mathrm{tr}\dot{\boldsymbol{D}}+(k_2+k_4)\left[\mathrm{tr}\left(\boldsymbol{D}^2\right)-(\mathrm{tr}\boldsymbol{D})^2\right]^{\cdot}\\ +(a_2\mathrm{tr}\boldsymbol{D}+a_3+2k_2\boldsymbol{W}(\boldsymbol{d})\cdot\boldsymbol{D})\,\boldsymbol{W}(\boldsymbol{d})\cdot\dot{\boldsymbol{D}}+2k_3\boldsymbol{D}\boldsymbol{d}\cdot\dot{\boldsymbol{D}}\boldsymbol{d},\end{aligned} \tag{4.80}$$

where

$$\mathrm{tr}\dot{\boldsymbol{D}} = \boldsymbol{I}\cdot\dot{\boldsymbol{D}}, \tag{4.81}$$

with $\boldsymbol{I}$ the identity for 3-space, and

$$\left[\mathrm{tr}\left(\boldsymbol{D}^2\right)-(\mathrm{tr}\boldsymbol{D})^2\right] = 2\left[\boldsymbol{D}^T-(\mathrm{tr}\boldsymbol{D})\,\boldsymbol{I}\right]\cdot\dot{\boldsymbol{D}}. \tag{4.82}$$

Thus,

$$\begin{aligned}\mathcal{W}_{\boldsymbol{D}} = (a_1+a_2\boldsymbol{W}(\boldsymbol{d})\cdot\boldsymbol{D}+2k_1\mathrm{tr}\boldsymbol{D})\,\boldsymbol{I}+2(k_2+k_4)\left[\boldsymbol{D}^T-(\mathrm{tr}\boldsymbol{D})\,\boldsymbol{I}\right]\\ +(a_2\mathrm{tr}\boldsymbol{D}+a_3+2k_2\boldsymbol{W}(\boldsymbol{d})\cdot\boldsymbol{D})\,\boldsymbol{W}(\boldsymbol{d})+2k_3\boldsymbol{\eta}\otimes\boldsymbol{d}.\end{aligned} \tag{4.83}$$

To obtain $\mathcal{W}_{\boldsymbol{d}}$ we hold $\boldsymbol{D}$ fixed, finding that

$$\mathcal{W}_{\boldsymbol{d}}\cdot\dot{\boldsymbol{d}} = (a_2\mathrm{tr}\boldsymbol{D}+a_3+2k_2\boldsymbol{W}(\boldsymbol{d})\cdot\boldsymbol{D})\,\dot{W}(\boldsymbol{d})\cdot\boldsymbol{D}+2k_3\boldsymbol{D}\boldsymbol{d}\cdot\boldsymbol{D}\dot{\boldsymbol{d}}, \tag{4.84}$$

where (cf. (4.6))

$$\dot{W}(\boldsymbol{d})\cdot\boldsymbol{D} = \mathrm{curl}\boldsymbol{d}\cdot\dot{\boldsymbol{d}}. \tag{4.85}$$

Accordingly,

$$\mathcal{W}_{\boldsymbol{d}} = (a_2\mathrm{tr}\boldsymbol{D}+a_3+2k_2\boldsymbol{W}(\boldsymbol{d})\cdot\boldsymbol{D})\,\mathrm{curl}\boldsymbol{d}+2k_3\boldsymbol{D}^T\boldsymbol{\eta}. \tag{4.86}$$

Here $\mathrm{curl}\boldsymbol{d} = (\mathrm{curl}\tilde{\boldsymbol{d}})_{|\omega}$ is the restriction to ω of the three-dimensional field $\mathrm{curl}\tilde{\boldsymbol{d}}$. This is given by [74]

$$\mathrm{curl}\boldsymbol{d} = \boldsymbol{g}^i\times\boldsymbol{d}_{,i} \tag{4.87}$$

where

$$\boldsymbol{g}^\alpha = \boldsymbol{a}^\alpha - d_n^{-1}d^\alpha\boldsymbol{n},\quad \boldsymbol{g}^3 = d_n^{-1}\boldsymbol{n},\quad \text{with}\quad d^\alpha = \boldsymbol{d}\cdot\boldsymbol{a}^\alpha, \tag{4.88}$$

and $\boldsymbol{d}_{,3} = \boldsymbol{\eta}$. Thus,

$$\mathrm{curl}\boldsymbol{d} = \boldsymbol{a}^\alpha\times\boldsymbol{d}_{,\alpha}+d_n^{-1}\boldsymbol{n}\times\left[\boldsymbol{\eta}-(\nabla\boldsymbol{d})\,\boldsymbol{d}\right]. \tag{4.89}$$

With these results, the constraints of Section 4.3 and the equilibrium equations and edge conditions of Section 4.4 yield a complete system for the determination of the position field $\boldsymbol{r}(\theta^\alpha)$, the leaflet director fields $\boldsymbol{d}^\pm$, $\boldsymbol{\eta}^\pm$ and the multipliers $\lambda^\pm$and $\mu^\pm$ on the bilayer surface.

Chapter 5

Conclusion

We now conclude this thesis with a brief review of the significant results and mention some suggests for further expanding on those results.

In Chapter 2, a simple model of lipid tilt and distension proposed in [77] inspired by parallel computational research in molecular dynamics was solved and plotted using COMSOL Multiphysics. A simple energy was introduced in (2.4) resulting in the equilibrium equations (2.22) and (2.23), which were then plotted using (2.24) as a choice for G. The results showed a tilt gradient affected by the presence of idealized embedded proteins. Future development of this idea would involve attempting to find forms of (2.4) that would precisely match results of simulations based on particle methods. Further work may then extend of this simple model to one in which predictions can be made and tested experimentally.

In Chapter 3, the equilibrium equations for a lipid bilayer with a comoving cytoskeletal membrane were derived, where (3.123) is the shape equation subject to the tangential equilibrium equations (3.116). This equation was used to predict the biconcave discoid shape of a human erythrocyte in equilibrium (Figure 3.5). A possible advancement of this model could be achieved by comparing a prediction made using (3.123) for an experimentally testable form of $\Sigma^{\alpha\beta}$.

In Chapter 4, the equilibrium equations (4.46) and (4.47) were derived for a lipid bilayer with asymmetric tilt fields in each leaflet as part of a complete system to determine the position field $\boldsymbol{r}(\theta^\alpha)$ and other necessary fields. The next step in exploring this result would be to propose an appropriate boundary value problem using this system of equations and solve it for some elementary problems in which asymmetric tilt fields would yield a different result than those of the standard symmetric tilt models.

Bibliography

[1] D. J. Steigmann A. Agrawal. "A model for surface diffusion of trans-membrane proteins on lipid bilayers". In: *Z. Angew. Math. Phys.* 62:3.549-563 (2011).

[2] D. J. Steigmann A. Agrawal. "Boundary-value problems in the theory of lipid membranes". In: *Contin. Mech. Therm.* 21.57-82 (2009).

[3] D. J. Steigmann A. Agrawal. "Coexistent fluid-phase equilibria in biomembranes with bending elasticity". In: *J. Elasticity* 93.63-80 (2008).

[4] D.J. Steigmann A. Agrawal. "Asymmetric lipid bilayers from the perspective of three-dimensional liquid crystal theory". In: *Cont. Mech. Thermodyn.* (2020), (doi: 10.1007/s0061-020-00919–8).

[5] W.M. Gelbat A. Ben Shaul I. Szleifer. "Organization and thermodynamics in micelles and bilayers". In: *J. Chem. Phys.* 83 (1985), pp. 3597–3611.

[6] H. Cohen A.I. Murdoch. "Symmetry considerations for material surfaces". In: *Arch. Ration. Mech. Anal.* 72.61-98 (1979).

[7] M. Tartibi et al. "Single-cell mechanics— an experimental-computational method for quantifying the membrane-cytoskeleton elasticity of cells". In: *Acta Biomater* 27.224–235 (2015).

[8] R. Aris. "Vectors, tensors and the basic equations of fluid mechanics". In: *Dover Publications* (1989).

[9] S. Mukhin et al. B. Kheyfets. "Origin of lipid tilt in flat monolayers and bilayers". In: *Phys. Rev. E.* 100.6-1 (2019), :062405.

[10] A.J. Baines. "The spectrin-ankyrin-4.1-adducin membrane skeleton: adapting eukaryotic cells to the demands of animal life." In: *Protoplasma* 244 (2010), pp. 99–131.

[11] V. Berdichevsky. "Variational principles of continuum mechanics: part I—fundamentals". In: *Springer* Berlin (2009).

[12] P. B. Canham. "The minimum energy of bending as a possible explanation of the biconcave shape of the human red blood cell". In: *J. Theor. Biol.* 26:1.61-81 (1970).

[13] P. G. Ciarlet. "An introduction to differential geometry with applications to elasticity". In: *Springer,* Dordrecht, (2005).

[14] M. Deserno. "Fluid lipid membranes: From differential geometry to curvature stresses". In: *Chem. Phys. Lipids* 185 (2015), pp. 11–45.

[15] M. Deserno. *Notes on Differential Geometry*. Carnegie Mellon University. May 2004. [Online]. URL: `https://www.cmu.edu/biolphys/deserno/pdf/diff_geom.pdf`.

[16] R. Skalak E. Evans. "Mechanics and thermodynamics of biomembranes". In: *CRC Press* Boca Raton (2015).

[17] E.A. Evans. "Bending Resistance and Chemically-Induced Moments in Membrane". In: *Biophys. J.* 14 (1974), pp. 923–31.

[18] J.B. Fournier. "Microscopic membrane elasticity and interactions among membrane inclusions: interplay between the shape, dilation, tilt and tilt-difference modes". In: *Eur. Phys. J.* B.11 (1999), pp. 261–272.

[19] F.C. Frank. "On the theory of liquid crystals". In: *Discuss. Faraday Soc.* 25.19-28 (1958).

[20] S. Klein G. Gompper. "Theory of Aqueous Surfactant Solutions". In: *J. Phys.* 1992.2 (1992), pp. 1725–44.

[21] C.-C. Wang H. Cohen. "On the response and symmetry of elastic and hyperelastic membrane points". In: *Arch. Ration. Mech. Anal.* 85.355-391 (1984).

[22] S.L. Zipursky et al. H. Lodish A. Berk. "Molecular Cell Biology 4th ed." In: *New York: W.H. Freeman* (2000).

[23] W. Helfrich H.J. Deuling. "The curvature elasticity of fluid membranes: A catalogue of vesicle shapes". In: *SIAM Journal on Applied Mathematics* 37 (1982), pp. 1335–45.

[24] W. Helfrich. "Elastic properties of lipid bilayers: theory and possible experiments". In: *Z. Naturforsch* 28c.693-703 (1973).

[25] Berg C. Howard. "Random Walks in Biology". In: *Princeton, N.J.* Princeton University Press.ISBN (1993), pp. 978-0-691-00064–.

[26] P. Vázquez-Montejo J. Guven M. M. Müller. "Isometric bending requires local constraints on free edges". In: *Math. Mech. Solids* 24:12.4051-4077 (2019).

[27] E. Boura et al. J. Hurley. "Membrane budding". In: *Cell* 143.6 (2010), pp. 875–87.

[28] S. Tristram-Nagle J.F. Nagle. "Structure of lipid bilayers". In: *Biochem. Biophys. Acta* 1469.(3) (2000), pp. 159–95.

[29] J. T. Jenkins. "The equations of mechanical equilibrium of a model membrane". In: *SIAM J. Appl. Math.* 32:4.755-764 (1977).

[30] S. Krishnaswamy. "A Cosserat-type model for the red blood cell wall". In: *Int. J. Eng. Sci.* 34:8.873-899 (1996).

[31] A. Boudaoud L. Beauzamy N. Nakayama. "Flowers under pressure: ins and outs of turgor regulation in development." In: *Ann Bot.* 114.(7) (2014), pp. 1517–33.

[32] S.E. Lux. "Anatomy of the red cell membrane skeleton: unanswered questions." In: *Blood* 127 (1993), pp. 187–199.

[33] S. May M. Fosnaric A. Iglic. "Influence of rigid inclusions on the bending elasticity of a lipid membrane". In: *Phys. Rev.* E74.051503 (2006).

[34] A. C. Pipkin M. G. Hilgers. "Energy-minimizing deformations of elastic sheets with bending stiffness". In: *J. Elasticity* 31.125-139 (2019).

[35] M. Kozlov M. Hamm. "Model of inverted amphiphilic mesophases". In: *Eur. Phys. J.* 6 (1998), pp. 519–28.

[36] M.M. Kozlov M. Hamm. "A consistent quadratic curvature-tilt theory for fluid membranes". In: *J. Chem. Hpys.* 151 (2019), p. 164108.

[37] M.M. Kozlov M. Hamm. "Elastic energy of tilt and bending of fluid membranes". In: *Eur. Phys. J.* E.3 (2000), pp. 323–335.

[38] M. Dembo M. Herant. "Active cellular protrusion: continuum theories and models". In: *Cambridge University Press* Cambridge.Cytoskeletal mechanics: models and measurements in cell mechanics (2006), pp. 204–224.

[39] L. Cattel M. L. Immordino F. Dosio. "Stealth liposomes: review of the basic science, rationale, and clinical applications, existing and potential". In: *Int. J. Nanomedicine* 1.(3) (2006), pp. 297–315.

[40] B. Hendrickson M. Shirani D. J. Steigmann. "Equilibrium theory for a lipid bilayer with a conforming cytoskeletal membrane". In: *Mathematics and Mechanics of Complex Systems* 8.1 (2020), pp. 69–99.

[41] B. Hendrickson M. Shirani D. J. Steigmann. "On the equations of equilibrium for asymmetric tilted lipid bilayers". In: (Manuscript submitted for publication 2021).

[42] I. Szeifer M. Uline. "Mode specific elastic constants for the gel, liquid-ordered, and liquid-disordered phases of DPPC/DOPC/cholesterol model lipid bilayers". In: *Faraday Discuss.* 161 (2013), pp. 177–91.

[43] M.M. Sperotto M. Venturoli B. Smit. "Simulation studies of protein-induced bilayer deformations, and lipid-induced protein tilting, on a mesoscopic model for lipid bilayers with embedded proteins." In: *Biophys J.* 88.(3) (2005), pp. 1778–98.

[44] l. Martinez-Balbuena et al. "Application of the Helfrich elasticity theory to the morphology of red blood cells". In: *American Journal of Physics* 89 (2021), pp. 465–76.

[45] S. May. "Protein-induced bilayer deformations: the lipid tilt degree of freedom". In: *Eur Biophys J.* 29.(1) (2000), pp. 17–28.

[46] R. Korenstein N. Ben-Dov. "Enhancement of cell membrane invaginations, vesiculation and uptake of macromolecules by protonation of the cell surface". In: *PLoS One* 7.4 (2012), :e35204.

[47] P.G. Gallagher N. Mohandas. "Red cell membrane: past, present, and future". In: *Blood* 112.10 (2008), pp. 3939–48.

[48] P. M. Naghdi. "The theory of shells and plates". In: *S. Flügge's Handbuch der Physik* VIa.2 (1972), pp. 425–640.

[49] P. Nelson. "Renormalization of chiral couplings in tilted bilayer membranes". In: *J. Phys.* 3 (1993), pp. 1535–69.

[50] J.C.C. Nitsche. "Boundary value problems for variational integrals involving surface curvatures". In: *Quart. Appl. Math.* 51:2.363–387 (1993).

[51] W. Noll. "A mathematical theory of the mechanical behavior of continuous media". In: *Arch. Ration. Mech. Anal.* 2.197-226 (1958).

[52] W. Noll. "On material frame-indifference". In: *Five contributions to natural philosophy* Available at http://www.math.cmu.edu/ wn0g/noll/FC.pdf. (2004).

[53] B. Martinac O. Hamil. "Molecular Basis of Mechanotransduction in Living Cells". In: *Physiological Reviews* 81.(2) (2001), pp. 685–740.

[54] F. Schmid O. Lenz. "Structure of symmetric and asymmetric 'ripple' phases in lipid bilayers". In: *Phys. Rev. Lett.* 98.104 (2007).

[55] T.R. Galimzyanov et al. O.V. Kondrashov. "Membrane-mediated interaction of amphipathic peptides can be described by a one-dimensional approach". In: *Phys. Rev.* E99.022401 (2019).

[56] T. Powers P. Nelson. "Rigid chiral membranes". In: *Phys. Rev.* 69 (1992), pp. 3409–12.

[57] A. Agrawal et al. P. Rangamani A. Benjamini. "Small scale membrane mechanics". In: *Biomech. Model Mechanobiol.* 13 (2014), p. 697.

[58] D.J. Steigmann P. Rangamani. "Variable tilt on lipid membranes". In: *Proc. R. Soc. A* 470.(2172) (2014), p. 20140463.

[59] G. Oster P. Rangamani D.J. Steigmann. "Role of Lipid Tilt in Endocytosis". In: *Biophysics J.* 102.(3) (2012), pp. 501–.

[60] L. Pan. "Super-resolution microscopy reveals the native ultrastructure of the erythrocyte cytoskeleton". In: *Cell Rep.* 22.5 (2018), pp. 1151–1158.

[61] J. Betten Q.S. Zheng and A.J.M. Spencer. "The formulation of constitutive equations for fibre-reinforced composites in plane problems: part I". In: *Arch. Appl. Mech.* 62.530–543 (2003).

[62] M. R. K. Mofrad R. D. Kamm. "Introduction, with the biological basis for cell mechanics". In: *pp. 1–17 in Cytoskeletal mechanics: models and measurements in cell mechanics* edited by M. R. K. Mofrad and R. D. Kamm.Cambridge University Press (2006), Cambridge.

[63] M. Caffrey R. Koynova. "Phases and phase transitions of the glycoglycerolipids". In: *Chem. Phys. Lipids* 69.3 (1994), pp. 181–207.

[64] E. G. Virga R. Rosso. "Adhesive borders of lipid membranes". In: *Proc. R. Soc. Lond. A* 455:1992.4145–4168 (2018).

[65] T. Galimzyanov et al. R.J. Molotkovsky. "Switching between successful and dead-end intermediates in membrane fusion". In: *Int.J. Mol. Sci* 18.2598 (2017).

[66] J.N. Reddy. "Theory and analysis of elastic plates and shells". In: *CRC Press* (2007), Taylor and Francis.

[67] T.J. Healey S. Dharmavaram. "On the equivalence of local and global area-constraint formulations for lipid bilayer vesicles". In: *Z. Angew. Math. Phys.* 66.2843-2854 (2015).

[68] F. Nedelec S. Dmitrieff. "Membrane Mechanics of Endocytosis in Cells with Turgor". In: *PLoS Comput Biol.* 11.10 (2015), :e1004538.

[69] R.J. Molotkovsky et al. S.A. Akimov. "Model of membrane fusion: continuous transition to fusion pore with regard of hydrophobic and hydration interactions". In: *Cell Biol.* 8.153 (2014).

[70] V.V. Aleksandrova et al. S.A. Akimov. "Interaction of amphipathic peptides mediated by elastic membrane deformations". In: *Membr. Cell Biol.* 11.206 (2017).

[71] L. E. Scriven. "Dynamics of a fluid interface: equation of motion for Newtonian surface fluids". In: *Chem. Eng. Sci.* 12:2.98–108 (1960).

[72] D. Stamenovic. "Models of cytoskeletal mechanics based on tensegrity". In: *pp. 103–128 in Cytoskeletal mechanics: models and measurements in cell mechanics* edited by M. R. K. Mofrad and R. D. Kamm.Cambridge University Press (2006), Cambridge.

[73] D. J. Steigmann. "Applications of polyconvexity and strong ellipticity to nonlinear elasticity and elastic plate theory". In: *pp. 265–299 in Poly-, quasi- and rank-one convexity in applied mechanics* vol. 516.edited by J. Schröder and P. Neff (2010), Springer, Vienna.

[74] D. J. Steigmann. "Continuum theory for elastic sheets formed by inextensible crossed elasticae". In: *Int. J. Non-Linear Mech.* 106.324–329 (2018).

[75] D. J. Steigmann. "Irreducible function bases for simple fluids and liquid crystal films". In: *Z. angew. Math. Phys.* 54.462–477 (2003).

[76] D. J. Steigmann. "Tension-field theory". In: *Proc. R. Soc. Lond. A* 429:1876.141–173 (1990).

[77] D.J. Steigmann. "Mechanics and Physics of Lipid Bilayers". In: *Lecture delivered as part of course CHM ENG C294A at UC Berkeley, September 26th, 2017* (2017).

[78] D.J. Steigmann. "Mechanics and physics of lipid bilayers". In: *CISM Course: The Role of Mechanics in the Study of Lipid Bilayers* 577 (D.J. Steigmann, ed.)Springer, Singapore (2018), pp. 1–61.

[79] D.J. Steigmann. "On the relationship between the Cosserat and Kirchhoff-Love theories of elastic shells". In: *Math. Mech. Solids* 4.275-88 (1999a).

[80] P. Schiavone T. Belay C.I. Kim. "Mechanics of a lipid bilayer subjected to thickness distension and membrane budding". In: *Mathematics and Mechanics of Solids* 23.(1) (2018), pp. 67–84.

[81] P. Nelson T. Powers. "Fluctuating membranes with tilt order". In: *J. Phys.* 5 (1995), pp. 1671–8.

[82] R.A. Toupin. "Elastic materials with couple-stresses". In: *Arch. Ration. Mech. Anal.* 11.385–414 (1962).

[83] R. Lipowsky U. Seifert K. Berndl. "Shape transformations of vesicles: Phase diagram for spontaneous- curvature and bilayer-coupling models". In: *Phys. Rev. A* 44.1182-1202 (1991).

[84] D.M. Gilligan V. Bennett. "The spectrin-based membrane skeleton and micron-scale organization of the plasma membrane." In: *Annu. Rev. Cell Biol.* 9 (1993), pp. 27–66.

[85] B. Babnik et al. V. Kralj-Iglic. "Quadrupolar ordering of phospholipid molecules in narrow necks of phospholipid vesicles". In: *J. Stat. Phys.* 125.727 (2006).

[86] A. Escalada et al. V.A. Frolov. "Geometry of membrane fission". In: *Chem. Phys. Lipids* 185.129 (2015).

[87] P.V. Bashkirov et al. V.A. Frolov. "Membrane curvature and fission by dynamin: mechanics, dynamics and partners". In: *Biophysics J.* 98.2a (2010).

[88] E.G. Virga. "Variational theories for liquid crystals". In: *Chapman Hall* London (1994).

[89] K. Olbrich et al. W. Rawicz. "Effect of chain length and unsaturation on elasticity of lipid bilayers". In: *Biophys. J* 79 (2000), pp. 328–39.

[90] A.C. Pipkin W.B. Wang. "Inextensible networks with bending stiffness". In: *Quart. J. Mech. Appl. Math.* 39:3.343–359 (1986).

[91] M. Deserno X. Wang. "Bending Resistance and Chemically-Induced Moments in Membrane". In: *The Journal of Physical Chemistry B* 120.26 (2016), pp. 6061–73.

[92] Y.Z. Xia Z.C. Ou-Yang J.X. Liu. "Geometric methods in the elastic theory of membranes in liquid crystal phases". In: *World Scientific* Singapore (1999).

[93] Q.S. Zheng. "Irreducible function bases for simple fluids and liquid crystal films: a new derivation". In: *Z. angew. Math. Phys.* 54.478–483 (2003).